농학박사학위논문

바실러스 섭틸리스로부터 생합성 된 Micrococcin P2 및 Thiocillin IV의 특성에 관한 연구

Biosynthesis and Characterization of Micrococcin P2 and Thiocillin IV in *Bacillus subtilis*

2023년 8월

서울대학교 대학원
농생명공학부 응용생명화학전공
손 영 진

A Dissertation for the Degree of Doctor of Philosophy

Biosynthesis and Characterization of Micrococcin P2 and Thiocillin IV in *Bacillus subtilis*

August 2023

Young-Jin Son
Applied Life Chemistry Major
Department of Agricultural Biotechnology
Seoul National University

바실러스 섭틸리스로부터 생합성 된 Micrococcin P2 및 Thiocillin IV의 특성에 관한 연구

Biosynthesis and Characterization of Micrococcin P2 and Thiocillin IV in *Bacillus subtilis*

지도교수 권 용 훈

이 논문을 농학박사학위논문으로 제출함
2023년 5월

서울대학교 대학원
농생명공학부 응용생명화학전공

손 영 진

손영진의 박사학위논문을 인준함
2023년 7월

위 원 장	오 기 봉	(인)
부 위 원 장	권 용 훈	(인)
위 원	김 상 민	(인)
위 원	권 문 혁	(인)
위 원	강 민 경	(인)

Biosynthesis and Characterization of Micrococcin P2 and Thiocillin IV in *Bacillus subtilis*

Advisor: Yonghoon Kwon

A Dissertation Submitted in Partial Fulfillment
of the Requirement for the Degree of

DOCTOR OF PHILOSOPHY

to the Faculty of
Applied Life Chemistry Major,
Department of Agricultural Biotechnology

at

SEOUL NATIONAL UNIVERSITY

by

Young-Jin Son

Date Approved

_____

Ki-Bong Oh

Yonghoon Kwon

Sang-Min Kim

Moonhyuk Kwon

Min-Kyoung Kang

Abstract

The emergence of antimicrobial resistance has become a significant public health concern, highlighting the urgent call for developing new antibiotics with novel mechanisms of action. Thiopeptides, a class of natural products, hold great promise for developing new antibacterial agents. This dissertation describes studies to leverage promising thiopeptide scaffolds into clinical treatments by harmonizing chemical and biological studies. In Chapter 1, the reconstruction of thiocillin gene clusters obtained from *Bacillus cereus* ATCC 14579 led to the selective biosynthesis of micrococcin P2 in *Bacillus subtilis* 168. The biosynthetic micrococcin P2 displayed structural characteristics similar to those of the authentic micrococcin P2 and demonstrated effective inhibition against Gram-positive pathogens, *Mycobacterium tuberculosis*, and *Clostridioides difficile*. Through extensive *in vitro* assays using clinical isolates, time-kill studies, pharmacokinetic analysis, and *in vivo* animal efficacy studies, micrococcin P2 was identified as a promising anti-*C. difficile* agent. Furthermore, in the presence of a hydroxide ion, micrococcin P2 can be selectively converted to micrococcin acid, a hydrolyzed product that serves as a crucial intermediate for semi-synthesis. Therefore, micrococcin P2 holds significant value for the development of new anti-*C. difficile* antibiotics and warrants further exploration. In Chapter 2, the focus is on the scalable biosynthesis and characterization of thiocillin IV. Thiocillin IV is believed to be a congener of O-methylated micrococcin P2, although the exact structure requires elucidation. The biosynthesis of thiocillin IV was achieved by

expressing *tclO*, a gene encoding an O-methyltransferase, along with the genes responsible for micrococcin P2 biosynthesis in a *Bacillus* strain. By incorporating the precursor peptide genes and optimizing the culture conditions, a production level reached to 2.4 mg/L of culture. Through extensive analysis, the structure of thiocillin IV was determined to be O-methylated micrococcin P2 exclusively at the 8-Thr position. The distinct inhibitory mechanisms of thiocillin IV exhibited promising biological activity against Gram-positive pathogens, without showing cross-resistance to conventional antibiotics. However, the protein stability of recombinant TclO hindered its purification process. Nevertheless, *in vivo* feeding studies confirmed that micrococin P2 was not O-methylated by TclO, providing valuable insights into the biosynthetic pathway and its role in the modification process. Finally, this study has significantly enhanced the understanding of thiopeptides and provided novel ways to tackle the spreading antibiotic resistance problem.

Key words: antibiotics, thiopeptide, thiocillin gene cluster, biosynthesis, microbial production

***Student Number*:** 2019-37399

Contents

Chapter 2: Biosynthesis and Characterization of Thiocillin IV

List of Figures

List of Tables

List of Abbreviations

^{13}C	Carbon-13
^{1}H	Proton
ACN	Acetonitrile
ATCC	American Type Culture Collection
BHI	Brain heart infusion
calcd	Calculated
CDI	*Clostridioides difficile* infection
Chl	Chloramphenicol
CIP	Ciprofloxacin
CLSI	Clinical and Laboratory Standards Institutes
COSY	Correlation spectroscopy
CV	Column volume
d	Doublet (spectral)
dd	Doublet of doublet (spectral)
dt	Doublet of triplet (spectral)
ddd	Doublet of doublet of doublet (spectral)
DMSO	Dimethyl sulfoxide
ELISA	Enzyme-linked immunosorbent assay
gDNA	Genomic DNA
GST	Glutathione S-transferase
h	Hours

HMBC	Heteronuclear multiple-bond correlation spectroscopy
HSQC	Heteronuclear single-quantum correlation spectroscopy
HRMS	High resolution mass spectrometry
Hz	Hertz
IBD	Inflammatory bowel disease
IPA	Isopropyl alcohol
J	Coupling constant
LB	Luria-Bertani
LC-MS	Liquid chromatography-Mass spectrometry
LPS	Lipopolysaccharide
m	Multiplet (spectral)
MALDI-TOF	Matrix-assisted laser desorption/ionization time-of-flight
MBP	Maltose binding protein
MeOH	Methanol
MHZ	Megahertz
MIC	Minimum inhibitory concentration
m/z	Mass-to-charge ratio
MRSA	Methicillin-resistant *Staphylococcus aureus*
Ni-NTA	Nickel-nitrilotriacetic acid
NMR	Nuclear magnetic resonance
OD	Optical density
PCR	Polymerase chain reaction
q	Quartet (spectral)

RiPP	Ribosomally synthesized and post-translationally modified peptide
RP-HPLC	Reverse phase-high performance liquid chromatograpy
rpm	Rotation per minutes
Rt	Retention time
s	Singlet (spectral)
Ser	Serine
TFA	Trifluoroacetic acid
Thr	Threonine
TOCSY	Total correlation spectroscopy
UPLC-MS	Ultra-performance liquid chromatography-mass spectrometry
VAN	Vancomycin
VRE	Vancomycin-resistant *enterococci*
δ	Chemical shift

General Introduction

A brief history of antibiotics

The origin of the term "antibiotic" can be traced back to the word antibiosis, which was first used as an antonym to symbiosis by Paul Vuillemin in 1890, when he described antagonistic action between different microorganisms (e.g., fungi and bacteria; or bacteria and protozoa) (Dhingra et al., 2020). Later, the word "antibiotic" was used to describe naturally occurring secondary metabolites produced by bacteria and fungi possessing either growth-inhibitory (bacteriostatic) or killing (bactericidal) activities against bacteria or fungi (Bérdy, 2012).

Perhaps, many people are familiar with the somewhat accidental discovery of penicillin by Sanford Fleming on September 03, 1928 (Hare, 1982). In 1940, Howard Flory and Ernest Chain published a paper describing the purification of sufficient penicillin for clinical trials (Chain et al., 1940). Their works eventually led to dramatic improvements in general health and sanitation, at least in North America and the UK (Walsh, 2003; Aslam et al., 2018). Another major figure in the history of antibiotics, Selman Waksman, proposed a new screening platform for antibiotic discovery. As per Waksman's platform *Streptomyces* isolated from the soil were grown on solid media and screened for antimicrobial activity against a sensitive indicator strain (Lewis, 2013). Waksman received the 1952 Nobel Prize for the discovery of streptomycin—the first antibiotic isolated using this approach (Waksman,

1953). Due to the simplicity of this platform, it has become widely accepted and highly successful. Following this development, introducing new molecular entities by global pharmaceutical companies has resulted in an intense and competitive race. The period between the 1950s and 1970s was the golden age of discovering novel antibiotics classes (Figure 1) (Walsh, 2003).

Figure 1. Timeline of antibiotic discovery.

Timeline showing new classes of antibiotic used in the clinic. The period from 1950 to 1970 is known as the "golden era" of antibiotics research. At the bottom of the timeline are dates related to antibiotic discovery and AMR, including the first reports of drug-resistant strains. Here antibiotics are colored according to their origin: green = actinomycetes, blue = other bacteria, purple = fungi and orange = synthetic. Figure 1 adapted from Hutchings et al., 2019.

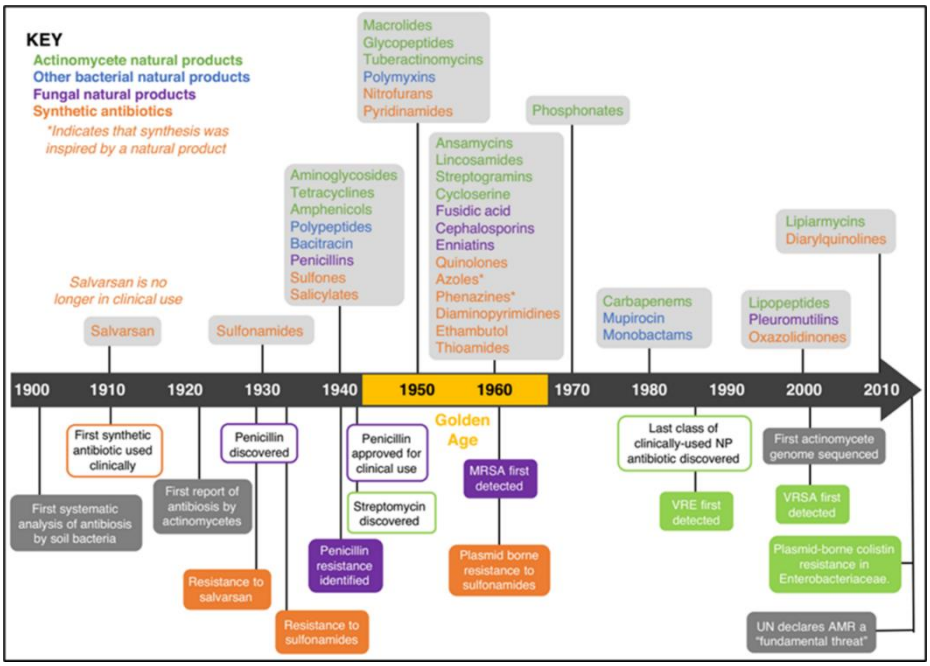
KEY
Actinomycete natural products
Other bacterial natural products
Fungal natural products
Synthetic antibiotics
*Indicates that synthesis was inspired by a natural product
Salvarsan is no longer in clinical use
Salvarsan
Sulfonamides
Aminoglycosides
Tetracyclines
Amphenicols
Polypeptides
Bacitracin
Penicillins
Sulfones
Salicylates
Macrolides
Glycopeptides
Tuberactinomycins
Polymyxins
Nitrofurans
Pyridinamides
Ansamycins
Lincosamides
Streptogramins
Cycloserine
Fusidic acid
Cephalosporins
Enniatins
Quinolones
Azoles*
Phenazines*
Diaminopyrimidines
Ethambutol
Thioamides
Phosphonates
Carbapenems
Mupirocin
Monobactams
Lipopeptides
Pleuromutilins
Oxazolidinones
Lipiarmycins
Diarylquinolines
1900
1910
1920
1930
1940
1950
1960
1970
1980
1990
2000
2010
Golden Age
First systematic analysis of antibiosis by soil bacteria
First synthetic antibiotic used clinically
First report of antibiosis by actinomycetes
Resistance to salvarsan
Penicillin discovered
Resistance to sulfonamides
Penicillin resistance identified
Penicillin approved for clinical use
Streptomycin discovered
MRSA first detected
Plasmid borne resistance to sulfonamides
Last class of clinically-used NP antibiotic discovered
VRE first detected
First actinomycete genome sequenced
VRSA first detected
Plasmid-borne colistin resistance in Enterobacteriaceae.
UN declares AMR a "fundamental threat"

Global spread of antibiotic resistance

The introduction of antibiotics into clinical use was undoubtedly the most remarkable medical advancement of the 20th century. In addition to treating bacterial infections, antibiotics have enabled many modern medical procedures, including cancer treatment, organ transplantation, and open-heart surgery (Hutchings et al., 2019). However, the misuse of antibiotics has led to a drastic increase in antimicrobial resistance (AMR) and the ineffectiveness of some antibiotics. Due to the rapid outbreak of antibiotic-resistant bacteria around the world, antibiotics are becoming less effective, posing a severe threat to human health (Ventola, 2015). Antibiotic resistance occurs naturally in response to exposure and selection, but antibiotic misuse and abuse significantly promote its emergence and spread (Ferri et al., 2017). For example, an O'Neill report predicts that 10 million people will die annually from AMR by 2050 (Sugden et al., 2016). In the United States, antibiotic-resistant bacteria kill more than 2 million people a year, and in the EU, 35,000 people (including 33,000 patients) died this year from selected multi-drug-resistant (MDR) bacterial infections (Abda et al., 2020). Therefore, the dangers of “superbugs” have led policymakers to recognize this threat to human health and propose additional subsidies (Hall, 2018).

Reports of resistance to almost all major classes of antibiotics have emerged, with the identification of multi-drug-resistant, extensively-drug-resistant (XDR), and pan-drug-resistant (PDR) bacteria. In this context, PDR bacteria refer to those that display resistance to all approved antibiotic classes.

The Centers for Disease Control and Prevention (CDC) 2019 antibiotic resistance threats report has classified 18 antibiotic-resistant bacteria and fungi (not including viruses and parasites) into urgent, serious, or concerning threats (Dadgostar, 2019). Many of these bacteria impose significant clinical and financial burdens on patients, their families, and the US healthcare system. However, despite the urgent need for new antibiotics, the development pipelines for dealing with particularly lethal multidrug-resistant Gram-negative bacteria are limited (Renwick et al., 2016). Pharmaceutical and biotechnology companies are reluctant to invest in new antibiotics because the market is risky and relatively unprofitable (Grabowski et al., 2002). Given the difficulty in developing antibiotics pipelines, the best hope for developing a new generation of anti-infective drugs may be discovering new natural products (Theuretzbacher et al., 2020). Such products are a likely source of new antibiotics due to their chemical diversity and high efficacy.

Urgent need to discover novel antibiotics

Drug-resistant infections are a serious threat to human health, and antibiotic resistance is getting worse. According to a 2017 report, the prevalence of resistance to levofloxacin, an antibiotic used to treat various *H. pylori* infections, in the Asia-Pacific region increased from about 2% before 2000 to 27% between 2011 and 2015. (Matsumoto et al., 2019). More antimicrobial agents are clearly needed, but such drugs still need to be developed. Fewer new antibiotics are reaching the market; the last entirely original class was

discovered in the late 1980s (Taubes, 2008). While it is easy to identify substances that kill bacteria, it is much more challenging to discover and develop substances that also show low toxicity to humans. Aside from the research difficulty, other barriers include the fact that the research and development process is time-consuming (i.e., 10–15 years) and expensive (i.e., $1.5 billion to develop a new antibiotic). It often fails to generate the desired result.

Historically, the development of many antibiotics using the high-throughput screening system has failed, and most of the best antibiotics have been sourced from natural products. (e.g., β-lactams, aminoglycosides, tetracyclines, and glycopeptides) (Walsh and Wright, 2005). Of the ~28,000 antibiotics sourced from natural products that have been discovered over the past few decades, >0.1% are in clinical use (Maarten et al., 2018). Most of natural products are unsuitable for drugs due to implementation problems including efficacy, toxicity, stability issues, or limited ability to culture diverse microbes in laboratory environments (Wright, 2017). Nevertheless, some of these natural products are worthy of reinvestigation. Many natural products discovered using Waksman's platform are not being developed as antibiotics. The reasons for this include low production yields, the structure of the natural product, and that too few sources of culturable bacteria have been identified (Harvey et al., 2015). Recently, the advance of massive microbial fermentation, sequencing, and DNA manipulation technologies have made providing new molecular structures for antibiotic developments easier, partially by enabling us

to overcome the shortcomings of as-yet unused resources (Foulston, 2019). Therefore, developing antibiotics based on natural products remains a promising strategy.

Overview of RiPPs

Ribosomally synthesized and post-translationally modified peptides (RiPPs) constitute a large and structurally diverse class of natural products (Arnison et al., 2013). Many RiPP-like materials have been newly identified, largely due to improvements in sequencing technology during the 21st century. (Kloosterman et al., 2020a). Many researchers have focused on RiPPs because they present a group of natural products that provide novel molecular entities and mechanisms of action (Caesar et al., 2021). Thus, even though they have not been extensively studied, there is significant potential for RiPPs to become a significant source of new antibiotics.

RiPPs are synthesized from the ribosomal synthesis of linear precursor peptides (structural peptides) that are typically 20 to 110 residues in length (Sukmarini, 2022). The precursor peptide, coded by structural genes, consists of an N-terminal leader peptide and the C-terminal core peptide. The N-terminus leader peptides serve as recognition sequences and are directly bound by specific biosynthetic proteins (Burkhart et al., 2015). In contrast, the C-terminus core region is modified post-translationally, resulting in mature RiPPs (Cheung et al., 2016) (Figure 2). Leader peptides provide binding affinity, selectivity, and allosteric effectors to activate biosynthetic enzymes and/or

discontinue enzymatic reactions (Ortega and Van Der Donk, 2016). When the core peptide undergoes post-translational modification, the leader peptide remains unmodified and serves as a recognition sequence for biosynthetic enzymes (Mordhorst et al., 2023).

During the last enzymatic reaction, the leader peptide, which serves no purpose other than specific recognition, is removed (Oman and Van Der Donk, 2010). In contrast, the core peptides are changed during RiPP biosynthesis. Following modification by biosynthetic genes, the core peptide goes through various intermediates until the leader peptide is removed (Hetrick and van der Donk, 2017). Therefore, by varying the leader peptides present in the substrate-specific binding region, core peptides can serve multiple processes (Burkhart et al., 2017a).

The leader peptide-guided strategy for the biosynthesis of RiPPs results in highly evolvable pathways (Bowers et al., 2010a). Many post-translational processing enzymes recognize the specific leader peptide but are highly tolerant of mutations in the core peptide (Rodríguez, 2022). Mutational studies of core peptide genes have generated different mature structures, showing differences in stability and biological activity (Fleming et al., 2019). Moreover, core region engineering studies have further demonstrated the plasticity of biosynthetic enzymes. The relatively small number of enzymes involved in maturation pathways also facilitates natural selection, which results in multiple pathways selecting for the same types of chemical structures.

Figure 2. A window into RiPP biosynthesis.

(A) Schematic of the RiPP biosynthetic pathway. All RiPPs are first synthesized from ribosomal precursor peptides (structural peptides). This linear peptide generally consists of a core peptide region preceded by a leader peptide. With the termination of RiPP biosynthesis (usually macrocyclization), the modified precursor peptide ~~then~~ undergoes proteolysis, and the leader peptide is removed. This leads to a mature RiPP. Representative RiPP biosynthetic gene clusters are shown, wherein each gene encodes a color-coded biosynthetic enzyme based on the modification it catalyzes. The dotted circles represent amino acids within the leader peptide. Full circles represent amino acids within the core region. (B) Chemical structures of select RiPP subfamily members. Structural features defining a particular RiPP subfamily are shown in blue. Additional PTMs are shown in red. Figures 2A and 2B are adapted from Ortega and Van Der Donk, 2016.

A

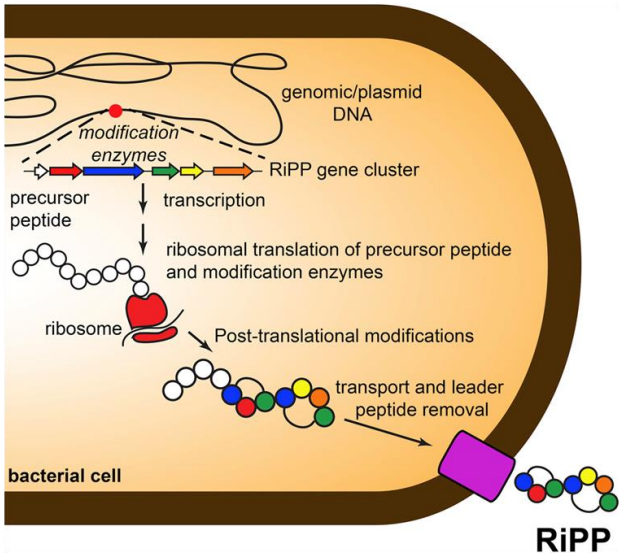
genomic/plasmid DNA
modification enzymes
RiPP gene cluster
precursor peptide
transcription
ribosomal translation of precursor peptide and modification enzymes
ribosome
Post-translational modifications
transport and leader peptide removal
bacterial cell
RiPP

B

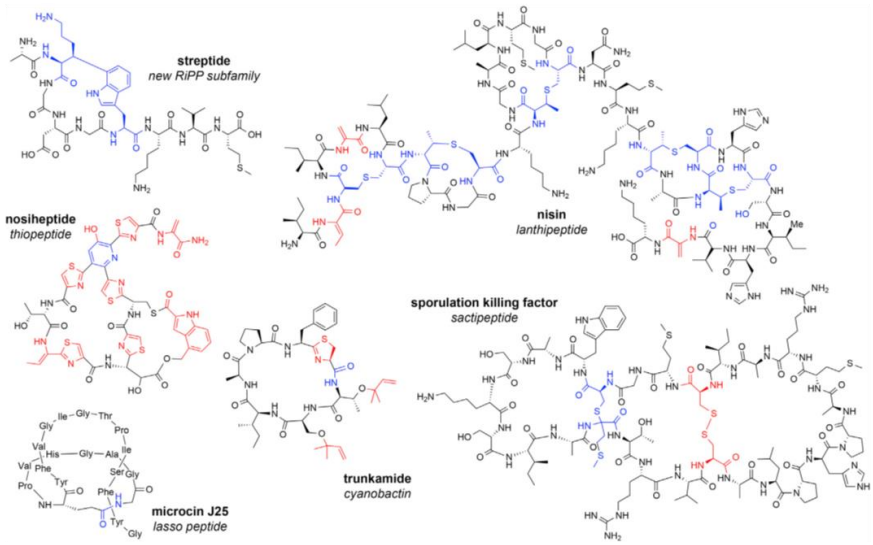
streptide
new RiPP subfamily
nosiheptide
thiopeptide
nisin
lanthipeptide
sporulation killing factor
sactipeptide
trunkamide
cyanobactin
microcin J25
lasso peptide

Thiopeptide

Thiopeptides, a subclass of RiPPs, are natural products that feature sulfur-rich, highly modified azol(in)e heterocycles, dehydroalanine/dehydrobutyrine (dha/dhb) residues, and a class-defining six-membered nitrogen-containing macrocyclic structure (Vinogradov and Suga, 2020). They are produced in ribosomal peptides that contain high amounts of cysteine, threonine, and serine (Cox et al., 2015). Those residues change to form heterocycles or dehydrated structures. Many thiopeptides also include structures such as a quinaldic-containing, or indolic acid-containing secondary macrocycle, or possess C-terminal amidation, methylation, oxidation, or glycosylation (Hudson and Mitchell, 2018).

Due to their novel chemical structures and powerful antibacterial properties, thiopeptides have become an important focal point of antibiotic research (Bennallack et al., 2014). They display potent antimicrobial activity toward Gram-positive pathogens, including methicillin-resistant *Staphylococcus aureus* (MRSA), drug-resistant *Streptococcus pneumoniae*, and vancomycin-resistant *Enterococci* (VRE), all of which are designated as "serious threats" by the CDC (Bagley et al., 2005). Remarkably, some thiopeptides also exhibit potent activity against *Mycobacterium tuberculosis,* non-tuberculosis mycobacteria (NTM), and *Clostridioides. difficile* (Leeds et al., 2012; Zheng et al., 2015; Degiacomi et al., 2016; Kim et al., 2019).

The first reported thiopeptide was isolated from a sewage sample in Oxford, United Kingdom, in 1948 (Su, 1948). Approximately 80 members of

the thiopeptides family have been identified (Bailly, 2022). The macrocyclic ring size (which can be 26-, 29-, 32- or 35-membered) of an individual thiopeptide determines its intrinsic biological target (Just-Baringo et al., 2014) (Figure 3).

For example, 26-membered rings, such as micrococcin P1, nosiheptide, and thiostrepton, are known to selectively bind to a cleft between ribosomal protein L11 (protein L11) and 23S ribosomal RNA (rRNA) (Burkhart et al., 2017b). This region is known as the "GTPase-associated center" and 26-membered thiopeptides prevent polypeptide translocation along template mRNA in the 50S ribosomal subunit (Harms et al., 2008) (Figure 4). A conserved sequence exists on all prokaryotic 23S rRNAs that bind to 26-membered thiopeptides. Mutations at N-terminus proline-rich regions in ribosomal protein L11 or 23S rRNA adenine 1067 or adenine 1095 confer resistance to 26-membered thiopeptides (Baumann et al., 2010). Thiopeptides containing 29-membered macrocyclic rings, such as GE2270A, GE37468, and thiomuracin, compete for the aminoacyl-tRNA binding site on the prokaryotic EF-Tu (LaMarche et al., 2012). The biological targets of thiopeptides containing 32 or 35-membered macrocyclic rings remain unknown (Chan and Burrows, 2021).

Figure 3. Structures of representative thiopeptide.

Micrococcin P1/P2, thiostrepton, nosiheptide, GE2270A and berninamycin. There are 26-membered rings on micrococcin P1/P2, thiostrepton and nosiheptide, 29-membered rings on GE2270A, and 35-membered rings on berninamycin.

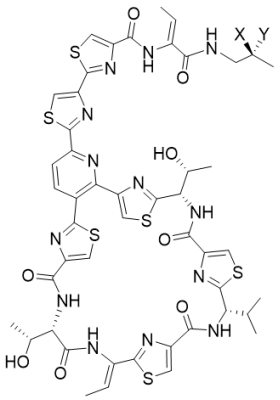

micrococcin P2, X,Y = O
micrococcin P1, X = OH, Y = H

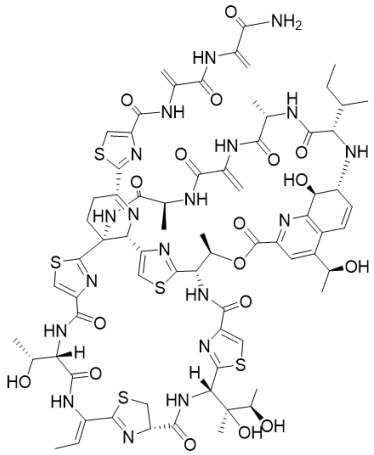

Thiostrepton

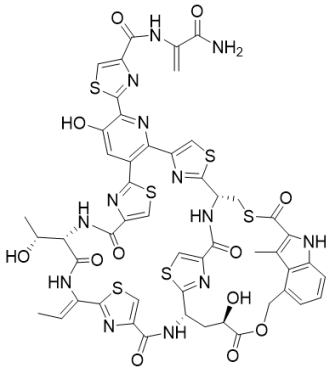

Nosiheptide

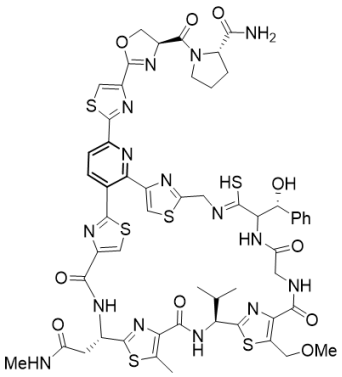

GE2270A

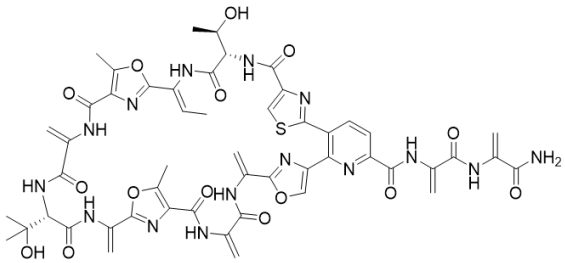

Berninamycin A

Figure 4. The proposed mechanisms of 26- and 29-membered thiopeptide antibiotics.

a) 29-membered antibiotics GE2270A bind and inhibit the formation of the EF-Tu–amino acyl-tRNA complex. Inhibition of EF-Tu lead to translational block and bacterial growth. b) The undisturbed state of a ribosome. The C-terminal domain (CTD) of protein L11 interacts with helix 43 and 44 of the 23S rRNA. The N-terminal domain of protein L11 is associated with protein L7. EF-G (Elongation factor G) interacts with the NTD of protein L7 and helix 43 and 44. EF-G converts GTP to GDP for proper ribosomal activity. c) Although micrococcin does not inhibit EF-G's binding to L7, it interferes with the binding to the 23s rRNA helices, interfering with the ribosomeal function. The figure was adapted from a Chan and Burrows, 2021.

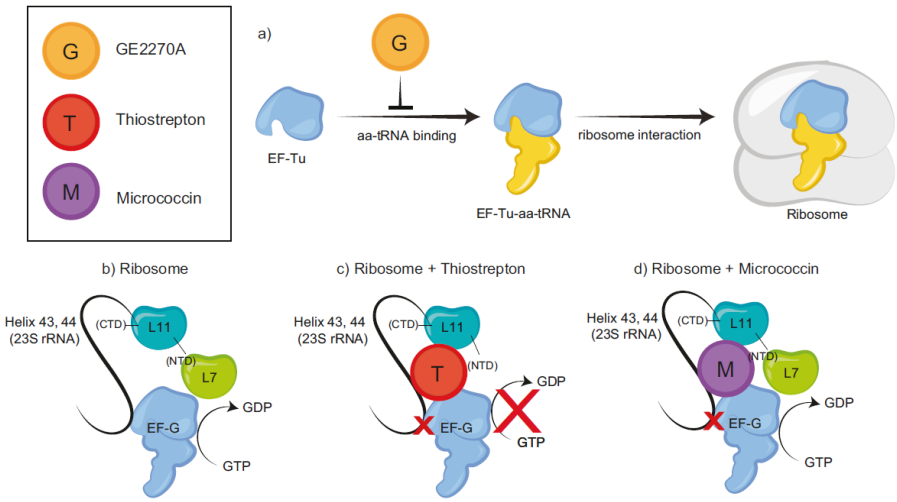
G
GE2270A
T
Thiostrepton
M
Micrococcin
a)
G
EF-Tu
aa-tRNA binding
EF-Tu-aa-tRNA
ribosome interaction
Ribosome
b) Ribosome
Helix 43, 44
(23S rRNA)
(CTD)
L11
(NTD)
L7
EF-G
GDP
GTP
c) Ribosome + Thiostrepton
Helix 43, 44
(23S rRNA)
(CTD)
L11
T
(NTD)
EF-G
GDP
GTP
d) Ribosome + Micrococcin
Helix 43, 44
(23S rRNA)
(CTD)
L11
M
(NTD)
L7
EF-G
GDP
GTP

Summary of research chapters

These research chapters provide the results of biological synthesis and characterization of micrococcin P2 and thiocillin IV.

Chapter 1 describes the efforts to engineer a pathway for biosynthesis in *Bacillus subtilis*. The thiocillin biosynthetic gene cluster, which initially produced eight substances, was reconstituted to produce only MP2. With biosynthesized MP2, antimicrobial and biological activities against pathogenic bacteria were investigated. Notably, MP2 showed *in vitro* anti-*C. difficile* activity and promising *in vivo* efficacy in mouse *C. difficile* infection model. Finally, the base hydrolysis products of MP2 could be exploited to establish a semi-synthesis platform for developing thiopeptide antibiotics.

Chapter 2 reports the structural elucidation and biological study of thiocillin IV. In order to biosynthesize thiocillin IV, candidate gene *tclO* was found and expressed with the MP2 biosynthetic genes. With the incorporation of precursor peptide genes and cultural optimization, production yield was raised to sufficient purification for structure characterization. The purified thiocillin IV structure was identified as O-methylated micrococcin P2 at the 8-Thr position. Thiocillin IV showed promising biological activity toward Gram-positive pathogens and became inactive in the presence of protein L11 N-terminus proline mutations.

Chapter 1. Biosynthesis of Micrococcin P2 and Biological Evaluation

Introduction

Since Su's first discovery of thiopeptides in 1948, approximately 80 members of this family have been identified (Su, 1948). In 1955, Fuller isolated an antibiotic from *Bacillus pumilus* sourced from East Africa soil samples (Abraham et al., 1956). They observed that the difference between these two substances was related to their optical rotation: $[\alpha]^{21}$ +116 for the Su micrococcin, $[\alpha]^{21}$ +62 for Fuller's. Fuller's micrococcin was later shown to be a 7:1 mixture of two compounds: micrococcin P1 (MP1) and micrococcin P2 (MP2) (Ciufolini and Lefranc, 2010). Structural determination of micrococcin P1 was conducted (Walker et al., 1977; Bycroft and Gowland 1978) and was ultimately established by total synthesis (Lefranc and Ciufolini, 2009). These results showed that MP2 structures were almost identical to MP1 structures, except that a terminal alcohol group was changed to a ketone group (Hwang et al., 2022).

Until recently, it was debated whether thiopeptide was synthesized ribosomally or nonribosomally (Arndt et al., 2009). Before 2009, when the thiocillin biosynthesis gene cluster was discovered in *Bacillus cereus* ATCC 14579, there was no sufficient evidence to support the hypothesis that thiopeptides are produced ribosomally (Morris et al., 2009). The pioneering efforts by Walsh to understand the biosynthesis of thiocillin have substantiated the notion that the well-coordinated action of enzymes can afford the synthesis

of thiopeptides via post-translational modifications (Brown et al., 2009) (Figure 5A).

Bioinformatic analysis of the *B. cereus* genome yielded a sequence encoding a 52-residue peptide composed of a leader peptide (38-residues) and a structural peptide (containing the Cys/Thr/Ser rich sequence H_2N-SCTTCVCTCSCCTT-CO_2H; 14-residues) (Bowers et al., 2010a). The translated linear precursor is modified by a series of tailoring enzymes (Liao et al., 2009). The precursor peptide (TclE) is translated that includes a structural portion comprised of 14 residues rich in serine, cysteine, and threonine at the C-terminus. This region contains the amino acids that will constitute the thiopeptide itself. This sequence is preceded by the 38 residues of the N-terminus leader peptide, which is cleaved during final biosynthesis.

Thiocillins were synthesized by a highly well-coordinated network of biosynthetic enzymes (Figure 5B). The elucidation of the comprehensive biosynthetic cluster in *Macrococcus caseolyticus str 115* provides insights into the underlying mechanisms of micrococcin P1 biosynthesis (Bewley et al., 2016). The structural peptide's core regions contain six cysteines that are transformed into thiazoles by TclI, TclJ, and TclN. TclI is an Ocin–ThiF-like protein containing a proposed RiPP precursor peptide recognition element (Schwalen et al., 2018). TclJ is a Thiazole/Oxazole-Modified Microcinfamily cyclodehydratase that converts core peptide cysteines to thiazolines and TclN, an FMN-binding McbC-type dehydrogenase, subsequently oxidizes thiazolines to thiazoles (Arnison et al., 2013).

Figure 5. Scheme of thiocillin synthesis by the *tcl* cluster of *Bacillus cereus* ATCC 14579

(A) The *tcl* gene cluster from *B. cereus* ATCC 14579 with predicted enzymatic functions. To biosynthesize thiopeptides, thiazole formation (Blue), dehydration (Red), decarboxylation (Green), and macrocyclization (Pink) reactions are required. Three other modifications by *tclD*, *tclS*, and *tclO* make structurally diverse thiocillin congeners by Val-6 hydroxylation, Thr-14 dehydrogenation, and Thr-8 O-methylation. (B) TclI/J are capable of recognizing core peptide cysteine residues to produce thiazoline. TclN oxidizes thiazoline to thiazole. To attach a dehydroalanine /dehydrobutyrine group corresponding to the dehydrated form of Ser/Thr, glutamylation by tRNAglu and glutamate-mediated eliminating reaction is required. During the biosynthesis of thiocillin, terminal Thr-14 residues of the core peptide also experience decarboxylation and macrocyclization via mediating enzymes related to the maturation of bioactive thiocillins. (C) Structure of eight thiocillin congeners. The *B. cereus tcl* gene cluster has the capability to synthesize a collection of eight structurally similar enzymatic products from precursor peptide (TclE).

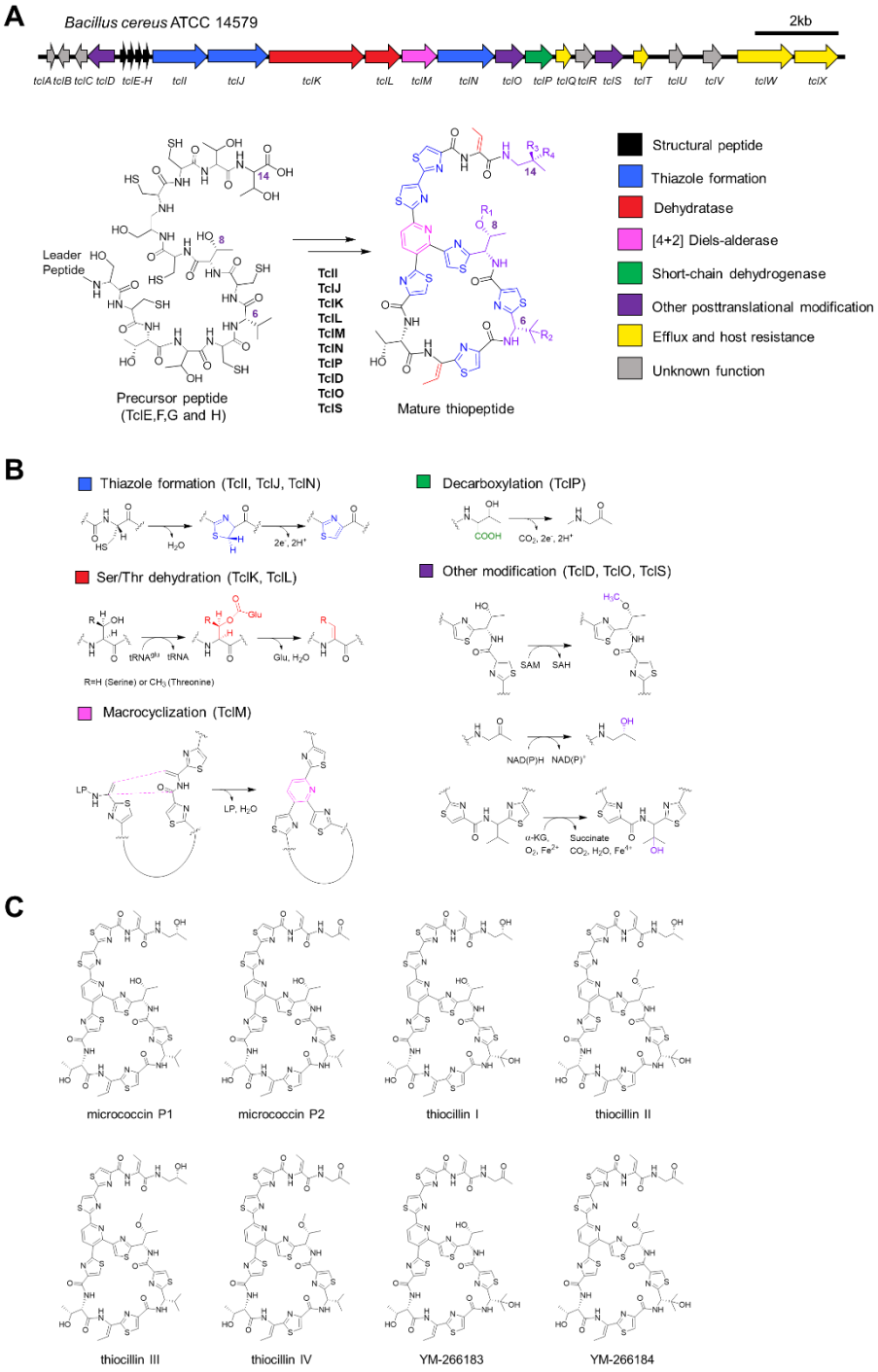
A
Bacillus cereus ATCC 14579
2kb
tclA tclB tclC tclD tclE-H tclI tclJ tclK tclL tclM tclN tclO tclP tclQ tclR tclS tclT tclU tclV tclW tclX
Leader Peptide
Precursor peptide (TclE,F,G and H)
TclI
TclJ
TclK
TclL
TclM
TclN
TclP
TclD
TclO
TclS
Mature thiopeptide
Structural peptide
Thiazole formation
Dehydratase
[4+2] Diels-alderase
Short-chain dehydrogenase
Other posttranslational modification
Efflux and host resistance
Unknown function
B
Thiazole formation (TclI, TclJ, TclN)
Decarboxylation (TclP)
Ser/Thr dehydration (TclK, TclL)
R=H (Serine) or CH3 (Threonine)
Other modification (TclD, TclO, TclS)
Macrocyclization (TclM)
C
micrococcin P1
micrococcin P2
thiocillin I
thiocillin II
thiocillin III
thiocillin IV
YM-266183
YM-266184

After its cysteines are converted into thiazoles, TclP-mediated decarboxylation of Thr-14 occurs, and this is required for the subsequent peptide reaction to progress via Ser/Thr dehydration (TclKL) (Ovchinnikov et al., 2021). TclK and TclL show homology to the N- and C-terminal domains of the known antibiotic Ser/Thr dehydratase NisB (Bewley et al., 2016). Dehydrating of core peptide Ser/Thr residues occurs via glutamylation (TclK) and is followed by elimination (TclL) dehydratases (Garg et al., 2013). Finally, a well-characterized protein TclM-mediated [4+2] Diels-alder reaction forms nitrogen-containing central pyridines (i.e., 6-membered) (Bower et al., 2010b). Simultaneously, leader peptides are released and marking the biosynthetic reaction ends. The other modification enzymes (i.e., TclD, TclO, TclS) contribute to the structural variety of thiocillins by hydroxylation, methylation, and reduction processes (Son et al., 2023). Notably, from the *tcl* gene cluster of *B. cereus* ATCC 14579, various compounds such as micrococin P1 and P2, thiocillin I-IV, and YM-266183/266184 have been identified using NMR and/or high-resolution mass spectra (Brown et al., 2009).

Several studies on the *tcl* gene cluster of *B. cereus* ATCC 14579 have explored final product variation through the investigation of structural gene variation, alanine scanning of core peptide residues, and site-directed mutagenesis of biosynthetic genes (Acker et al., 2009; Bowers et al., 2010a). Furthermore, *in vitro* synthesis of thiocillin-like compounds has been achieved by utilizing the macrocyclizing enzyme TclM in combination with synthesized core peptide fragments and leader peptides (Wever et al., 2015). The

biosynthetic gene cluster (*pbt*) of the 29-membered GE2270 compound from *Planobispora rosea* ATCC 53733 has been successfully expressed in the heterologous host strain *Streptomyces coelicolor* M1146 (Flinspach et al., 2014). Additionally, the biosynthesis of GE37468 from *Streptomyces* ATCC 55365 has been demonstrated in the model host *Streptomyces lividans* TK24 (Young TS and Walsh CT, 2011).

Among the *B. cereus* thiopeptide product, the biosynthesis of MP2 was predicted to require the fewest biosynthetic enzymes based on its molecular structure (Son et al., 2023). In this chapter, micrococcin P2 was exclusively synthesized by reconstitution of the *tcl* gene cluster in *Bacillus subtilis* 168. This gene cluster was able to be minimized to a considerably smaller size (i.e., from 24 to 8 genes) based on the predicted enzymatic functions. Biosynthesized product appears to have identical structural features compared to totally synthesized MP2. Moreover, the antimicrobial activity of MP2 was extensively investigated against serious human pathogens, including MRSA, VRE, *M. tuberculosis*, and *C. difficile*. MP2 is a promising *C. difficile* treatment option since it is noncytotoxic, shows an inhibitory effect of proinflammatory cytokine production, and is more effective in a dextran sodium sulfate (DSS)-induced mouse *C. difficile* infection model than some Food and Drug Administration (FDA)-approved drugs.

Materials and Methods

Plasmid construction for MP2 synthesis

For the expression of recombinant proteins in *Escherichia coli*, the coding sequence of selected *tcl* genes (*tclE, I, J, K, L, M, N, P*) was amplified from the genomic DNA of *B. cereus* ATCC 14579. The amplified genes were cloned into pET28a (Novagen; for fusing N-terminus His_6-tag), pGEX4T-1(GE Healthcare; for fusing N-terminus glutathione S-transferase (GST) tag), or pHMT-pET28a vector (for fusing N-terminus His_6-tag-maltose binding protein (MBP)-tev protease recognition site).

To construct a micrococcin P2 biosynthesis gene clusters in *B. subtilis* 168 strain, a pUC19 vector was altered by inserting xylose inducible promoter (xylR-P_{xylA}), *cat* (chloramphenicol acetyltransferase), and *amyE* (α-amylase) homologous sites. The *amyE*, xylR-P_{xylA} sequences were amplified from *B. subtilis* 168 genomic DNA, and the *cat* gene was obtained from pDG1661. In order to construct pANJ-165, the eight selected *tcl* genes (*tclE, I, J, K, L, M, N, P*) were amplified from *B. cereus* ATCC 14579 genomic DNA with appropriate primer pairs (listed in Table 2). The *tclE* gene was cloned in pET21a, then transferred to the expression vector for introducing the RBS sequence and C-terminus His_6-tag sequence. *Tcl* genes were amplified and cloned sequentially (*tclE-IJ-KL-MN-P*) using the gibson assembly cloning kit (NEB, Ipswich, MA, USA). Gibson assembly reaction mixture was transformed into chemically competent *E. coli* DH5α cells, and positive transformants were selected for on LB agar supplemented with 100 μg/mL ampicillin. Genomic DNA from *B.*

cereus ATCC 14579 and *B. subtilis* 168 was prepared using a Wizard® Genomic DNA Purification Kit (Promega, Madison, WI, USA). Target DNA amplification was conducted by Phusion High-Fidelity DNA Polymerase (Thermo Scientific, Waltham, MA, USA). Recombinant DNA was purified using QIAGEN mini prep kits according to the protocol provided (QIAGEN, Valencia, CA, USA) and sequences were confirmed through sequencing (Bionics, Daejeon, Republic of Korea). The sequences of oligonucleotides used for cloning are listed in Table 2.

B. subtilis **strain construction**

Before introducing the plasmid pANJ-165, *B. subtilis* 168 strain was exposed to four-times of MP2 (2 μg/mL) to induce spontaneous mutation that confers resistance to MP2. In MP2 resistant stain, the *rplK* gene (protein L11 encoding gene) was sequenced, and alternation in *rplK* gene (ΔP22) was associated with MP2 resistance. MP2-resistant strain with a single-codon deletion in the *rplK* gene was used for the MP2 biosynthesis experiment.

B. subtilis 168 transformations were conducted as described previously (Bennallack et al., 2016). Briefly, cells were grown on LB agar without antibiotics, then used to inoculate a 3 ml liquid culture of LB. Cells were grown overnight at 37°C, 200 rpm for 16 h. 0.33 ml of overnight culture was combined with 5 ml of warm, freshly prepared starvation medium 1 (SM1) and incubated at 37°C, 200 rpm for 4 h. Following incubation in SM1, an equal volume of pre-warmed starvation medium 2 (SM2) was added and cells were

further incubated for 2 h under the same conditions. After 1 h, cells are competent and ready for a transformation. pANJ-165 was added to competent *B. subtilis* and incubated for 1 h. Transformants were selected in LB-chloramphenicol (Chl; 10 μg/mL) agar. Following selection, colonies were screened in starch-containing LB-agar media with Lugol's solution, *B. subtilis* genomic DNA was purified, and PCR confirmed chromosomal gene integration.

Purification and analysis of MP2

MP2-producing starter cultures (3 mL) were grown in LB for 16 h at 37°C. Larger cultures (0.5 L of LB in 2 L culture flasks) were inoculated with 500 μL of starter culture and grown for 24 h at 37°C with shaking at 200 rpm. (LB supplemented with 1% xylose, 5 μg/mL Chl, and 10 μg/mL tryptophan). Cells were harvested by centrifugation (4,000 × *g*, 30 min), resuspended in 50 mL methanol, vortexed vigorously, and allowed to sit for at least 20 min. Sodium sulfate (15 g) was added to the methanolic extracts. The mixture was then filtered through Whatman filter paper (no. 1), and the methanol was removed by vacuum. The dried solid dissolved and extracted by ethyl acetate and removed on a rotary evaporator. The crude residue was then dissolved in 40 mL of 1:1 super solvent (3:1 isopropyl alcohol/chloroform mixture by volume): water. The biphasic solution was transferred to a 5 mL separatory funnel, extraction, and the organic layer was removed. The aqueous layer was extracted twice, and the combined organic solvents were dried with Na_2SO_4 and evaporated. MP2 was finally purified by preparative reversed-phase high-

performance liquid chromatography (RP-HPLC) on a Gilson 321-Kinetex 5 μm Biphenyl 100 Å column (Phenomenex, Torrance, CA, USA). 30–100% acetonitrile (ACN)-0.1% trifluoroacetic acid (TFA), 60 min gradient to obtain pure compounds. Biosynthesized MP2 was characterized by ultra-performance liquid chromatography-mass spectrometry (UPLC-MS; Waters, Milford, MA, USA) with an ACQUITY UPLC BEH C18 1.7 μm column (Waters, Milford, MA, USA), and ^{1}H and ^{13}C NMR.

In vitro MIC determination of bacteria

For these studies, test organisms consisted of reference strains from the American Type Culture Collection (ATCC; Manassas, VA, USA), and clinical isolates-were obtained from Professor Jin-Hwan Kwak lab, at Handong Global University in Republic of Korea. Details on the strains used in the MIC test are described in Table 4. *In vitro* susceptibility testing of organisms other than *C. difficile* was determined by the microtiter broth serial dilution method by the Clinical and Laboratory Standards Institute (CLSI) guidelines (Clinical and Laboratory Standards Institute, 2018). The MIC for *C. difficile* was determined by the agar dilution method according to CLSI guidelines. The antimicrobial agents (vancomycin, linezolid, and ciprofloxacin) were purchased from Sigma-Aldrich (St Louis, MO, USA) and used as the quality control agent. Each compound was tested in the concentration range prepared with a double series of dilutions in 32–0.06 μg/mL range. The medium employed for testing in the broth microdilution assay was cation-adjusted Mueller Hinton broth (CAMHB;

BD Difco, Sparks, MD, USA). A standardized inoculum was added to each 96-well microtiter plate (final 5×10^5 CFU in 0.1 mL) and incubated with serially diluted antibiotics at 37°C. After 18–24 h, the plates were inspected and the MIC was scored visually as the lowest concentration of antibiotic where no growth is apparent by visual inspection for turbidity.

C. difficile MIC test was performed using brucella agar (BD Difco, Sparks, MD, USA) supplemented with hemin (5 μg/mL), vitamin K1 (1 μg/L), and 5% sheep blood. Before the MIC test, the liquid Brain Heart Infusion (BHI) medium (BD Difco, Sparks, MD, USA) with yeast extract (BD Difco, Sparks, MD, USA) medium was placed in the anaerobic chamber (90% nitrogen, 5% hydrogen, 5% carbon dioxide; Coy Laboratory Products Inc., Grass Lake, MI, USA) to remove oxygen from the broth for a day. A day before the experiment, the bacteria were incubated in 4 ml of BHIS medium. Dilute the cultured bacteria using a BHIS medium to make it about 1×10^7 CFU/ml. The diluted cultures were dropped 10 μl each on a brucella agar plate containing antibiotics (10^5 CFU/spot), and the results were observed after incubating them in an anaerobic chamber for more than 18 h.

M. tuberculosis strain H37Rv was obtained from ATCC (ATCC 27294). Of the 15 clinical *M. tuberculosis* isolated strains were obtained from TB Specimen Biobank., Masan National Tuberculosis Hospital (MNTH; Masan, Republic of Korea). All the isolates were identified as *M. tuberculosis* using Acid-Fast Bacilli (AFB) stain and MTB immunochromatographic detection kit (SD Biosensor, Suwon, Republic of Korea). The drug susceptibility of *M. tuberculosis* strains was determined using the resazurin

microtiter assay (REMA) under aerobic conditions. The resazurin solution was prepared in 0.02% (w/v) solution in sterile distilled water using resazurin sodium salt powder (Sigma-Aldrich, St Louis, MO, USA) and filter sterilized. Bacteria from exponential-phase cultures were harvested and adjusted to an OD_{600} of 0.0001 in a 96-well microtiter plate. Two-fold serial dilutions of compounds were prepared from 10 μM to 10 nM micrococcin P2. Plates were then incubated at 37°C. After 7–12 days of incubation, 40 μL of 0.025% resazurin was added to the wells. Fluorescence was measured using a SpectraMax® M3 Multi-Mode Microplate Reader (Molecular Devices, Sunnyvale, CA, USA). Concentrations required to inhibit bacterial growth by 50% (IC_{50}) were determined by fitting the curves with a sigmoidal dose-response using GraphPad Prism software version 6.05 (GraphPad Software, Inc., San Diego, CA, USA).

Time-kill kinetics of micrococcin P2 against *C. difficile*

The time-kill studies were performed by the method of CLSI (CLSI, 1999). Test organisms were incubated in brain heart infusion (BHI; BD Difco, Sparks, MD, USA) broth with 0.5% yeast extract for 18 h at 37°C in an anaerobic chamber and diluted with fresh broth to approximately 10^5 CFU/mL. Vancomycin and MP2 were added to the cultures of 1/2, 1, 2, and 4 × the MIC. Samples were collected at 0, 3, 6, and 24 h afterinoculation, and serial 10-fold dilutions were performed. The number of viable cells was determined on BHI agar containing 5% defibrinated sheep blood after 24 h of incubation. The

plates were incubated at 37°C in an anaerobic chamber. Antimicrobials were considered bactericidal at the lowest concentration that reduced the original inoculum by 3 $\log_{10}$ CFU/mL at each of the periods and bacteriostatic if the inoculum was reduced by 0 to 3 $\log_{10}$ CFU/mL.

Cellular toxicity

Cytotoxicity was tested against the human cell lines SH-SH5Y and HEK293T using CCK-8 cell viability assay. Each cell line was grown in Dulbecco's Modified Eagles Medium (DMEM; Gibco, New York, NY, USA) supplemented with 1% penicillin/streptomycin (Gibco, New York, NY, USA) and 10% fetal bovine serum (FBS; Gibco, New York, NY, USA) at humidified incubator containing 5% CO_2 at 37°C. For a test, cells were plated at a density of 5000 cells/well in 100 µL of cell culture medium in a 96-well microplate. MP2 were treated in triplicate with 1.25 µM to 40 µM to the cells for 48 h at 37°C. Finally, 10 µL of the CCK-8 reagent (Dojindo, Rockville, MD, USA) was added into each well, and OD_{450} was measured using a microplate reader (Biotek, Vermont, VT, USA) after incubation for 2 h at 37°C. The cell viability was normalized to DMSO control.

ELISA assay of pro-inflammatory cytokines

Mouse monocyte-macrophage RAW 264.7 cells were maintained in RPMI-1640 medium (Gibco, New York, NY, USA) supplemented with 10% heat-inactivated FBS at 37°C in a humidified incubator with 5% CO_2. To investigate

the effect of MP2 on cytokine levels from LPS-treated cells. RAW 264.7 cells (2×10^5 cells/mL) seeded into 24-well plates were treated with 5, 10, 20, and 40 μg/mL of MP2 with 1 mg/L LPS. After 24 h, the concentrations of IL-6 and IL-1β in the RAW 264.7 cell culture supernatants were determined using an ELISA kit, according to the manufacturer's instructions (R&D Systems, Minneapolis, MN, USA).

Rat pharmacokinetic studies

Rat pharmacokinetic studies were conducted at DGMIF (Daegu-Gyeongbuk Medical Innovation Foundation). Sprague-Dawley rats (7–8-week-old; five males and females per group) were administrated either 10 mg/kg orally or 2 mg/kg intravenously of MP2, which was formulated with 2.5% DMSO, 47.5% Labrasol, 30%, polyethylene glycol 400, and 20% deionized water. Blood samples were collected via jugular vein at pre-dose and post-dose at 5, 15, and 30 min, 1, 2, 4, 6, and 8 h. Plasma was prepared and stored frozen at -80°C until bioanalysis. To each plasma sample, 20 μL was added 180 μL of ACN with the internal standard and was subsequently vortexed at 4°C for 5 min followed by centrifugation at 15,000 rpm for 5 min. The resulting supernatant was measured using liquid chromatography-tandem mass spectrometry (LC-MS/MS) by Triple Quad 5500 (Applied Biosystems, Foster City, CA, USA) with a lower limit of quantification (LLOQ) of 10 ng/mL.

Mouse CDI-IBD comorbidity infection model

All animal experiments were conducted by the ethical guidelines of the Ethics Review Committee for Animal Experimentation at Handong Global University (Republic of Korea, protocol #HGU-20211214-20). C57BL/6J male (4 weeks old male weighing 20 to 22 g, Daehan Bio Link Co., Ltd. Eumseong, Republic of Korea) 5 mice per group was used in *C. difficile* infection model. Mice were maintained in animal chambers kept at 23℃ ± 2℃ with 55% ± 20% relative humidity. 2.5% dextran sodium sulfate (DSS; MP biomedical, Irvine, CA, USA) was inoculated with drinking water for 5 days to cause colitis in mice. A single dose of clindamycin (20 mg/kg) was injected a day before *C. difficile* ribotype 027 challenge intraperitoneally.

C. difficile ribotype 027 was grown on a blood agar plate and incubated for two days at 37℃ in an anaerobic chamber and subcultured on 70:30 sporulation medium to facilitate the sporulation of *C. difficile* ribotype 027. Briefly, the sporulation medium consists of 70% SMC (Bacto peptone 90 g, protease peptone 5 g, NH_4SO_4 1 g, tris base 1.5 g, agar 15 g per liter) and 30% BHIS (BHI agar with 0.5% yeast extract) agar. For inoculation, bacterial colonies were suspended in 0.9% saline solution and further diluted with saline solutions to adjust OD_{600} = 1.0 at 1/10 of the original saline solutions. Groups of five male C57BL/6J mice were injected orally with a single 0.5 mL dose of the bacterial suspension. 30 mg/kg of each drug (vancomycin, fidaxomicin, micrococcin P2) was dissolved in a vehicle, and 0.25 mL was inoculated after 6 h of infection through oral gavage (every 24 h for 5 days).

Table 1. List of strains and plasmids used in this study.

Strains	Genotype or Description	Source
Escherichia coli		
DH5α	Host strain for cloning	Enzynomics
BL21(DE3)	Protein expression host	Enzynomics
Bacillus subtilis		
168	*trpC2*	ATCC 23857
168R	*trpC2 rplK*ΔP22	This study
AJ-002	*trpC2 rplK*ΔP22 *amyE::xylR-*P_{xylA}*-tclEEEEIJKLMNP cat*	This study
Bacillus cereus	Source of *tcl* genes. Thiocillins producer	ATCC 14579
Plasmids		
pET28a	Plasmid for protein expression	Novagen
pGEX4T-1	Plasmid for protein expression, GST source.	GE Healthcare
pMal-c2X	Source of MBP gene	NEB
pHMT-pET28a	Plasmid for protein expression	Lab stock
pDG1661	Source of *cat* genes	BGSC
pANJ-23	Kan^R, pET28a with *tclE*	This study
pANJ-26	Kan^R, pET28a with *tclI*	This study
pANJ-27	Kan^R, pET28a with *tclJ*	This study
pANJ-28	Kan^R, pET28a with *tclK*	This study
pANJ-29	Kan^R, pET28a with *tclL*	This study
pANJ-30	Kan^R, pET28a with *tclN*	This study
pANJ-31	Kan^R, pET28a with HMT-*tclM*	This study
pANJ-34	Kan^R, pET28a with *tclP*	This study
pANJ-36	Amp^R, pGEX 4T-1 with *tclI*	This study
pANJ-37	Amp^R, pGEX 4T-1 with *tclE*	This study
pANJ-38	Kan^R, pET28a with HMT-*tclI*	This study
pANJ-60	Amp^R, pGEX 4T-1 with *tclEIJKLMNP*	This study
pANJ-67	*xylR-*P_{xylA} for *amyE* integrative vector, *E. coli ori*, binary vector (Amp^R in *E. coli*, Chl^R in *B. subtilis)*	Hwang et al., 2022

pANJ-165	Derivative of pANJ-67; *xylR*-P_{xylA}-*tclEIJKLMNP*	Hwang et al., 2022
pANJ-194	Derivative of pANJ-67; *xylR*-P_{xylA}-*tclEEEEIJKLMNOP*	This study

Table 2. The sequences of oligonucleotides used in this study.

Primer	Sequence (5' to 3')
Oligonucleotides used in *E. coli* study	
TclE-F	GCGGATCCATGAGTGAAATTAAAAAAGCATTAAATAC
TclE-R	GGAATTCCTCGAGTTAAGTTGTACAACAACTGCATG
H_6-TclI-F	CCTGGTGCCGCGCGGCAGCCATATGGTAAATATACCTTTGAAAGATATAG
GST-TclI-F	CGCGGATCCATGGTAAATATACCTTTGAAAGATATAG
TclI-R	TCAGTGGTGGTGGTGGTGGTGCTCGAGCTAACTTTCTATTAATATTGCTCCAAC
TclJ-F	CCTGGTGCCGCGCGGCAGCCATATGAATAAGGAAGTCCTTATAATCAG
TclJ-R	TCAGTGGTGGTGGTGGTGGTGCTCGAGTTATGGGAAAGGATGAGGAGTTAC
TclK-F	CCTGGTGCCGCGCGGCAGCCATATGAAACCAATAAACTATGTACCAC
TclK-R	TCAGTGGTGGTGGTGGTGGTGCTCGAGTTAAAAAACCTCAACTAAAAATTCTACAC
TclL-F	CCTGGTGCCGCGCGGCAGCCATATGAACGAGAATAATTTTATATGGAAGG
TclL-R	TCAGTGGTGGTGGTGGTGGTGCTCGAGTCATCCCTTTCTACTCTTATACAATG
TclM-F	CCAATTCATATGGAGCAGTATCATAAAATTGTATTAACTGG
TclM-R	CCAATTCTCGAGTCAATATCTTTGTAAGTCTTCAACATTATTATC
TclN-F	CCTGGTGCCGCGCGGCAGCCATATGTTGAAGACTTACAAAGATATTGAAG
TclN-R	TCAGTGGTGGTGGTGGTGGTGCTCGAGTCATACATAAAATTGTTCTCCTTTAGTT
TclP-F	GCGGATCCATGAACTCTATCAAACAATTTAATTTT
TclP-R	GGAATTCTCGAGCTAGTGTAATGTATAACCACC
Oligonucleotides used in *B. subtilis* study	
amyE-F	GATTGTACTGAGAGTGCACCATATGTTTGCAAAACGATTCAAAACC
amyE-R	CCCGGGTACCGAGCTCGAATTCCGTATCATGCGACTCTACC
cat-F	CGACCTGCAGGCATGCAAGCTTGCACCCATTAGTTCAACAAAC
amyE-R	ATGACCATGATTACGCCAAGCTATCAATGGGGAAGAGAACCGC
xylR-F	ACGGAATTCGAGCTCGGTACCGAACTCCTTTTTCATATGAGAAGG
CRE-R	TTCTAGAGGATACCCGGGTACCTTAGTAAACCACTTTGTTTGCGCTTCC
TclE-F	GATATACATATGAGTGAAATTAAAAAAGCATTAAATAC
TclE-R	GGAATTCCTCGAGTTAAGTTGTACAACAACTGCATG
TclI-F	GTTTACTAAGGTACCCGGGATCCGTTTGTTCCCTTTATAGAAAGG

TclJ-R	TCAGTGGTGGTGGTGGTGGTGCTCGAGTTATGGGAAAGGATGAGGAGTTAC
TclK-F	TCCTCATCCTTTCCCATAACATTTTTTATGAAAGATGG
TclL-R	TCAGTGGTGGTGGTGGTGGTGCTCGAGTCATCCCTTTCTACTCTTATACAATG
TclM-F	ATAAGAGTAGAAAGGGATGACTTAAATGGAGCAGTATC
TclN-R	TCAGTGGTGGTGGTGGTGGTGCTCGAGTCATACATAAAATTGTTCTCCTTTAGTT
TclP-F	AAGGAGAACAATTTTATGTATGACGGAAAACGGGTGAATC
TclP-R	TCAGTGGTGGTGGTGGTGGTGTCGAGATCTAGTGTAATGTATAACCACC
Pxyl-F	GGAGGAAGCGGAAGAATGAAG (integration)
pUC-R1	GGTACCGAGCTCGAATTC (integration)
amyE-F	GGCTGCTTCCTAATGCAGG (integration)
pUC-R2	CGGTAAGTCCCGTCTAGCCT (integration)

* The recognition site of the restriction enzymes was underlined

Results

Thiocillin gene cluster analysis and plasmid construction

The recent total synthesis and structural characterization of MP2 prompted us to initiate biosynthesis (Hwang et al., 2022). In order to biosynthesize MP2 from *B. cereus tcl* genes, amino acid sequences of 24 *tcl* genes were analyzed to presume the function of enzymes (Table 3). Protein functions were assigned by blastp comparisons of their predicted protein products. Based on the proposed biosynthetic pathways for micrococcin P2 synthesis, structural peptides were first synthesized ribosomally as unmodified linear peptides and were then subjected to subsequent reactions to sequentially form thiazole from cysteine (i.e., via TclI, TclJ, and TclN). MP2 structural peptides then underwent C-terminus decarboxylation (via TclP), Ser/Thr elimination (via TclL and TclK), and lastly macrocyclization (via TclM) (Bewley et al., 2016). Finally, among the 24 *tcl* genes, eight biosynthetic genes (t*clE, I, J, K, L, M, N, P*) were selected to construct plasmids for micrococcin P2 synthesis.

Except for these selected biosynthetic genes, several other genes in the *tcl* gene cluster were excluded from the biosynthetic reconstruction due to their presumed unknown functions (*tclB, C, R, V*), transporter functions (*tclW, X*), and transcriptional regulation (*tclA, U*). TclQ and TclT are identical copies of the same gene in the *tcl* gene cluster. Both genes, homologs of 50S ribosomal protein L11 located near the ribosomal GTPase center, are known to be involved in the mechanism of action of MP1 (Porse et al., 1999; Agrawal et al.,

2001). Protein L11 translated from the *tcl* gene cluster may confer immunity by replacing native L11 to protect ribosomes from thiopeptide that this self-immunity-related gene planned to solve by spontaneous resistance. Precursor peptides were ribosomally synthesized from four copies of structural genes (*tclE, F, G, H*) which had highly similar gene encoding sequences except for some silent mutation that did not affect to amino acid sequence. Among them, the *tclE* gene was chosen for precursor peptide in MP2 biosynthesis. Other predicted biosynthesis genes (*tclD, O, S*) were rationally excluded for selective biosynthesis of MP2.

E. coli is widely regarded as the preferred prokaryotic system for successful heterologous gene expression (Kaur et al., 2018). Prior to biosynthesizing MP2 in *E. coli*, it was necessary to determine that the chosen enzymes could be expressed with sufficient protein stability and minimal cell toxicity. Separately, eight genes were cloned in the pET28a vector and expressed in *E. coli* BL21(DE3). The corresponding proteins (i.e., *tclE, I, J, K, L, M, N,* and *P*) could be purified as soluble proteins. Nevertheless, *tclI* gene, which may be involved in the first biosynthetic step of cysteine to thiazoline conversion, failed to be purified as soluble protein. Despite efforts such as codon optimization, low-temperature induction, and fusion with soluble tags (i.e., MBP and GST), the complete TclI protein sequence could not be obtained in a soluble form (data not shown). The results indicated that the TclI protein was not expressed in *E. coli*, so *B. subtilis* was chosen as the biosynthesis host. It is worth noting that *B. cereus* and *B. subtilis* belong to the same subgroup in

terms of classification, and they share similarities in codon bias, protein expression conditions, tRNA usage, and other physiological characteristics. These similarities suggest a high level of compatibility for the expression of *tcl* biosynthetic genes in *B. subtilis* (Miao et al., 2020).

To construct the pUC19 vector as an *E. coli-B. subtilis* binary vector system, the *B. subtilis amyE* homologous region (~1kb) was cloned on both ends of the construct, and the chloramphenicol resistance gene (*cat*) was used as a marker for *B. subtilis* selection. A xylose-inducible expression system was also developed to examine gene suppression, particularly for the toxic gene *tclI* (Bhavsar et al., 2001). Under this xylose regulating system, all genes involved in synthesizing thiocillins (i.e., *tclE, I, J, K, L, M, N,* and *P*) were successfully cloned one after another. The final plasmid contained micrococcin P2 biosynthetic genes and was designated as pANJ-165 and used in subsequent research (Figure 6).

Figure 6. Functional gene cluster analysis and reconstruction for micrococcin P2 synthesis.

(A) Scheme of the reconstructed plasmid pANJ-165. Genes were constructed using targeted homologous recombination sites (*amyE*) and a tight regulating system (i.e., a xylose inducible system). Thiazole formation-, Ser/Thr dehydration-, decarboxylation-, and macrocyclization-mediating enzymes were selected for biosynthesis (B) Predictive biosynthetic pathways for micrococcin P2. The 14-amino acid core peptide (TclE) undergoes post-translational modification and is transformed into the bioactive thiopeptide MP2.

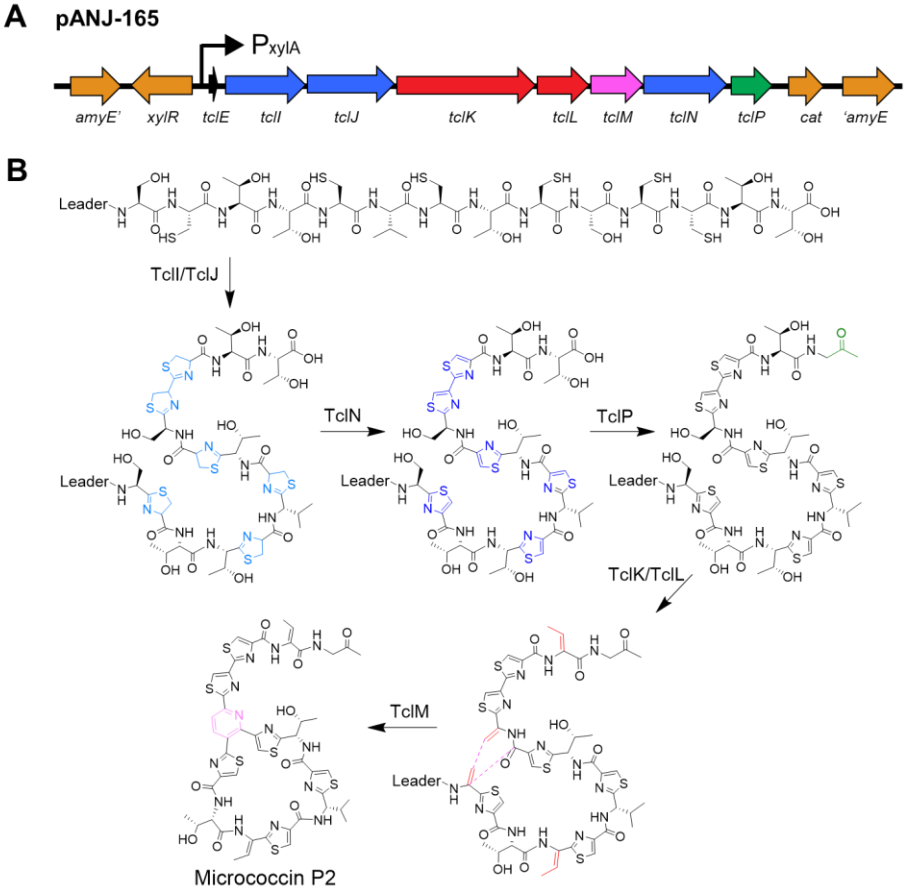
A
pANJ-165
PxylA
amyE'
xylR
tclE
tclI
tclJ
tclK
tclL
tclM
tclN
tclP
cat
'amyE
B
Leader
TclI/TclJ
TclN
TclP
TclK/TclL
TclM
Micrococcin P2

Table 3. Functional analysis of thiocillin gene cluster.

Gene	Product	Function
tclX	MFS transporter	Efflux
tclW	ABC transporter ATP-binding protein	Efflux
tclV	spermidine N1-acetyltransferase	Unknown
tclU	MerR family transcriptional regulator	Unknown
tclT	50S ribosomal protein L11	Host resistance
tclS	Short chain dehydrogenase	Reduction
tclR	hypothetical protein	Unknown
tclQ	50S ribosomal protein L11	Host resistance
tclP	Short chain dehydrogenase	Decarboxylation
tclO	class I SAM-dependent methyltransferase	Methylation
tclN	SagB/ThcOx family dehydrogenase	Thiazole formation
tclM	Cyclization	Macrocyclization
tclL	lantibiotic biosynthesis protein	Elimination
tclK	lanthionine biosynthesis protein	Elimination
tclJ	putative cytoplasmic protein	Thiazoline
tclI	putative lantibiotic biosynthesis protein	Thiazoline
tclH	thiocillin/thiostrepton family thiazolyl peptide	Structural gene
tclG	thiocillin/thiostrepton family thiazolyl peptide	Structural gene
tclF	thiocillin/thiostrepton family thiazolyl peptide	Structural gene
tclE	thiocillin/thiostrepton family thiazolyl peptide	Structural gene
tclD	phytanoyl-CoA dioxygenase family protein	Hydroxylation
tclC	glyoxalase/bleomycin resistance protein /dioxygenase superfamily protein	Unknown
tclB	xanthine permease	Unknown
tclA	Lrp/AsnC family transcriptional regulator	Unknown

Enzymatically synthesized micrococcin P2 comparable to an authentic standard

The plasmid pANJ-165 was transformed into the *B. subtilis* 168R strain to functionally identify the cloned gene cluster. The 168R strain has been designed to induce structural changes in ribosomal protein L11 (*rplK*) to confer protection from intracellularly emerging thiopeptides that might otherwise exert potent antibacterial action.

Transformants (AJ-002) were confirmed with antibiotic selection and cultured in xylose-containing media. Xylose-induced *B. subtilis* cell extracts were then analyzed using UPLC-MS, revealing that the inserted exogenous pANJ-165 formed a distinctive peak that differed from the untransformed control. This new emerging peak was detected at 350 nm, a key absorbance in the peak for thiopeptide. The purified material and the authentic standard showed the same retention time and mass in UPLC-MS, which suggested that the inducible constructs worked as intended (Figure 7A). Therefore, reorganized enzymes resulted in an exclusive production.

The identity of biosynthetic product was then further confirmed via RP-HPLC purification from *B. subtilis* extract. To increase the production yield, additional three copies of the *tclE* gene (precursor peptide encoding gene) were placed into the pANJ-165 plasmid to obtain pANJ-194. Compared with the NMR spectra of authentic MP2, only small differences are observed, mainly for exchangeable (i.e., OH and NH) protons. (Figure 7B and 7C).

Figure 7. Structural analysis of enzymatic micrococcin P2.

(A) UPLC-MS analysis of methanol extracted samples for pANJ-165 transformed *B. subtilis* and authentic standard of MP2. (B) ^{1}H-NMR Spectra of fermented (top) vs. synthetic MP2 (150 MHz, CD_3OD) small differences exist only at the level of exchangeable protons (OH and NH) (C) ^{13}C-NMR Spectra of fermented (top) vs. synthetic MP2 (150 MHz, CD_3OD).

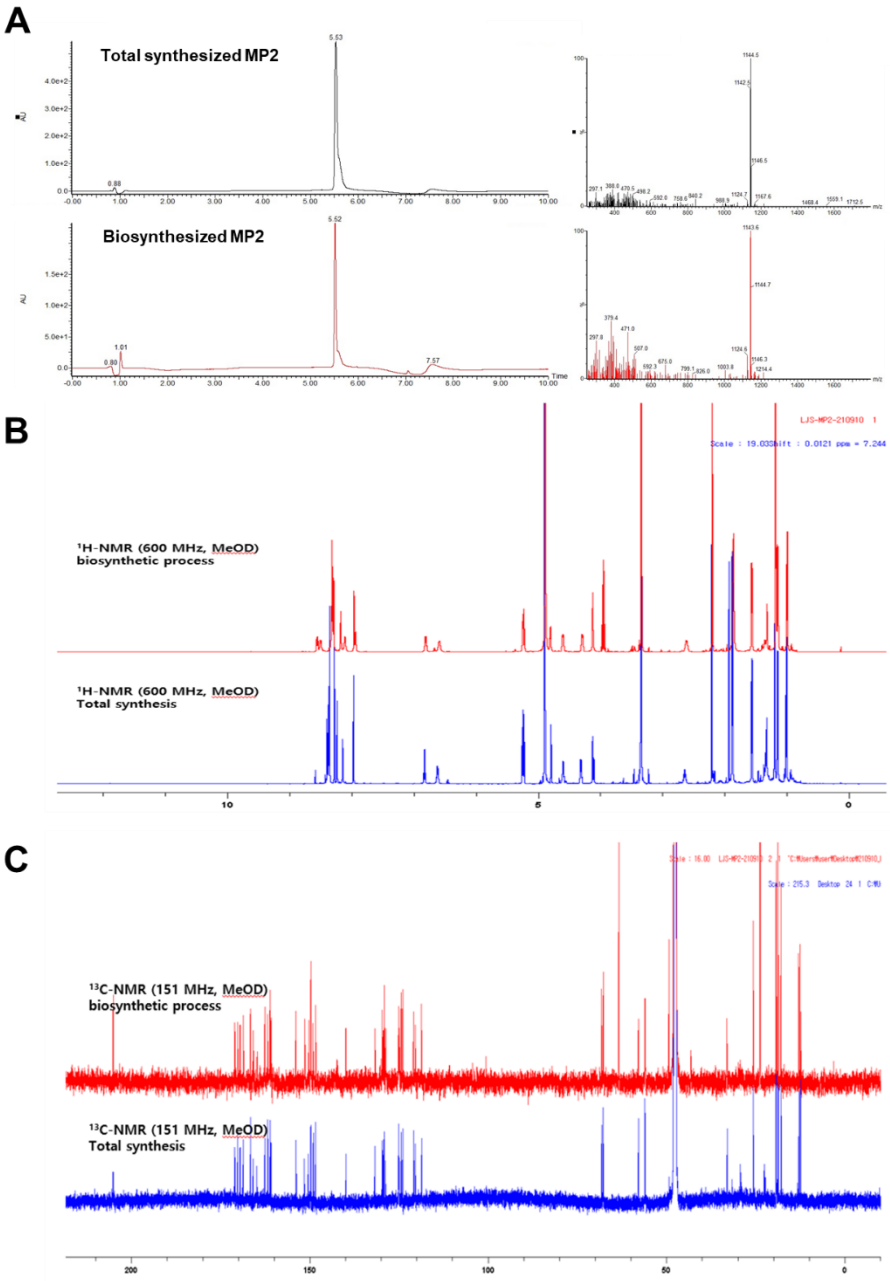
A
Total synthesized MP2
Biosynthesized MP2
B
¹H-NMR (600 MHz, MeOD)
biosynthetic process
¹H-NMR (600 MHz, MeOD)
Total synthesis
C
¹³C-NMR (151 MHz, MeOD)
biosynthetic process
¹³C-NMR (151 MHz, MeOD)
Total synthesis

***In vitro* antimicrobial activity of micrococcin P2**

Using LC-MS and NMR, the biosynthesized compound was identified as chemically identical to authentic MP2. However, since the bioactivity of MP2 has not yet been reported, its antimicrobial activity was confirmed determining minimal inhibitory concentration (MIC) of severely pathogenic bacteria. Wide range of pathogens were selected, including both Gram-positive and Gram-negative. These antibiotic-resistant pathogens cause nosocomial infections and are associated with increased rates of illness and death in the intensive care unit (Boyce, 2007).

Pure MP2 was found to possess antimicrobial activity comparable to vancomycin, but this was limited only to Gram-positive organisms (i.e., it was inactive against Gram-negative bacteria). MP2 also inhibited the growth of antibiotic-resistant clinical isolates (i.e., MRSA and VRE) with excellent MIC because MP2 offered a completely different mechanism of action to currently used antibiotics. The antimicrobial activities of biosynthetic and authentic MP2 were identical within experimental error (Table 4). MP2 showed comparable potency to vancomycin against *C. difficile,* an organism that is designated as an urgent threat by the CDC (Zhu et al., 2018).

Tuberculosis (TB) is caused by *M. tuberculosis* that most often affect the lungs (Zaman, 2010). In 2018, an estimated 10 million people fell ill with TB worldwide, and 1.5 million people died (including 214,000 people with HIV infection) (Gabrovska, 2022). TB is a major problem worldwide due to the spread of drug-resistant *M. tuberculosis* (Tacconelli et al., 2018). Previously,

MP1 exhibited potent activity against the H37Rv strain of *M. tuberculosis* (IC_{50} = 32 nM) by its novel mode of action (Degiacomi et al., 2016). Therefore, MP2 was tested against the H37Rv strains and clinical isolates of *M. tuberculosis*. Representative results are provided in Table 5. MP2 was active, even against XDR strains that were resistant to first- and second-line anti-tuberculosis agents.

Table 4. Comparison of the activity of synthetic and fermented MP2 vs other common antibiotics against various microorganisms (MICs, µg/ml).

Strain		Synthetic MP2	Fermented MP2	CIP	VAN	LIN
Gram-(+)	ATCC					
S. aureus	25923^{MS}	0.125	0.25	0.25	0.5	2
	29213^{MS}	0.125	0.125	0.5	0.5	1
	43300^{MR}	1	1	1	0.5	4
	CI^{VR}	1	1	>32	>32	8
S. epidermidis	12228	1	1	0.25	2	4
	CI^{MS}	0.125	0.25	>32	1	1
	Cl^{MR}	0.125	0.125	>32	0.5	1
E. faecalis	19433	0.25	0.25	1	1	2
	Cl^{VR}	0.125	0.25	>32	>32	2
	Cl^{LR}	0.125	0.25	32	1	>32
E. faecium	19434	0.5	0.5	8	0.5	4
	Cl^{VR}	1	1	32	>32	2
	Cl^{LR}	0.125	0.125	16	0.5	32
B. subtilis	6688	>32	>32	<0.06	0.25	4
C. difficile	9689	1	1		1	
Gram -(-)						
E. coli	25922	>32	>32	<0.06	>32	>32
K. pneumoniae	10031	>32	>32	<0.06	>32	32
P. aeruginosa	27853	>32	>32	0.5	>32	>32
A. baumannii	17904	>32	>32	0.25	>32	>32

Abbreviations: MS = methicillin susceptible; MR = methicillin resistant; CI = clinical isolates; MP2 = micrococcin P2; CIP = ciprofloxacin; VAN = vancomycin; LIN = linezolid; LR = linezolid resistant; VR = vancomycin resistant

Table 5. Activity of MP2 against to *M. tuberculosis* isolates.

Strain	Resistance	Reference	IC_{50}
H37Rv	SUS	INH^S, RIF^S, MXF^S, AMK^S	89 nM
704	SUS	INH^S, RIF^S, MXF^S, AMK^S	199 nM
1443	SUS	INH^S, RIF^S, MXF^S, AMK^S	356 nM
2577	SUS	INH^S, RIF^S, MXF^S, AMK^S	354 nM
2656	SUS	INH^S, RIF^S, MXF^S, AMK^S	208 nM
2318	MDR	INH^R, RIF^R, MXF^S, AMK^S	73 nM
2400	MDR	INH^R, RIF^R, MXF^S, AMK^S	169 nM
6393	MDR	INH^R, RIF^R, MXF^S, AMK^S	51 nM
5027	MDR	INH^R, RIF^R, MXF^S, AMK^R	2.3 uM
2180	MDR	INH^R, RIF^R, MXF^R, AMK^S	304 nM
4027	MDR	INH^R, RIF^R, MXF^R, AMK^S	44 nM
3836	XDR	INH^R, RIF^R, MXF^R, AMK^R	375 nM
4691	XDR	INH^R, RIF^R, MXF^R, AMK^R	94 nM
30	XDR	INH^R, RIF^R, MXF^R, AMK^R	114 nM
9845	XDR	INH^R, RIF^R, MXF^R, AMK^R	722 nM
8301	XDR	INH^R, RIF^R, MXF^R, AMK^R	209 nM

Abbreviations: SUS = susceptible; MDR = multi-drug resistant; XDR = extensively-drug resistant; INH = isoniazid; RIF = rifampicin; MXF = moxifloxacin; AMK = amikacin. *In vitro* activity evaluation against *M. tuberculosis* isolates was carried out in collaboration with Dr. Da-kyum Lee at the Masan National Tuberculosis Hospital in Republic of Korea.

MP2 shows a potent antimicrobial effect against *C. difficile*

C. difficile is a Gram-positive, spore-forming, toxin-producing, anaerobic species that representing a serious health threat (Zhu et al., 2018). Currently, only two antibiotics (i.e., vancomycin and fidaxomicin) are approved by the FDA for treating *C. difficile* infection (CDI) (Dai et al., 2022). This organism causes severe diarrhea with life-threatening complications, including toxic megacolon, pseudomembranous colitis, and systemic inflammatory response syndrome (Stelzmueller et al., 2007).

MP2 showed potent activity against the type strain of *C. difficile* ATCC 9689 (Table 4). Then, MP2 was screened against *C. difficile* clinical isolates collected by Professor Hyunjoo Pai at Hanyang Medical School in Republic of Korea from 2008 to 2018. These clinical isolates were selected for covering different multilocus sequence typing (MLST), PCR ribotyping, and the presence of genes encoding toxin A, toxin B, and binary toxin. MP2 was found to be active against all clinical isolates of *C. difficile*. Moreover, it showed an *in vitro* MIC value that was comparable to vancomycin (Table 6).

MIC results indicated that MP2 was effective in all the tested clinical isolates, so MP2 concentration and exposure time were varied and examined to determine how *C. difficile* inhibition differed. The comparative killing kinetics of MP2 and vancomycin were assessed against a hypervirulent *C. difficile* ribotype 027 strain. The ribotype 027 strain is responsible for a worldwide epidemic of nosocomial disease, significantly higher morbidity, and is related to severe complications associated with infection (Valiente et al., 2014). The

killing curves for MP2 and vancomycin showed different patterns (i.e., bacteriocidal and bacteriostatic, respectively. Therefore, these data show that MP2 kills *C. difficile* ribotype 027 more efficiently than vancomycin. A significant reduction in bacterial count (2.5–3.3 $\log_{10}$ units) was achieved at doses between 1 and 4 times the MIC value. A reduced bacterial count of only 1.5–2.0 $\log_{10}$ units was observed with the less efficacious vancomycin under identical conditions (Figure 8).

Figure 8. Time-kill assay of *C. difficile* ribotype 027.

Twenty-four hour time-kill curves for micrococcin P2 (A) and vancomycin (B) against *C. difficile* ribotype 027. MP2 exerts bactericidal action against *C. difficile* at 2× MIC, whereas vancomycin is bacteriostatic at all tested concentrations. CON = control (drug untreated), CFU = colony forming unit, LOD = limit of detection. The time-kill assay of *C. difficile* has been conducted in Professor Jin-Hwan Kwak lab, at Handong Global University in Republic of Korea.

A

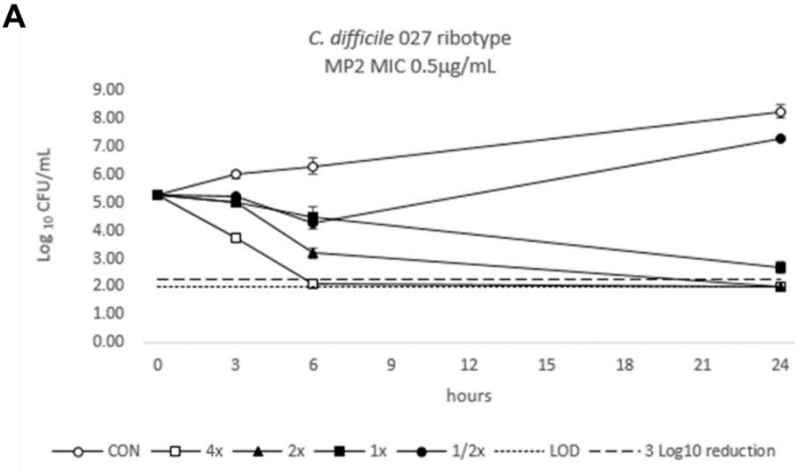
C. difficile 027 ribotype
MP2 MIC 0.5µg/mL
Log 10 CFU/mL
9.00
8.00
7.00
6.00
5.00
4.00
3.00
2.00
1.00
0.00
0
3
6
9
12
15
18
21
24
hours
CON
4x
2x
1x
1/2x
LOD
3 Log10 reduction

B

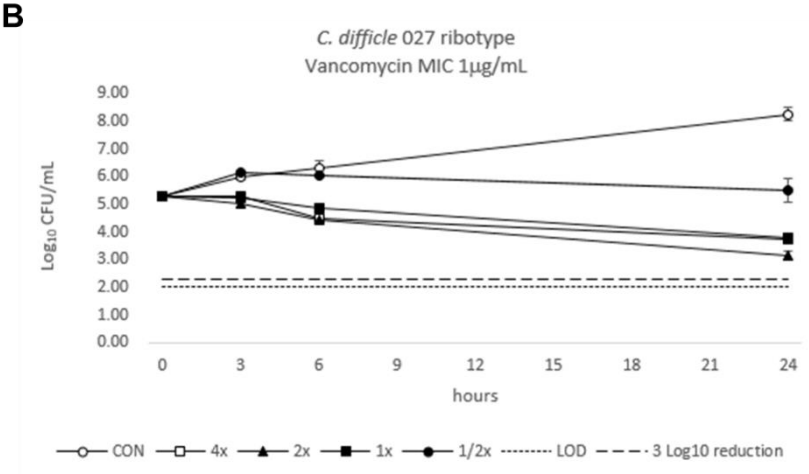
C. difficle 027 ribotype
Vancomycin MIC 1µg/mL
Log10 CFU/mL
9.00
8.00
7.00
6.00
5.00
4.00
3.00
2.00
1.00
0.00
0
3
6
9
12
15
18
21
24
hours
CON
4x
2x
1x
1/2x
LOD
3 Log10 reduction

Table 6. *In vitro* activity of MP2 against *C. difficile* clinical isolates.

Clade	Ribotype	Number	MLST	Toxin	MICs, µg/ml	
					VAN	micrococcin P2
1	RT018	10	ST17	A^+B^+	1	0.5
	RT001	4	ST3	A^+B^+	2	1
	RT002	4	ST8	A^+B^+	1	1
	RT012	3	ST54	A^+B^+	2	1
	RT014	3	ST14	A^+B^+	1	1
	RT015	3	ST35	A^+B^+	1	1
	RT293	2	ST129	A^+B^+	1	1
2	RT027	3	ST1	$A^+B^+CDT^+$	1	0.5
3	RT130	5	ST5	$A^+B^+CDT^+$	1	0.5
	nt	3	ST221	$A^+B^+CDT^+$	2	1
4	RT017	10	ST37	A^-B^+	1	0.5
5	RT078	3	ST11	$A^+B^+CDT^+$	1	1

Abbreviations: MLST = multilocus sequence typing; VAN = vancomycin; RT = ribotype; ST = sequence type; nt = nontypable; A = toxin A; B = toxin B; CDT = *C. difficile* binary toxin. *In vitro* MIC of *C. difficile* isolates has been conducted in Professor Hyunjoo Pai lab, at Hanyang University in Republic of Korea.

Micrococcin P2 is a noncytotoxic agent for the prevention of proinflammatory signaling

The severe pathogenesis of CDI is accompanied by an upregulation of cytokines, especially interleukins IL-1β, IL-6, and IL-8 (Czepiel et al., 2014). Interestingly, vancomycin upregulates IL-1β and IL-6, which correlate with CDI severity, while fidaxomicin reduces the production of IL-1β, thereby exerting a cytoprotective effect (Koon et al., 2018; Saleh et al., 2019). It has been suggested that IL-1β and IL-6 concentrations ~~are~~ positively correlated with *C. difficile* pathogenesis. Proinflammatory cytokines are induced by the treatment of lipopolysaccharide (LPS). However, a significantly diminished expression of IL-6 and IL-1β has been observed in mouse monocyte-macrophage RAW 264.7 cells treated with micrococcin P2. This finding suggests that MP2 possesses appreciable anti-inflammatory and noncytotoxic effects and potent antibiotic properties (Figure 9). These results clearly warrant further evaluation of MP2 and its derivatives for the treatment of *C. difficile* infection.

Figure 9. Cellular toxicity and inhibitory effect of cytokine production.

Cytotoxicity of micrococcin P2 on HEK293T cell (A) and SH-SY5Y cell (B). There is no appreciable toxicity even at 40 μM. Triton X-100 has been used as the negative control. (C, D) ELISA results of proinflammatory cytokine production in the presence of LPS by RAW cells: (C) IL-1b; (D) IL-6. Micrococcin P2 showed reduced cytokine levels than LPS-treated cells. Dexamethasone (Dex, 10 μM) is used as a control.

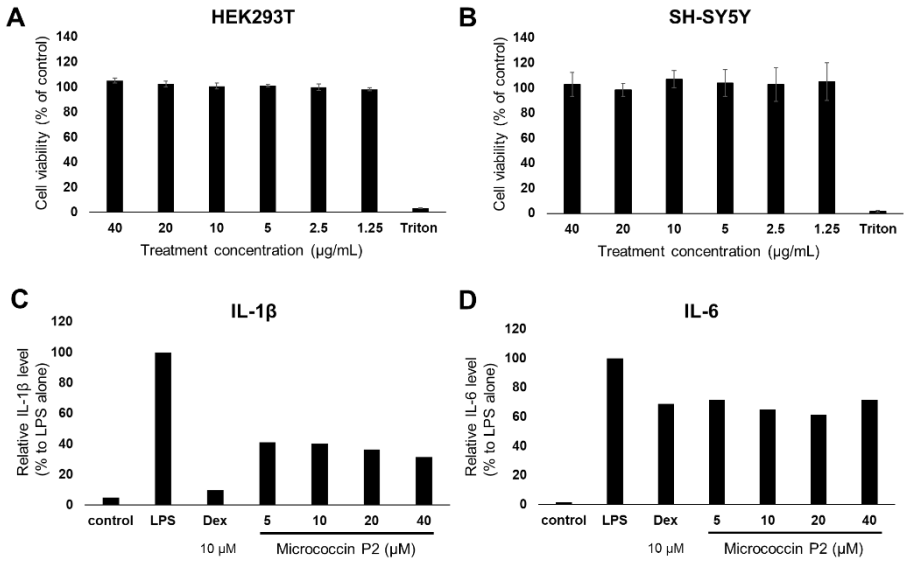
A
HEK293T
Cell viability (% of control)
140
120
100
80
60
40
20
0
40
20
10
5
2.5
1.25
Triton
Treatment concentration (μg/mL)
B
SH-SY5Y
Cell viability (% of control)
140
120
100
80
60
40
20
0
40
20
10
5
2.5
1.25
Triton
Treatment concentration (μg/mL)
C
IL-1β
Relative IL-1β level (% to LPS alone)
120
100
80
60
40
20
0
control
LPS
Dex
10 μM
5
10
20
40
Micrococcin P2 (μM)
D
IL-6
Relative IL-6 level (% to LPS alone)
120
100
80
60
40
20
0
control
LPS
Dex
10 μM
5
10
20
40
Micrococcin P2 (μM)

Micrococcin P2 shows ideal pharmacological properties

Since *C. difficile* targets primarily the lumen of the large intestine, a good CDI agent should possess very low bioavailability (LaMarche et al., 2012; Daniels LM and Kufel WD., 2018). Compounds with poor oral availability are desirable for *C. difficile* treatment since a high concentration of compound remains at the site of infection, resulting in low systemic exposure (Jarrad et al., 2015). Indeed, vancomycin, fidaxomicin, and most existing anti-CDI agents in the current pipeline are known to show poor bioavailability (Oka et al., 2021). Thus, to evaluate MP2 as a treatment option for CDI, pharmacokinetic studies of MP2 were conducted in SD rats. Oral administration of MP2 to rats resulted in blood plasma levels below the quantification limit (BQL – lower than 10 ng/mL; Table 7). Thus, the very low oral bioavailability of MP2 observed here suggests promising pharmacoproperties for an oral anti-CDI agent.

Table 7. Pharmacokinetic properties of micrococcin P2.

	Oral (10mg/kg)	Intravenous (2mg/kg)
$T_{1/2}$ (h)	BQL	0.8 ± 0.2
AUC_{last} (hr * ng/mL)	BQL	374.0 ± 97.7
Cl_observed (mL/min/kg)	BQL	88.9 ± 23.6
MRT_observed (hr)	BQL	0.4 ± 0.1
Vss_observed (L/kg)	BQL	2.1 ± 0.1

Abbreviations: $T_{1/2}$ = half-life; AUC = area under curve; Cl = clearance; MRT = mean retention time; Vss = volume of distribution at steady state; BQL = below quantification level.

In vivo efficacy assessed using a mouse CDI-IBD infection model

The mouse *C. difficile* infection model was adopted due to evaluate potent antibacterial activity and optimal pharmacokinetic characteristics of MP2. An established *in vivo* model, in which mice (C57BL/6J) are initially treated with DSS to induce acute Inflammatory Bowel Disease (IBD), then infected with *C. difficile* to induce CDI-IBD comorbidity (Zhou et al., 2018). These IBD-induced animals are highly susceptible to infection by *C. difficile*. Such a model is a good indicator of the therapeutic potential of MP2 for the treatment of CDI-IBD. Using this system, the efficacy of MP2, vancomycin, and fidaxomicin (i.e., the only FDA-approved drugs to treat *C. difficile* infection) were compared. In the case of *C. difficile*-infected mice, all vehicle-treated animals died by the end of day 3. However, 5/5 mice from the 30 mg/kg MP2 group survived until the end of day 14 (i.e., a survival rate of 100%), while for both the vancomycin- and fidaxomicin-treated groups, 4/5 mice survived until day 14 (i.e., both showed a survival rate of 80%) (Figure 10). Thus, in this CDI-IBD animal model, MP2 showed superior results relative to vancomycin and fidaxomicin, indicating that MP2 may be a promising option for curing *C. difficile* infections.

Figure 10. *In vivo* protection efficacy against *C. difficile* infection.

(A) Animal study design. Schematic representation of the timeline of *C. difficile* infection and treatment. (B) A representative experiment comparing micrococcin P2, vehicle alone, and FDA-approved drugs (i.e., vancomycin and fidaxomicin) at 30 mg/kg via oral gavage once daily. Animals were infected with *C. difficile* spores on day 0 of the study. Treatment was administered once daily from days 1 to 5. Animals were observed up to day 14. QD: *quaque die* (once per day), PO: *per os* (by mouth). *In vivo* efficacy of MP2 in *C. difficile* infection model has been conducted in Professor Jin-Hwan Kwak lab at Handong Global University in Republic of Korea.

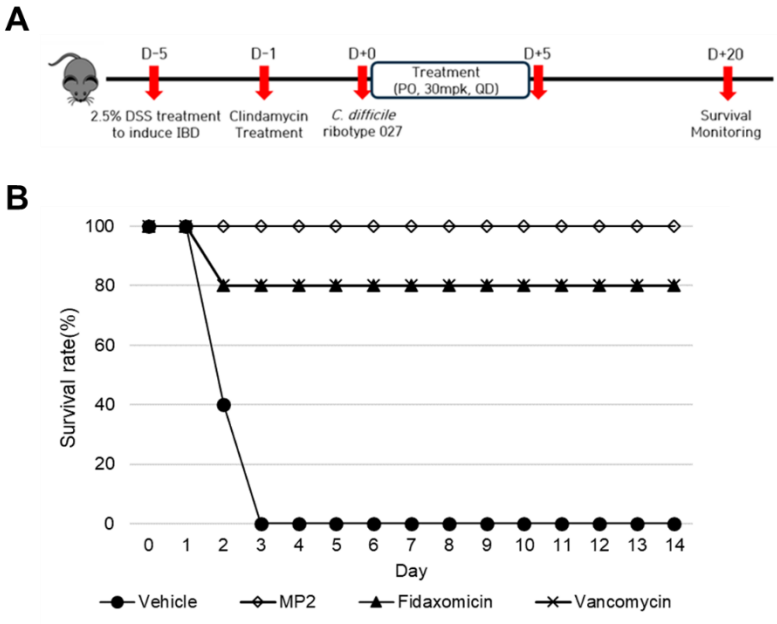
A
D-5
D-1
D+0
D+5
D+20
Treatment
(PO, 30mpk, QD)
2.5% DSS treatment
to induce IBD
Clindamycin
Treatment
C. difficile
ribotype 027
Survival
Monitoring
B
Survival rate(%)
100
80
60
40
20
0
0 1 2 3 4 5 6 7 8 9 10 11 12 13 14
Day
Vehicle
MP2
Fidaxomicin
Vancomycin

Discussion

Micrococcin P2 showed similar chemical properties to thiocillin structural congeners. Due to their similar chemical properties, MP2 was difficult to separate and obtain as a purified compound. To overcome this issue, in this chapter, MP2 was biosynthesized as a single product from the rationally clustered *B. cereus* ATCC 14579 *tcl* gene clusters. This is the first report of MP2 synthesis using eight genes from the *tcl* cluster of *B. cereus* ATCC 14579. In the next step, purified MP2 was used to characterize its structural properties as well as to evaluate its biological activity against key pathogens.

Strategic biosynthesis of micrococcin P2

In *B. cereus* ATCC 14579, eight structurally similar thiocillin compounds can be synthesized from *tcl* clusters, and five compounds were commonly produced in the host (Brown et al., 2009). By excluding putative post-translational modification enzymes such as valine hydroxylase (*tclD*), O-methyltransferase (*tclO*), and oxidoreductase (*tclS*) in the *tcl* clusters, selective synthesis of MP2 was achieved. Therefore, establishing a biosynthetic expression system in *B. subtilis* offers several advantages over the original host, *B. cereus*.

First, there are advantages to biosafety and engineering. *B. cereus* strains can cause food poisoning and are difficult to genetically manipulate (Ehling-Schulz et al., 2019). *B. subtilis* 168 strain is a model laboratory Gram-positive bacterium that is easy to transform and can be engineered using simple

transformation protocols (Harwood et al., 2013). *B. subtilis* has also been widely used to produce heterologous proteins to permit the study of protein function in a well-characterized system, and this can be more easily manipulated than the native host organism (Cui et al., 2018).

B. subtilis is also commonly used as an industrial cell factory to produce vitamins, inositol, acetoin, hyaluronan, and many other chemicals (Tang et al., 2023). Heterologous synthesis in *B. subtilis* offers a flexible and efficient method for producing and studying proteins that can be used in various applications. *B. subtilis* can apply to large-scale production of a target protein for research or commercial applications (Khadye VS et al., 2021).

Moreover, *B. subtilis* is a Gram-positive model organism in which it is feasible to apply accumulated experimental data to optimize the expression system, including strong promoters and other genetic modifications (Xiang et al., 2020). Furthermore, excellent expression systems with good genetic stability are available for this organism, and it has no strong codon preference (Su et al., 2020). Finally, *B. subtilis* species is Generally Regarded as Safe, which is highly desirable from a regulatory standpoint (Guan et al., 2015).

Micrococcin P2 shows novel antibiotic properties

Thiopeptides exhibit antibacterial effects, especially against Gram-positive (Just-Baringo et al., 2014). Purified MP2 showed potent antibacterial inhibitory effects against the Gram-positive pathogens, *M. tuberculosis*, and *C. difficile*, but was not active against Gram-negative pathogens. MP2 exhibited similar antibacterial activities between clinical isolates and susceptible strains. The

potent antibacterial effect and absence of cross-resistance are powerful strengths of MP2 as a candidate antibiotic.

Along with its potent antibacterial activity, MP2 also possesses other essential characteristics for developing CDI drugs. Usually, orally administrated drugs are absorbed into the body and show their biological effects based on their mode of action. However, in the case of antibiotics for *C. difficile*, it is critical that administrated drugs were not absorbed and delivered to the infected site (i.e., the large intestine) to expose the pathogen to high drug concentration. Pharmacokinetic studies revealed that MP2 possesses very low oral bioavailability, which is ideal for the development of orally administrated anti-CDI agents and is therefore an ideal characteristic for its intended use as an oral non-absorbed treatment for *C. difficile* infection.

MP2 has antibiotic properties, immune control properties, and offers an optimal administration path for the treatment *C. difficile* infection. Chemical optimization based on MP2 structure can be an effective privileged scaffold for developing new antibiotics. These results warrant further evaluation of MP2 and its derivatives for the treatment of *C. difficile* infection.

Micrococcin P2 as an intermediate of a semisynthetic procedure

Recently, Novartis tried to engage in phase 2 clinical trials of *C. difficile* infection using a compound called LFF571, derived from the 29-member thiopeptide GE2270A (Leeds, 2016). GE2270A showed great potency against Gram-positive bacteria, including *C. difficile*, but its poor aqueous solubility hindered development as antibiotics was hindered by its poor aqueous solubility

(LaMarche et al., 2011). To find related candidate compounds to be used against *C. difficile* infection, Novartis tried to establish semi-synthesis methods to exploit the chemical architectures of GE2270A and improve aqueous solubility without reducing antibacterial potency (Figure 11). Antibiotic semi-synthesis is the process of modifying natural antibiotics to improve their efficacy or chemical properties (Wright et al., 2014). By combining medicinal chemistry and semi-synthesis methods, the poor aqueous solubility of GE2270A was overcome (LaMarche et al., 2012). LFF571's featured properties included increased solubility and low absorption into the body. These properties enabled Novartis to engage in preclinical and clinical trials via a semi-synthesis from natural products strategy (LaMarche et al., 2011; Mullane et al., 2015).

This strategy also could be applied to 26-membered thiopeptides. Many researchers have tried to develop antibacterial agents based on the thiopeptide structure (Naidu et al., 2004; Myers et al., 2010; Fan et al., 2021). Nevertheless, poor aqueous solubility, bioavailability, and complex molecular structures have prevented medicinal chemists from improving their chemical properties (Ovchinnikov et al., 2021). MP1 was degraded in acidic and basic conditions, but hydrolyzed products could not be served as core intermediates for semi-synthesis (Ciufolini and Lefranc, 2010). MP1 proved to be relatively resistant to base hydrolysis and gave rise to an intractable mixture of unreacted MP1 and a multitude of products (Hwang et al., 2022).

Figure 11. Structural optimization of LFF571 with enhanced solubility.

Using a semi-synthesis approach, a natural product is modified via chemical reactions to produce a new compound with improved properties. Conversion of GE2270A to the more water-soluble clinical candidate LFF571 offers a promising route for the commercialization of this important class of ribosome-binding antibiotics. Medicinal chemistry experiments mainly focused on enhancing aqueous solubility and antibacterial effects. Novartis conducted a phase 2 trial with LFF571 to treat *C. difficile* infection. LFF 571 was non-inferior to vancomycin as a cure in a phase II trial, but its development was discontinued (Mullane et al., 2015).

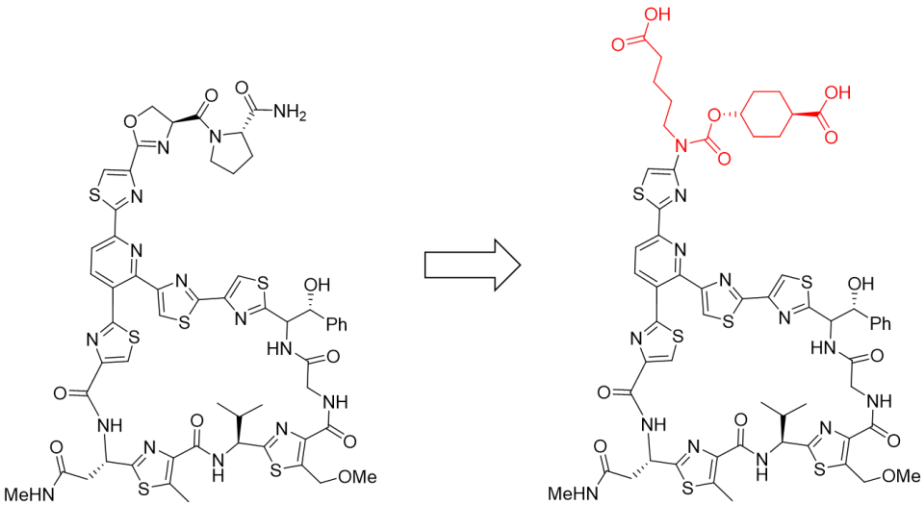

GE2270A

H_2O Solubility = < 0.001 mg/mL
MIC *C. diff* = 0.015 mg/mL

LFF571

H_2O Solubility = 12 mg/mL
MIC *C. diff* = 0.03 mg/mL

MP2 has almost the same structural characteristic as MP1 without a terminal alcohol to ketone group. This minor structural difference does not affect its antimicrobial spectrum and/or antimicrobial activity. Under the basic conditions, MP2 was rapidly and cleanly converted into the desired product micrococcin P acid (compound 1.2 in Figure 12A), isolated in its pure form and with a 74% yield (Figure S1 and S2). It is speculated that base treatment promotes the equilibration of MP2 with a hemiamidal, which probably exists as an intramolecularly hydrogen-bonded structure (compound 1.3 in Figure 12B). Such an equilibration is impossible for MP1, which displays secondary alcohol on its side chain. The hydrogen bond in compound 1.3 is likely to activate the C=O group toward the nucleophilic addition of a hydroxide ion. The resulting tetrahedral intermediate (compound 1.4 in Figure 12B) incorporates an N atom (starred) of significantly lower basicity than an ordinary 2-piperazinone, which is in turn considerably less basic than a typical amine (Ishida et al., 1967; Ledneczki et al., 2017; Wang et al., 2006). The starred N functions as a considerably better leaving group, ultimately departing as compound 1.5 and unveiling compound 1.2. The latter presumably is rapidly deprotonated under basic conditions, but the corresponding lithium carboxylate is returned to a carboxylic acid state upon gentle acidic workup (Hwang et al., 2022).

For several reasons, MP2 is an ideal natural product for exploring the medicinal chemistry of thiopeptides: its mechanism of action has been well addressed, produced by a variety of bacterial species, molecular structure is relatively simple compared to other thiopeptides, and it retains the attractive

biochemical properties (potency, stability, *etc.*) of this chemical family. The last noteworthy point is the ability to convert into MP acid, thereby conserving a structurally feasible pharmacophore. Site-selective hydrolysis of MP2 is an important feature for establishing semi-synthesis platforms. MP acid could be supplied as the crucial intermediate~~s~~ for the clinically interesting analog~~ue~~s of the natural product (Traux and Romo, 2020). Large-scale production of drug candidates is an undoubtedly important part of passing the death-valley in drug development (Eastgate et al., 2017). Such semi-synthetic routes thus greatly simplify the rigorous Chemistry, Manufacturing & Control (CMC) issues associated with a drug candidate's advancement to the clinical stage (DiFeo, 2003). Future works should focus on supplying the core intermediate MP acid. These efforts highly support a journey to the development of first-in-class of 26-membered thiopeptides.

Figure 12. Mechanistic hypothesis of the highly chemoselective hydrolysis of MP2.

(A) Chemoselective hydrolysis of MP2. The hydrolyzed carboxylic acid may be used as a core intermediate of a semi-synthesis process. When using hydrolyzed carboxylic acid as a starting material, MP2 derivatives can be synthesized by amide coupling. (B) Mechanistic hypothesis for the difference in hydrolytic behavior between MP2 and MP1. The structural difference between MP1 and MP2 induced the formation of a six-membered tetrahedral intermediate and led to OH- mediated hydrolysis. compound 1.1: micrococcin P2, compound 1.2: micrococcin P acid, compound 1.3: intermediate 1, compound 1.4: intermediate 2, compound 1.5: hydrolyzed fragment. Reagent and conditions (a) $LiOH.H_2O$, THF/H_2O (1:1), 50℃, 16 h, 74%. Dr. Hee-Jong Hwang conducted the chemoselective hydrolysis of MP2 in A&J Science Co., Ltd. in Republic of Korea.

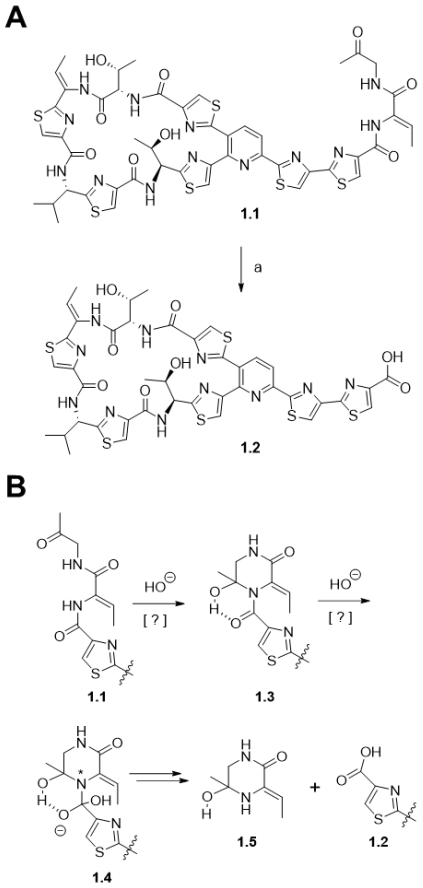
A
1.1
a
1.2
B
1.1
[?]
1.3
[?]
1.4
1.5
1.2

Chapter 2. Biosynthesis and Characterization of Thiocillin IV

Introduction

Thiopeptide gene clusters contain a structural gene (an unmodified polypeptide) that consists of an N-terminal leader peptide followed by a sequence rich in cysteine, threonine, and serine, which makes up the fundamental backbone of the thiopeptide (Haft et al., 2010). Several genes encoding cyclodehydratases and dehydrogenases are responsible for catalyzing the cyclization and subsequent oxidation of cysteine to thiazoles, and the synthesis of dehydrated amino acids, which conformationally restricts molecules (Dunbar et al., 2017). Furthermore, macrocyclization enzymes are speculated to promote the [4+2] heterocyclization that forms the core nitrogen-containing 6-membered ring (Yang and Van Der Donk, 2013).

The thiocillin biosynthetic gene cluster (i.e., *tcl* gene cluster) in *B. cereus* ATCC 14579 consists of 24 genes (Figure 13A) that deliver eight structurally different analogs of thiocillin via permutations in only three specific regions: Val-6 or C-hydroxylated Val-6 (R^2), Thr-8 or O-methylated Thr-8 (R^1), and the carbonyl or its reduced form of aminoacetone of Thr-14 (R^3) (R^1–R^3 are depicted in Figure 13B) (Bowers et al., 2010a). Other modified thiocillins have been synthesized with non-essential biosynthetic enzymes (Figure 13C). In addition to the genes involved in synthesizing micrococcin P2 (i.e., essential biosynthetic genes), notable candidate genes that present in the *tcl* cluster contributed to the thiopeptide modifications. TclD functionally annotated the SnoK-like protein and is predicted to add a hydroxyl group

selectively at Val-6 (Acker et al., 2009). TclS is predicted to be a short-chain dehydrogenase and is responsible for converting a terminal ketone group to alcohol (i.e., MP2 to MP1 conversion) (Bewley et al., 2016). TclO is anticipated to be an 8-threonine methylating enzyme since this protein shares a similar domain structure to other such enzymes, including its SAM-binding domain and its catalytic methyltransferase domain (Brown et al., 2009). The three enzymes mentioned above are not essential for building the 26-membered thiopeptide skeletons but work to modify existing structures (Son et al., 2022).

B. cereus ATCC 14579 mainly produced Val-6 hydroxylated metabolite thiocillin I (compound 2.3), thiocillin II (compound 2.4), YM266183 (compound 2.7), and YM266184 (compound 2.8) (Brown et al., 2009). When its putative nonheme iron-dependent dioxygenase gene (*tclD*) was removed, C-hydroxylation at Val-6 did not take place, and thiocillin IV was produced in very small amounts along with other non-hydroxylated thiocillin analogs (Brown et al., 2009). Available LC/MS data suggest that thiocillin IV may have Val-6, an amino-ketone group in the Thr-14 region, and an O-methyl group in Thr-8 (Brown et al., 2009). Because only small amounts of thiocillin IV have been synthesized, its structure has not been accurately identified and the prediction that the hydroxyl group is transformed into an O-methyl group at the Thr-8 site of MP2 is based solely on mass spectrometry data (Figure 13C).

This chapter reports the biosynthesis of thiocillin IV, the identification of key enzymes responsible for its O-methylation, structural characterization by NMR, and biological evaluations of thiocillin IV. To produce thiocillin IV, the *tclO* gene responsible for O-methylation was co-expressed with

micrococcin P2 biosynthesis enzymes in a *Bacillus* system. Purified thiocillin IV was structurally elucidated by LC-MS and NMR analyses. Furthermore, the antimicrobial activity of thiocillin IV was assessed. Finally, a mutational study confirmed that its antibiotic effects were exhibited through the same mechanism of action as MP2.

Figure 13. Schematic representation of thiocillin biosynthesis in *Bacillus cereus* ATCC 14579.

(A) 22 kb gene cluster contains 24 genes responsible for thiopeptide production. (B) The 52-aa precursor peptide (TclE, F, G, or H) undergoes 13 post-translational modifications to produce eight different thiocillin compounds. Eight post-translationally processed thiocillin compounds are classified by the variation of the R groups (violet colors: R^1, R^2, and R^3). The peptide residues are numbered, starting with the first residue after the leader peptide. (C) Structural congeners of micrococcin P2. All of extracted thiopeptides were posttranslationally modified structures comparing to MP2. Micrococcin P1 was dehydrogenated at Thr-14, thiocillin IV was O-methylated at Thr-8, and YM-266183 was hydroxylated at Val-6 rather than MP2. Colored areas indicate at green = Thr-8, blue = Val-6, Orange = Thr-14 in core peptide. The figure was adapted from a Son et al., 2023.

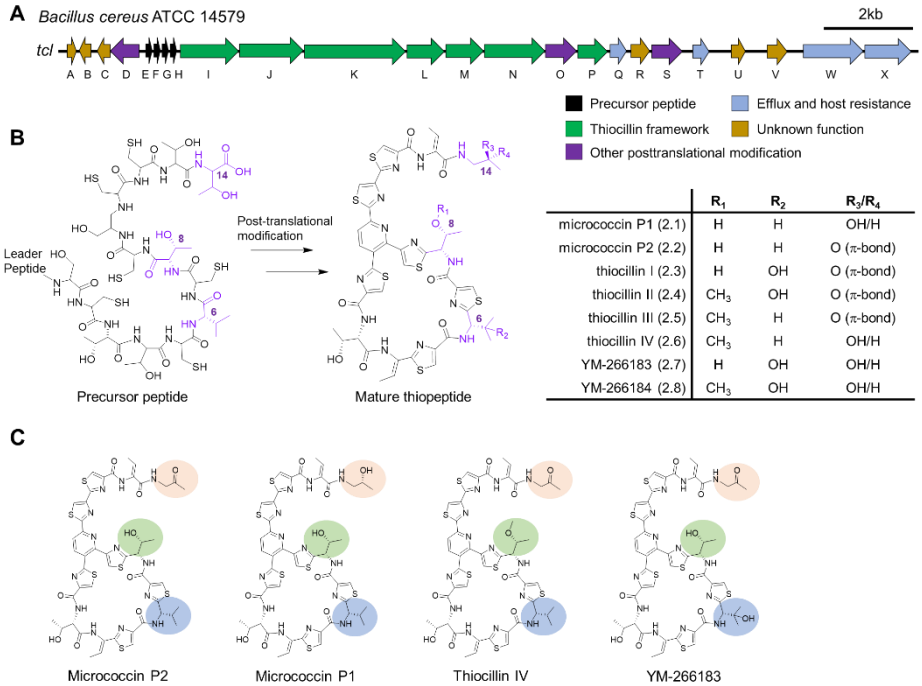

	R_1	R_2	R_3/R_4
micrococcin P1 (2.1)	H	H	OH/H
micrococcin P2 (2.2)	H	H	O (π-bond)
thiocillin I (2.3)	H	OH	O (π-bond)
thiocillin II (2.4)	CH_3	OH	O (π-bond)
thiocillin III (2.5)	CH_3	H	O (π-bond)
thiocillin IV (2.6)	CH_3	H	OH/H
YM-266183 (2.7)	H	OH	OH/H
YM-266184 (2.8)	CH_3	OH	OH/H

Materials and Methods

Chemical analysis

^{1}H, ^{13}C, and 2D NMR (HMBC, HSQC, and COSY, respectively) spectra were measured using a Bruker Avance III 600 MHz or 400 MHz spectrometer. The solvent signals were used as references, and the chemical shifts were converted to the TMS scale ($CDCl_3$: δ_C = 77.0 ppm; residual $CHCl_3$ in $CDCl_3$: δ_H = 7.26 ppm). High-resolution mass spectra (HR-MS) were obtained using a Thermo Scientific LTQ Orbitrap XL mass spectrometer in the positive ion mode with an electrospray ionization (ESI) source. Sample analysis and thiocillin IV quantifications were conducted using UPLC-MS. The gradient conditions were 30% to 95% ACN containing 0.1% TFA for 8 min at a flow rate of 0.3 mL/min. A UPLC-MS calibration curve was prepared using authentic micrococcin P2 as an external standard (Hwang et al., 2022). The extracts obtained from the thiocillin IV-producing *B. subtilis* cultures were analyzed against the calibration curve. Samples and MP2 standard peak areas were analyzed at 350 nm to quantify experimental production. All reported titers represent at least three independent experiments.

Generation of plasmids and strains

The plasmids and strains used in this study are listed in Table 8 and 9, respectively. pANJ-165, which harbors micrococcin P2 biosynthetic genes, was used as starting material. The *tclO* gene was amplified from *B. cereus* ATCC 14579 genomic DNA using appropriate primer pairs and was cloned into the

recombinant plasmid pANJ-199. Genomic DNA from *B. cereus* ATCC 14579 was prepared using a Wizard® Genomic DNA Purification Kit (Promega, Madison, WI, USA). To generate pANJ-229, three additional copies of the *tclE* gene were cloned sequentially into pANJ-199 vectors. The pANJ-253 plasmid was generated by removing the *xylR*-P_{xylA}-CRE-*tclE* region and reinserting *xylR*-P_{xylA}. pANJ-254 was constructed for integrating the *thrC* (i.e., the threonine synthase) locus of *B. subtilis* genomic DNA using a selection marker for the *spc* gene (i.e., the spectinomycin 9-adenylyltransferase) from pDG1661. pANJ-255, generated from pANJ-254, contained the *xylR*-P_{xylA}-CRE-*tclEEEE* construct and was used to confirm the expression of *tcl* genes. For pANJ-277, an N-terminus His_6-tag sequence was amplified from pET28a and a pANJ-278 His_6-tag sequence was introduced using synthesized DNA oligos. pANJ-280 and 281 were generated from pANJ-199. *B. subtilis* 168R was transformed into recombinant plasmids using a two-step protocol. Transformants were selected on LB plates containing 5 μg/ml of Chl. Following selection, colonies were screened in 1% starch-LB-agar with Lugol's solution, and chromosomal gene integration was confirmed by genomic DNA PCR. *E. coli* DH5α was used as a cloning host. Ligation and Gibson assembly were used for plasmid construction. All molecular biology-related enzymes and kits were purchased from Thermo Scientific (Waltham, MA, USA). Primer synthesis and sequencing services were performed by Bionics (Daejeon, Republic of Korea).

Extraction of thiocillin compounds

B. cereus ATCC 14579 and AJ-004 starter cultures (3 mL) were grown in LB medium for 20 h at 37°C. Larger cultures (100 mL LB in 500 mL flasks) were inoculated with 500 µL of starter culture and grown for 48 h at 37°C with shaking at 200 rpm. AJ-004 strain was grown in a medium supplemented with 0.5% xylose (TCI, Tokyo, Japan) and 5 µg/mL Chl. Cultures were harvested at 5,000 × g and lysed with 10 mL MeOH (HPLC grade, Merck, Darmstadt, Germany). After 20 min, the methanolic extracts were centrifuged at 12,000 × g for 10 min. The supernatants were subjected to UPLC-MS–for product analysis.

For larger cultures, the starter cultures were inoculated with 3 mL of starter culture and grown for 24 h at 37°C with shaking at 200 rpm. (0.4 L LB per 2 L culture flasks, supplemented with 1% xylose, 5 µg/mL Chl, and 50 µg/mL tryptophan (TCI, Tokyo, Japan). Cells were harvested by centrifugation (4,000 × g, 30 min), resuspended in methanol (100 mL for 1 L of culture), vortexed vigorously, and allowed to sit for 20 min. Sodium sulfate (15 g) was added to the methanol extract. The mixture was then filtered through Whatman filter paper (no. 1) and MeOH was removed under vacuum. Further purification was performed using ethyl acetate extraction. The solvents were removed from the crude extracts using a rotary evaporator. The crude residue was dissolved in 20 mL of a 1:1 ethyl acetate/water mixture. The biphasic solution was transferred to a 50 mL separatory funnel, shaken, and removed the organic layer. The aqueous layer was washed with 20 mL of super solvent (3:1 isopropyl

alcohol/chloroform mixture by volume) and the combined organics were dried over Na_2SO_4, filtered, and evaporated to dryness. Final purification was performed using RP-HPLC on a Gilson 321-Kinetex 5 μm Biphenyl 100 Å column (Phenomenex, Torrance, CA, USA). Thiocillin IV was eluted using 30–60% ACN-0.1% TFA (v/v) over 50 min at an 18 mL/min flow rate. The active fraction (retention time = 30–33 min) was collected for structural analysis.

Protein expression and purification

To obtain recombinant TclO protein, the ORF was amplified and cloned into pET28a or pGEX 4T-1 vectors. The recombinant construct was then transformed into BL21(DE3) cells and selected on LB-agar plates containing selection antibiotics (i.e., ampicillin 100 μg/ml). A single colony of transformed *E. coli* cells was cultured in liquid LB medium at 37°C until the OD_{600} = 0.5. TclO expression was induced by adding isopropyl-β-thiogalactopyranoside (IPTG) to a final concentration of 0.25 mM. Cells were then incubated at 17°C for 20 h before harvesting of cells by centrifugation, after which they were resuspended in a lysis buffer (i.e., 20 mM Tris-Cl, pH 7.4, 150 mM NaCl, 1 mM PMSF, and 5% glycerol). Harvested cells were then disrupted using a sonicator and centrifuged at 12,000 × g for 30 min at 4°C to remove cell debris. For His_6-TclO purification, clarified supernatant was loaded onto a Ni-NTA agarose (Thermo Scientific, Waltham, MA, USA), washed by adding 5-CV (column volume) of washing buffer (i.e., 20 mM Tris-Cl, pH 7.4, 150 mM NaCl, 10 mM imidazole) and 1-CV of elution buffer (i.e., 20, 50, 100, 150, or 250

mM of imidazole in washing buffer). For GST-TclO, the supernatant was filtered and loaded onto a Pierce glutathione agarose resin (Thermo Scientific, Waltham, MA, USA) which was pre-equilibrated with washing buffer (i.e., 20 mM Tris-Cl, pH 7.4, 150 mM NaCl, and 5% glycerol). The resin was then washed with wash buffer in a 10-CV and the bound protein was eluted with GST elution buffer (i.e., 50 mM Tris-Cl, 150 mM NaCl, 5% glycerol, and 10 mM reduced glutathione). All protein samples were then separated by SDS-PAGE using 10% acrylamide gels and stained with Gel Code Blue (Thermo Scientific, Waltham, MA, USA). Fractions containing the TclO were pooled and dialyzed against 1 L of wash buffer at 4°C for 24 h.

Micrococcin P2 spontaneous mutant generation

Micrococcin P2-resistant mutants were induced by plating approximately 10^{10} CFU of *S. aureus* on an LB agar medium containing four times the MIC (2 μg/mL). Following overnight incubation, colonies were streaked onto tryptic soy agar (BD Difco, Sparks, MD, USA) medium and resistance was confirmed by measuring the MIC against MP2. From the selected independent mutants, genomic DNA was purified to amplify 23s rRNA H43-44 region and *rplK* gene using the primers listed in Table 8. Genetic mutations responsible for MP2 resistance were identified by comparing the nucleotide sequences of the wild-type strain with those of resistant mutants. Five *rplK* spontaneous mutants were used to evaluate the antimicrobial activity of thiocillin IV.

Determination of minimum inhibitory concentration

The test organisms consisted of reference strains from the ATCC and clinical isolates (obtained from Prof. Jin-Hwan Kwak lab). *In vitro* susceptibility testing of organisms was performed using the microtiter broth serial dilution method, following the CLSI guidelines (Clinical and Laboratory Standards Institute, 2018). Each compound was tested in the concentration range prepared with a double series of dilutions in the range 32–0.06 μg/mL. The medium used in the broth microdilution assay was cation-adjusted Mueller Hinton broth (BD Difco, Sparks, MD, USA). A standardized inoculum of 5×10^5 CFU/mL in a volume of 0.1 mL was added to each 96-well microtiter plate well and incubated at 37°C. After 20 h, the plates were inspected, and the MIC values were determined as the lowest concentration of test compounds that inhibited cell growth.

Cellular toxicity

Cell cytotoxicity was determined against the human cell lines HEK293T using the CCK-8 cell viability assay. HEK293T cells were seeded in 96-well plates (5×10^3 cells/well) and cultured in DMEM (Gibco, New York, NY, USA) supplemented with 1% penicillin/streptomycin and 10% FBS (Gibco, New York, NY, USA) at humidified incubator adjusted 5% CO_2 at 37°C. The HEK 293T cells were treated in triplicate with 0.1 μM to 10 μM and then cultured for 48 h at 37°C. Finally, 10 μL CCK-8 reagent (Dojindo, Rockville, MD, USA) was added into each well, and viable cell signal was measured at 450 nm using

a microplate reader (Biotek, Vermont, VT, USA). The cell viability was normalized to DMSO control.

Statistical analysis

Data analysis and the generation of graphs were performed using GraphPad Prism 9 (GraphPad Software, Inc., San Diego, CA, USA). Data are presented as the mean ± standard deviation (SD). Statistical tests employed are indicated in the text and corresponding figure legend. Statistical significance was measured using a two-way analysis of variance (ANOVA) in GraphPad Prism 9 and a significant interaction was interpreted by a subsequent analysis with Tukey multiple comparison test. Asterisks indicate significance as follows: *, $p<0.05$; **, $p<0.01$; ***, $p<0.001$; ****, $p<0.0001$.

***In vitro* enzyme assay**

Dialyzed protein was concentrated using Amicon centrifugal filters (10 kDa cutoffs, Merck Millipore, MA, USA) and the resulting protein concentration was determined by Bradford reagent (Thermo Scientific, Waltham, MA, USA) with serial dilutions of bovine serum albumin used as standards. The prepared protein was then used for *in vitro* enzyme assays. For these assays, an enzyme reaction was performed in 0.1 M Tris-Cl buffer at pH 7.4, 150 mM NaCl, 1 mM SAM (S-adenosylmethionine), 20 μM MP2, and 10 μM of the GST-TclO in a total volume of 100 μL. After incubation at 37°C for 2 h, the reaction was terminated by adding 100 μL of ACN. After centrifugation (16,000 × g for 10

min), the supernatant was extracted and analyzed by UPLC-MS using the same analysis conditions described above.

In vivo micrococcin P2 feeding studies

AJ-005 and AJ-006 start cultures (3 mL) were grown in LB-Chl (5 μg/mL) for 20 h at 37°C. Start cultures were inoculated at a 1:100 dilution ratio into 10 mL LB (supplemented with 1% xylose and 5 μg/mL Chl in a 50 mL culture flask). Next, 10 μM micrococcin P2 was added to the AJ-005 culture. Diluted *B. subtilis* was cultured for 24 h at 37°C with shaking at 200 rpm. Cells were harvested by centrifugation (4,000 × g, 10 min), resuspended in methanol (500 μL for a 10 mL culture), vortexed vigorously, and allowed to stand for 20 min. Cell extracts were then clarified by centrifugation (15,000 × g, 10 min) and methanolic extracts were analyzed using an authentic thiocillin IV standard.

MALDI-TOF analysis of *tcl* intermediates

Cultured *Bacillus* strains (AJ-024 and AJ-026) were cultured (100 mL in 500 mL flasks) for 24 h before being harvested, sonicated, and clarified. Soluble fractions were then purified with Ni-NTA beads using an imidazole step gradient (i.e., 50 mM to 250 mM). Pooled purified fractions were concentrated using a Vivaspin (i.e., with a 3k-cut off, Sartorius, Goettingen, Germany). Concentrated and clarified protein samples were then analyzed by MALDI-TOF (in both linear and reflector modes). 3,5-Dimethoxy-4-hydroxy-cinnamic acid (sinapinic acid) was used as a matrix. MALDI-TOF mass spectra of *tcl*

intermediates were acquired using a MALDI-TOF 5800 system (Applied Biosystems, Foster City, CA, USA) equipped with a nitrogen laser (337 nm). These analyzes were performed at the National Center for Inter-University Research Facilities at Seoul National University.

Table 8. List of strains and plasmid used in this study.

Strains	Genotype or Description	Source
Escherichia coli		
DH5α	Host strain for cloning	Enzynomics
BL21(DE3)	Protein expression host	Enzynomics
Bacillus subtilis		
168	*trpC2*	ATCC 23857
168R	*trpC2 rplK*ΔP22	Hwang et al., 2022
BS-013	*trpC2 rplK*ΔP22 *amyE::xylR-*P_{xylA}*-tclEIJKLMNOP cat*	This study
AJ-004	*trpC2 rplK*ΔP22 *amyE::xylR-*P_{xylA}*-tclEEEE-IJKLMNPO cat*	This study
AJ-005	*trpC2 rplK*ΔP22 *amyE::xylR-*P_{xylA}*-tclIJKLMNOP cat*	This study
AJ-006	*trpC2 rplK*ΔP22 *amyE::xylR-*P_{xylA}*-tclIJKLMNOP cat, thrC:: xylR-*P_{xylA}*-tclEEEE spc*	This study
AJ-024	*trpC2 rplK*ΔP22 *amyE::xylR-*P_{xylA}*-tclIJKLNP cat, thrC:: xylR-*P_{xylA}*-ncohis-tclE spc*	This study
AJ-026	*trpC2 rplK*ΔP22 *amyE::xylR-*P_{xylA}*-tclIJKLNOP cat, thrC:: xylR-*P_{xylA}*-ncohis-tclE spc*	This study
Bacillus cereus	Source of *tcl* genes. Thiocillins producer	ATCC 14579
Plasmids		
pDG1661	Source of *spc* genes	BGSC
pGEX4T-1	Plasmid for protein expression	GE Healthcare
pET28a	Plasmid for protein expression	Novagen
pANJ-67	*xylR*-P_{xylA} for *amyE* integrative vector, *E. coli ori*, binary vector (Amp^R in *E. coli*, Chl^R in *B. subtilis)*	Hwang et al., 2022

pANJ-165	Derivative of pANJ-67; *xylR*-P_{xylA}-*tclEIJKLMNP*	Hwang et al., 2022
pANJ-199	Derivative of pANJ-67; *xylR*-P_{xylA}-*tclEIJKLMNOP*	Son et al., 2023
pANJ-229	Derivative of pANJ-67; *xylR*-P_{xylA}-*tclEEEE-IJKLMNOP*	Son et al., 2023
pANJ-245	Amp^R, BcTclO in pGEX4T-1	This study
pANJ-247	Kan^R, BcTclO in pET28a	This study
pANJ-253	Derivative of pANJ-67; *xylR*-P_{xylA}-*tclIJKLMNOP*	This study
pANJ-254	*thrC* integrative vector, *E. coli-B, subtilis*, binary vector	This study
pANJ-255	Derivative of pANJ-254; P_{xylA}-*tclEEEE*	This study
pANJ-277	Derivative of pANJ-254; *xylR-PxylA-pethis-tclE*	This study
pANJ-278	Derivative of pANJ-254; *xylR-PxylA-ncohis-tclE*	This study
pANJ-279	Derivative of pANJ-67; *xylR*-P_{xylA}-*tclIJKLNOP*	This study
pANJ-280	Derivative of pANJ-67; *xylR*-P_{xylA}-*tclIJKLNP*	This study

Table 9. The sequences of oligonucleotides used in this study.

Primer	Sequence (5' to 3')
TclO-F	AGGAGAACAATTTTATGTATGACGAATAAAACTAAAGGAGAAC
TclO-R	TCAGTGGTGGTGGTGGTGGTGCTCGAGCTAACGTTTTATTCCATTCAC
TclE-F	GGGGCTAGCTTTAAGAAGGAGATATACAT
TclE-R	GCTCTAGATTAAGTTGTACAACAACTGC
xylR-F	ACGGAATTCGAGCTCGGTACCGAACTCCTTTTTCATATGAGAAGG
xylR-R	TTCTAGAGGATACCCGGGTACCTTAGTAAACCACTTTGTTTGCGCTTCC
TclE4X-R	TATAAAGGGAACAAACGGATCCCCGGGTACCGCTTGGGCCCGTACG
GST-TclO-F	CCCGGATCCATGTATGAAAATAATGTAAAAGATAC
GST-TclO-R	AACCGCTCGAGCTAACGTTTTATTCCATTCAC
H6-TclO-F	GGCAGCCATATGTATGAAAATAATGTAAAAGATAC
H6-TclO-R	AGGTGCTCGAGCTAACGTTTTATTCCATTCAC
pET-TclE-F	GCGGATCCATGAGTGAAATTAAAAAAGCATTAAATAC
pET-TclE-R	GGAATTCCTCGAGTTAAGTTGTACAACAACTGCATG
Nco-H6-F	ATATACCATGGGCTCACATCATCATCATCATCATGGCGGCGGAAGTGAAATTAAAAAAGCATTAAATACAC
HiTclL-N-F	TATAAGAGTAGAAAGGGATGACGGGATTTTGGTAAAGGGAGGG
TclP-R-HI	TCAGTGGTGGTGGTGGTGGTGCTCGAGCTAGTGTAATGTATAACCACCATCAA
amyE-up-F	GGAGGAAGCGGAAGAATGAAG (integration)
amyE-up-R	GGTACCGAGCTCGAATTC (integration)
amyE-dn-F	GGCTGCTTCCTAATGCAGG (integration)
amyE-dn-R	CGGTAAGTCCCGTCTAGCCT (integration)
thrC-up-F	AAAACTGCAGCCCTCGCTCAAGCTGTCAT
thrC-up-R	TTGGAAGCTTTCATACACGGGCCGCTCC
thrC-dn-F	AACCGGCATATGAGGTTGGTTCATTCTCG
thrC-dn-R	GCGAATTCGCTGCCGCAGCAGCGGA
spc-F	GGCCTAGGTCTAGAGGATC
spc-R	ACGCGGCCCGACCTCGAGCT
rplK	GGCAACTAGCATGATATTTCGTC (sequencing)
23s rRNA	GAGGTAGAGCACTGTTTGGACG (sequencing)

* The recognition site of the restriction enzyme was underlined

Results

Plasmid design for thiocillin IV biosynthesis

Presumably, thiocillin IV shares structural similarities with MP2 and other thiocillin sister analogs. Although the precise structure of thiocillin IV is unknown, cumulative evidence suggests that thiocillin IV is an O-methylated congener of MP2 (Shoji et al., 1981) (Nagai et al., 2003).

Based on this hypothesis, clustered thiocillin biosynthetic genes from *B. cereus* ATCC 14579 were utilized. Previous efforts have culminated in the synthesis of MP2 through the reconstruction of the *tcl* gene cluster in a *B. subtilis* host, thus, demonstrating that enzymatically synthesized MP2 is identical to synthetic MP2 (Hwang et al., 2022). To obtain thiocillin IV, the gene responsible for O-methyl transfer during biosynthesis was identified. The gene *tclO*, proposed to encode an enzyme for Thr-8 O-methylation, was a strong candidate for converting micrococcin P2 to thiocillin IV. Two characteristics of *tclO* gene made it suitable to investigate: first, it is located in the *tcl* gene cluster. Second, based on its amino acid sequence, it is functionally annotated as a SAM-dependent methyltransferase that contains a conserved SAM-binding site (Figure 14). Therefore, the *tclO* gene was selected as a candidate gene for catalyzing O-methylation and synthesizing thiocillin IV almost exclusively.

Figure 14. Multiple sequence alignment of O-methyltransferses.

B. cereus ATCC 14579 tclO is compared with other O-methyltransferase: *Arabidopsis thaliana* gamma-tocoperol methyltransferase (AtTMT, GenBank: AAD02882.1); *Homo sapiens* Histone-lysine-N-methyltransferase (DOT1L, Range:1-416, GenBank: XP_005259716); *Bacillus cereus* malonyl-acyl carrier protein O-methyltransferase (BioC, GenBank: WP_000608914.1). Well conserved GxGxG signature motif was found in aligned SAM binding proteins. Highly conserved residues are in blue and similar residues are in yellow. Predicted SAM binding residues are noted (*). Amino acid alignment and figure was prepared using Bioedit software ver.7.2.6.

```
                    10        20        30        40        50        60        70        80
            ....|....| ....|....| ....|....| ....|....| ....|....| ....|....| ....|....| ....|....|
BcTclO   1  ---------- ---------- ---------- ---------- ---------- -----MYENN VKDTKDFYND IGHISWSVAP
AtTMT    1  MKATLAAPSS LTSLPYRTNS SFGSKSSLLF RSPSSSSSVS MTTTRGNVAV AAAATSTEAL RKGIAEFYNE TSGL-WEEIW
BioC     1  ---------- ---------- ---------- ---------- ---------- MINKTLLQKR FNGAAVSYDR YANV------
DOT1L    1  MGEKLELRLK SPVGAEPAVY PWPLPVYDKH HDAAHEIIET IRWVCEEIPD LKLAMENYVL IDYDTKSFES MQRLCDKYNR

                    90       100       110       120       130       140       150       160
            ....|....| ....|....| ....|....| ....|....| ....|....| ....|....| ....|....| ....|....|
BcTclO  26  SQHYHVGIFE LE------KD SMEDAQNRTV EYMARKVAAS L--------- ---------- ---------- -----LDVLL
AtTMT   80  GDHMHHGFYD PDSSVQLSDS GHKEAQTRMI EESLRFAGVT LEEEEK---- ---------- ---------- ----KIKKVV
BioC    24  ---------- --------QK KMAHSLLSIL KERYSETASI R--------- ---------- ---------- --------IL
DOT1L   81  AIDSIHQLWK GTTQPMKLNT RPSTGLLRHI LQQVYNHSVT LPEKLNNYEP FSPEVYGETS FDLVAQMIDE IKMTDDDLFV
            GxGxG motif
                    170       180       190       200       210       220       230       240
            .*.*.|....| ....|....| ....|..*.| ....|....| ....|....| ....|....| ***.|....| ....|...*|
BcTclO  66  DIGCGSGLTA VGISKKE-NC KIVGINISEK QLAIGKKLIS KE-------- KINSRVKLMN MDAHQLNFKS GMFDGAYALE
AtTMT  132  DVGCGIGGSS RYLASKF-GA ECIGITLSPV QAKRGNDLAA AQ-------- SLAHKASFQV ADALDQPFED GKFDLVWSME
BioC    50  ELGCGTGYVT EGLSKLFPKS HITAVDFAES MIAIDQTRQN ---------- --VKNVTFHC EDIERLRLEE S-YDVIISNA
DOT1L  161  DLGSGVGQVV LQVAAATNCK HHYGVEKADI PAKYDETMDR EFRKWMKWYG KKHAEYTLER GDFLSEEWRE RIANTSVIFV

                    250       260       270       280       290       300       310       320
            ....|....| ....|....| ....|....| ....|....| ....|....| ....|....| ....|....| ....|....|
BcTclO 137  S-IMHMN-RE KVDSEVHRVL KNGAPFSLCD -WYVK----- -KSLTPVEKR --FLETIT-- --LGKYITKE QYFSDYQTQN
AtTMT  203  S-GEHMPDKA KFVKEIVRVA APGGRIIIVT -WCHRNLSAG EEALQPWEQN --ILDKICKT FYLPAWCSTD DYVNILQSHS
BioC   117  T-FQWLNNLQ QVDRNLFQHL SIDGILLFST -FGHETFQEL HASFQRAKEE RNIKNETSIG ---QRFYSKD QLLHICKIET
DOT1L  241  NNFAFGPEVD HQFKERFANM KEGGRIVSSK PFAPLNFRIN SRNLSDIGTI MRVVELSPLK G-SVSWTGKP VSYYLHTIDR

                    330       340       350       360       370       380       390       400
            ....|....| ....|....| ....|....| ....|....| ....|....| ....|....| ....|....| ....|....|
BcTclO 201  ---------F MDIEIEEWSN KILPTY--KY WTTLLDEM-- ----KEKIPD HLLYVIEENS KVLSIHAIEK LGYLQVNGIK
AtTMT  278  ---------L QDIKCADWSE NVAPFWPAVI RTALGWKG-- ----LVSILR SGMKSIKGAL TMPLMHEGYK KGVIKFGIIT
BioC   192  GDVH-----V SETCYIESFT EVKEFLHSIR KVGAGNSNEG SYCQSPSIFR AMLRIYERDF TGNEGLMATY HALFIHITKE
DOT1L  320  TILENYFSSL KNPKLREEQE AARRRQQRES KSNAATPTKG PEGKVAGPAD APMDSGAEEE KAGAATVKKP SPSKARKKKL

                    410
            ....|....| ....|..
BcTclO 265  R--------- ------- 265
AtTMT  344  CQKPL----- ------- 348
BioC   267  GKR------ ------- 269
DOT1L  400  NKKGRKMAGR KRGRPKK 416
```

Strain construction and analysis of products

The candidate *tclO* gene was amplified and transferred to pANJ-165 (*amyE*::*xylR* P_{xylA}-*tclEIJKLMNP*: for MP2 biosynthesis) to generate pANJ-199 (*amyE*::*xylR* P_{xylA}-*tclEIJKLMNOP*) (Figure 15A). The stablished *B. subtilis* 168R strain was used as the host cell to carry the plasmid pANJ-199. In this 168R strain, changes in the ribosomal protein L11 (*rplK,* deletion of Pro22; ΔP22) were introduced to confer protection from intracellularly emerging thiopeptides that may exert potent antibacterial activity (Hwang et al., 2022).

After transforming pANJ-199, the BS-013 strain was selected and cultured for thiopeptide biosynthesis. The cultured *B. subtilis* cells were harvested and extracted with MeOH, followed by LC-MS analysis of the metabolites (Figure 15B). BS-013, *B. cereus* MeOH extracts, and authentic MP2 standards were injected to qualitatively compare their retention times and corresponding masses. Compound 2.6, hereafter referred to as 2.6, exhibited a relatively longer retention time (5.64 min) compared with the extracts from *B. cereus* (4.59–5.10 min) and the MP2 authentic standard (5.26 min) (Figure 15C and D). Chromatographic analysis suggested that 2.6 was by far the most non-polar. Moreover, compared with MP2, thiocillin IV had an additional mass of 14 Daltons (Figure S3). This indicated that thiocillin IV contained an extra methyl group, which explained its greasy behavior in this qualitative analytical method. Thiocillin IV emerged almost exclusively, and the possible other products were too small to be detected. Finally, efficient O-methylation was successfully mediated by *tclO*.

Figure 15. Synthesis and analysis of thiocillin products.

(A) Schematic map of *tclO* containing pANJ-199. (B) UPLC-MS analysis of the MeOH extract of *B. cereus*, pANJ-199 transformed BS-013 strain MeOH extract, and MP2 standard. (C) Structure of micrococcin P2 and thiocillin IV. The only difference is in the 8'-threonine side-chain. (D) Mass data corresponding to the thiopeptide compounds.

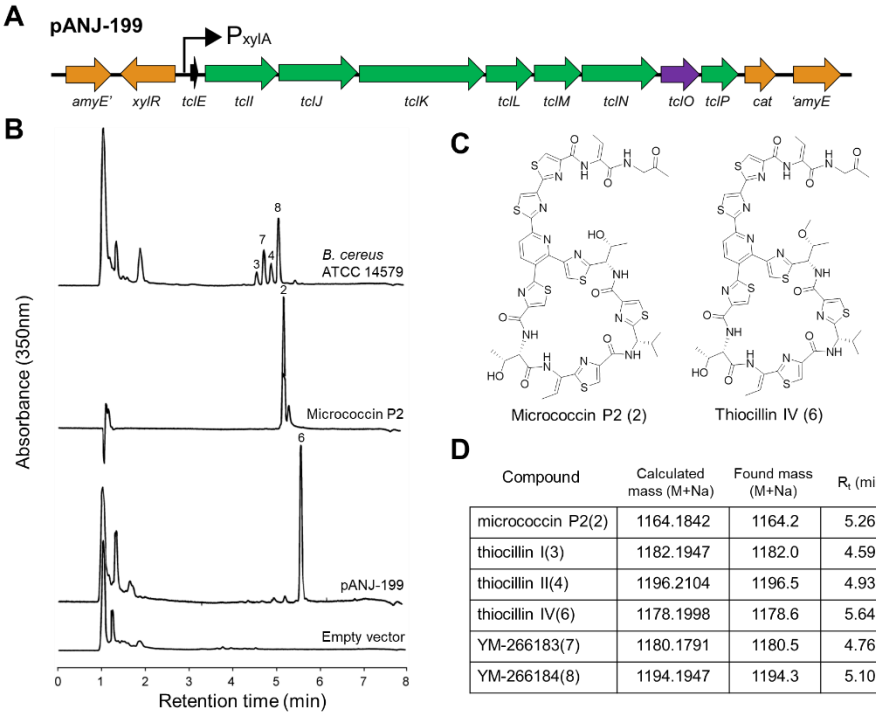

Compound	Calculated mass (M+Na)	Found mass (M+Na)	R_t (min)
micrococcin P2(2)	1164.1842	1164.2	5.26
thiocillin I(3)	1182.1947	1182.0	4.59
thiocillin II(4)	1196.2104	1196.5	4.93
thiocillin IV(6)	1178.1998	1178.6	5.64
YM-266183(7)	1180.1791	1180.5	4.76
YM-266184(8)	1194.1947	1194.3	5.10

De novo* thiocillin IV production in *B. subtilis

To fully elucidate the exact chemical structure of 2.6, a sufficient amount of high-purity product had to be acquired. The initial BS-013 strain produced a minute amount of 2.6 (~ 0.2 mg/L) in the LB-0.5% xylose condition (Data not shown). To increase the production yield, three additional copies of the *tclE* gene (precursor peptide gene) were inserted into the pANJ-199 plasmid to obtain pANJ-229. This plasmid was transformed to obtain the AJ-004 strain. Further optimization studies on combining the inducer and fermentation times were conducted under simple flask-shaking conditions. The xylose concentration was varied in the LB media between 0.5% and 4% to examine the effects of the induction conditions (Figure 16A). The accumulation rate of 2.6 was evaluated over a 72 h incubation period. Cellular density was also measured to find favorable growth culture conditions and confirm that the intracellular production of 2.6 did not inhibit growth (Figure 16C).

The insertion of three copies of the *tclE* gene and incubating the *B. subtilis* system with 1% xylose for up to 72 h significantly increased the production of 2.6 from ~0.2 mg/L to 2.4 mg/L (Figure 16B). Increasing the xylose concentration (2% and 4%) decreased yield and disturbed cell growth (Figure 16C and D). It can be assumed that a higher concentration of xylose may interfere with the growth of *B. subtilis* by affecting the expression of the construct for thiocillin biosynthesis through suboptimal osmotic pressure (Helle et al., 2003). Nonetheless, this study constitutes the first biosynthetic

optimization of thiocillin IV, in which the exclusive formation and fermentation of thiocillin IV have been established.

Figure 16. Effect of xylose concentration in AJ-004 strain.

Effect of xylose concentration in the AJ-004 strain. Time course measurement of the synthesized product (A, and B) and cellular density (C, and D) in the culture condition. Maximum production at 2.37 mg/L was achieved by 72 h of culture at 1% xylose containing the LB medium. The individual black circles depict the population means from each biological replicate. Statistical significance was analyzed using two-way ANOVA and Tukey multiple comparison test. *$p < 0.05$, **$p < 0.01$, ***$p < 0.001$, and ****$p < 0.0001$. # indicates significant xylose concentration, time, and xylose concentration-time interaction in a two-way ANOVA ($p < 0.0001$). The error bars were derived by the standard error ($n = 3$).

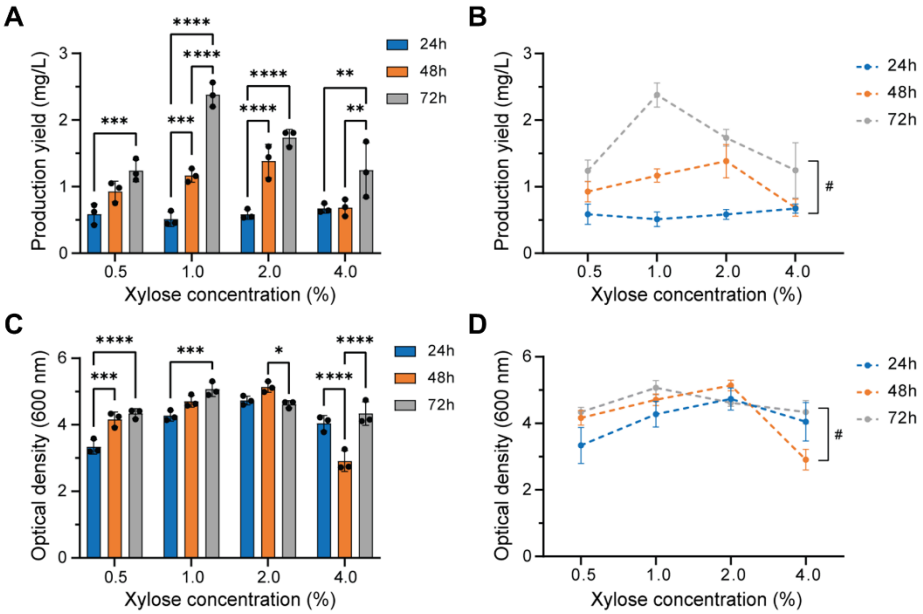
A
B
C
D
Production yield (mg/L)
Optical density (600 nm)
Xylose concentration (%)
0.5
1.0
2.0
4.0
24h
48h
72h
***
****
**
*
#

Purification and structural elucidation of thiocillin IV

Under the optimized culture conditions, a reasonable amount of 2.6 was isolated and purified using a preparative HPLC system. 2.6 showed a UV absorption pattern similar to that of MP2, indicating that it has an extended π-conjugation system from the central pyridine core with three attached thiazoles (Figure S4). This is the key chromophoric feature widely observed in thiopeptides (Engelhardt et al., 2010). HR-ESI-MS ion data corroborated that 2.6 exhibited a strong molecular ion with the correct composition, C49H49N13O9S6 (m/z 1156.2169 $[M + H]^+$, calculated 1156.2178), with an extra methyl group in MP2 (Figure S5). This methyl group likely resulted from the activity of TclO.

To elucidate the precise location of the O-methyl group, the complete assignment of the ^{1}H and ^{13}C resonances of thiocillin IV was determined using 1D and 2D NMR studies (Figures S6-S14). A combined 1D and 2D NMR analysis indicated that the O-methyl group was situated in the Thr-8 region (Figure 17). The HMBC correlations between 28-H / 26-C, 27-H / 25-C, and 27-H / 26-C supported analysis. Furthermore, the HMBC correlation between 25-H / 23-C, 25-H / 24-C, 23-H / 24-C, 23-H / 21-C, and 19-H / 21-C revealed the proximity of the O-methyl group to the adjacent thiazole, and the connected pyridine core (Figure 17, S7 and S8). Therefore, these NMR studies indicated that the enzymatic transfer of a methyl group is only allowed in the Thr-8 region.

The complete assignment of thiocillin IV was further facilitated by 2D TOCSY studies, in which protons sharing the same spin systems, such as the

protons (18-H and 19-H) at the central pyridine core, the protons (34-H, 35-H, 36-H, and 37-H) at 6-Val, the olefin protons (44-H and 45-H, 7-H and 8-H), and 3-Thr (48-H, 49-H, and 50-H), were identified (Figure S14). The other assignments were confirmed by the HMBC correlations in Table 10.

Figure 17. Key 2D NMR correlations for the structural assignment of thiocillin IV.

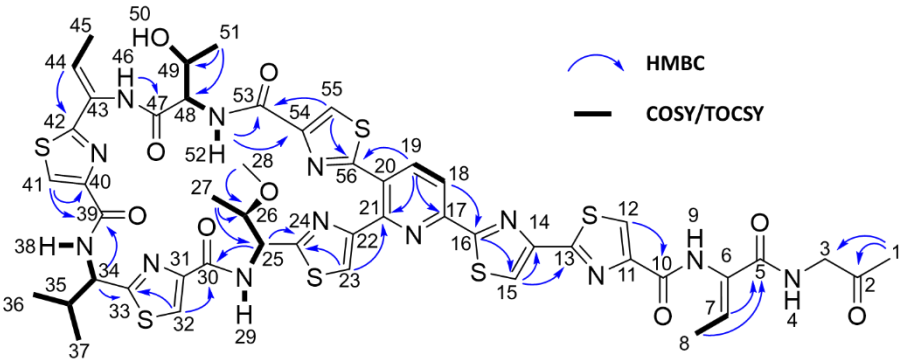
HMBC
COSY/TOCSY

Table 10. Assignment of $^{1}H/^{13}C$ chemical shifts for thiocillin IV in $CDCl_3$.

Position	$\delta^{1}H$	$\delta^{13}C$	Position	$\delta^{1}H$	$\delta^{13}C$	Position	$\delta^{1}H$	$\delta^{13}C$
1	2.28	27.6	20	-	121.3	39	-	169.8
2	-	203.6	21	-	154.6	40	-	149.7
3	4.19-4.11	50.1	22	-	152.3	41	8.17-8.14	124.2
4	ND[a]	-	23	7.74	119.1	42	-	167.3
5	-	164.4	24	-	171.5	43	-	128.8
6	-	128.6	25	5.4	55.9	44	6.49	128.8
7	6.89	128.8	26	4.19-4.11	76.3	45	1.86	14.1
8	1.86	13.9	27	1.16	15.4	46	8.71[b]	-
9	8.57[b]	-	28	2.85	56.5	47	-	167.4
10	-	166.7	29	8.08-7.99[b]	-	48	4.96	57.5
11	-	164.7	30	-	161.1	49	4.51-4.44	67.6
12	7.92	123.5	31	-	149.5	50	4.51-4.44[b]	-
13	-	160.4	32	8.08-7.99	123.8	51	1.69	18.3
14	-	150.4	33	-	159.7	52	7.79[b]	-
15	8.20	124.8	34	5.25	55.7	53	-	168.3
16	-	162.8	35	2.53	33.4	54	-	159.6
17	-	149.1	36	1[c]	20[c]	55	8.26	121.2
18	8.30	119.4	37	1.2[c]	19.3[c]	56	-	150.3
19	8.17-8.14	139	38	8.08-7.99[b]	-			

a. A corresponding peak is not seen.
b. NH, and OH.
c. Diastereotopic methyl groups are tentatively assigned between the two chemical shifts.

Antimicrobial activity and mode of action of thiocillin IV

The complete structural assignment and availability of sufficient quantities of thiocillin IV enabled the determination of its antibiotic activity against various pathogenic bacteria. The antibiotic activity of thiocillin IV was tested, and the results are outlined in Table 11. It is widely accepted that the macrocyclic cores of thiopeptides are pharmacophores that exert potent activity against Gram-positive pathogens (Bagley et al., 2005). The potent antibacterial activity of thiocillin IV was comparable to that of vancomycin. However, its activity was confined to Gram-positive bacteria. Thiocillin IV exhibited very low cytotoxicity in the mammalian cell lines, such as HEK293T cells (Figure 18), and showed no cross-resistance with clinically utilized antibiotics, like vancomycin and ciprofloxacin (Table 11).

Antibiotic resistance to 26-membered thiopeptides is conferred by a point mutation in the binding target (protein L11). To examine the mode of binding of thiocillin IV, spontaneous *S. aureus* mutants were generated. The genetic sequences of these mutants in the target regions (*rplK* gene, 23s rRNA H43, and H44 regions) revealed that the proline-rich N-terminal regions of protein L11 were altered. All mutations occurred at the N-terminus of the proline residues of *rplK*. Different proline mutations led *S. aureus* to gain resistance to MP2 and thiocillin IV, suggesting that the mode of action exerted by thiocillin IV followed the same pattern as MP2 (Table 12). The mutants were also tested for cross-resistance to ciprofloxacin and vancomycin. Although the antibacterial activity of thiocillin IV was completely abolished, vancomycin

and ciprofloxacin were unaffected by this mutation (Table 12). Thiocillin IV had the same mode of action as micrococcin P2 and showed no cross-resistance to vancomycin and ciprofloxacin.

Figure 18. Cytotoxicity assay of thiocillin IV and vancomycin on HEK293T cells.

Cell viability was normalized to DMSO control and 1% Triton X-100 was used as a positive control. No toxicity was observable up to 10 μg/mL of thiocillin IV. Individual points on the graph represent individual assessment datapoints.

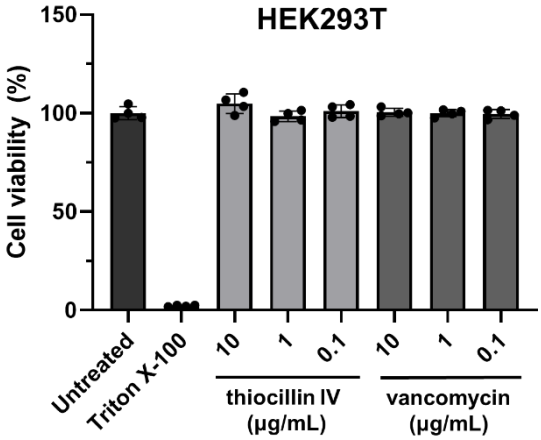
HEK293T
Cell viability (%)
150
100
50
0
Untreated
Triton X-100
10
1
0.1
10
1
0.1
thiocillin IV
(µg/mL)
vancomycin
(µg/mL)

Table 11. Comparison of the antimicrobial activity of MP2 and thiocillin IV vs. others antibiotics.

Strain		MIC (µg/mL)			
		MP2	Thio IV	VAN	CIP
MSSA	ATCC 25923	0.5	0.5	0.5	0.25
MRSA	ATCC 43300	0.5	1	0.5	0.5
VRE	Clinical isolate	0.5	0.5	>32	1
E. coli	ATCC 25922	>32	>32	>32	0.06
A. baumannii	ATCC 17904	>32	>32	>32	0.25
P. aeruginosa	ATCC 27853	>32	>32	>32	0.5

Abbreviations: MP2 = micrococcin P2, Thio IV = thiocillin IV, VAN = vancomycin, CIP = ciprofloxacin, MSSA = methiocillin-susceptible *Staphylococcus aureus*; MRSA = methicillin-resistant *Staphylococcus aureus*, and VRE = vancomycin-resistant *Enterococcus faecalis*.

Table 12. Minimum inhibitory concentration values in *S. aureus* protein L11 mutants.

Strain	Protein L11	MIC (μg/mL)			
		MP2	Thio IV	VAN	CIP
S. aureus	WT	0.5	0.5	0.5	0.25
Mutant 1	P25L	>32	>32	0.5	0.25
Mutant 2	P21S	>32	>32	0.5	0.25
Mutant 3	P25R	>32	>32	0.25	0.25
Mutant 4	P22L	>32	>32	0.5	0.25
Mutant 5	P21L	>32	>32	0.5	0.25

Abbreviations: *S. aureus* = *Staphylococcus aureus* ATCC 25923, MP2 = micrococcin P2, Thio IV = thiocillin IV, VAN = vancomycin, CIP = ciprofloxacin,

Micrococcin P2 is not the substrate of TclO

Thus far, the exclusive formation of thiocillin IV was obtained by introducing the *tcl*O gene into pANJ-165 (i.e., the original plasmid responsible for MP2 biosynthesis). During thiopeptide biosynthesis, the leader peptide is believed to act as an anchor that facilitates the binding of various enzymes to synchronize extensive enzymatic modifications of linear peptides and to aid in the maturation of thiopeptides following final enzymatic cleavage (Arnison et al., 2013). It is widely accepted that the biosynthesis of thiopeptides involves a series of post-translational modifications of a linear peptide containing the leader peptide. (Cogan, et al., 2017; Wever et al., 2016; Jin et al., 2017; Mahanta et al., 2017). However, if TclO can recognize macrocyclized thiopeptides as a substrate, then methylation of the Thr-8 site may open new opportunities for the development of valuable libraries of thiopeptide analogs. In brief, this effort might provide the groundwork for an efficient medicinal chemistry study of thiopeptides.

To verify this hypothesis, a recombinant His_6-TclO protein was constructed and expressed in BL21(DE3). There was no observed technical issue during the cloning, induction, cell lysis, and separating soluble fractions. However, problems occur during the lysate filtering steps. The filtration of the His_6-TclO lysate immediately clogged a conventionally used 0.45 μm syringe filter. Even a larger pore size (i.e., a 0.8 μm syringe filter) filtration was unsuccessful. The experiment could not proceed further despite rapid protein purification due to the TclO protein stability issues. Nevertheless, after

purification was completed (approximately 10 min at 0°C), visible protein aggregates were observed in the 100, 150, and 250 mM eluted fractions (Figures 19A and 19B). According to SDS-PAGE analysis, these precipitated fractions contained the majority of the recombinant His_6-TclO. Therefore, without the soluble tag, the purification of the TclO protein is not possible due to its poor protein stability.

To obtain soluble protein, *tclO* ORF was cloned to the pGEX4T-1 vector for fusion with the N-terminus GST and affinity column chromatography yielded purified recombinant enzyme at a purity of 75% as assessed by SDS-PAGE (Figure 19C). The enzyme was reacted with SAM to determine whether the purified enzyme could methylate MP2 *in vitro*. However, UPLC analysis results implied that the purified enzyme and other control samples did not produce methylated thiocillin IV (Figure 19D). The absence of an enzyme reaction may be caused by issues with the MP2 (not recognized) or protein itself (i.e., inactive protein).

Therefore, *B. subtilis* was revisited to address issues related to the stability of TclO protein. In *B. subtilis*, *tcl* enzymes were present in an active form, that biosynthetic genes were reconstructed to pANJ-253 (*amyE:: xylR-PxylA-tclIJKLMNPO*) and pANJ-255 (*thrC:: xylR-PxylA-tclEEEE spc*: structural peptides) to split structural genes and biosynthetic genes (Figure 20A). *B. subtilis* strains AJ-005 (pANJ-253) and AJ-006 (pANJ-253 + pANJ-255) were then cultured in the presence of 1% xylose to induce the expression of *tcl* genes (Figure 20B). In addition, 10 μM of MP2 was treated with AJ-005

to determine whether induced TclO recognizes and methylates correctly in cultured *Bacillus* cells (Figure 20B). Cells were harvested, extracted, and the results were analyzed via comparison to an authentic standard. A thiocillin IV production test was performed on strain AJ-006 to confirm *tcl* gene expression (Figure 20C). Thiocillin IV was synthesized when the *tclE* gene was expressed with the biosynthetic gene (AJ-006), whereas MP2 fed to AJ-005 was retained in its unmethylated form (Figure 20C). These results indicated that internalized MP2 was exposed to translated TclO, but TclO could not continue the methylation. Thus, TclO-mediated methylation did not occur since MP2 was not its correct substrate.

Figure 19. TclO purification and *in vitro* enzyme assay.

Purification of H_6-TclO. (A) SDS-PAGE analysis of purified fraction (i.e., on a 15% polyacrylamide gel). (B) Precipitated purified TclO protein. E1-E5 fractions correspond to SDS-PAGE fractions. (C) SDS-PAGE analysis of purified GST-TclO (i.e., on a 10% polyacrylamide gel) (D) *In vitro* enzymatic reaction of GST-TclO with MP2. UPLC-MS results show that in TclO does not recognize MP2 as a substrate. As a result, the enzymatic reaction did not occur. M: Protein size marker, S: Soluble fraction F: Flow through, E1: 20 mM E2: 50 mM, E3: 100 mM, E4: 150 mM, E5: 250 mM imidazole.

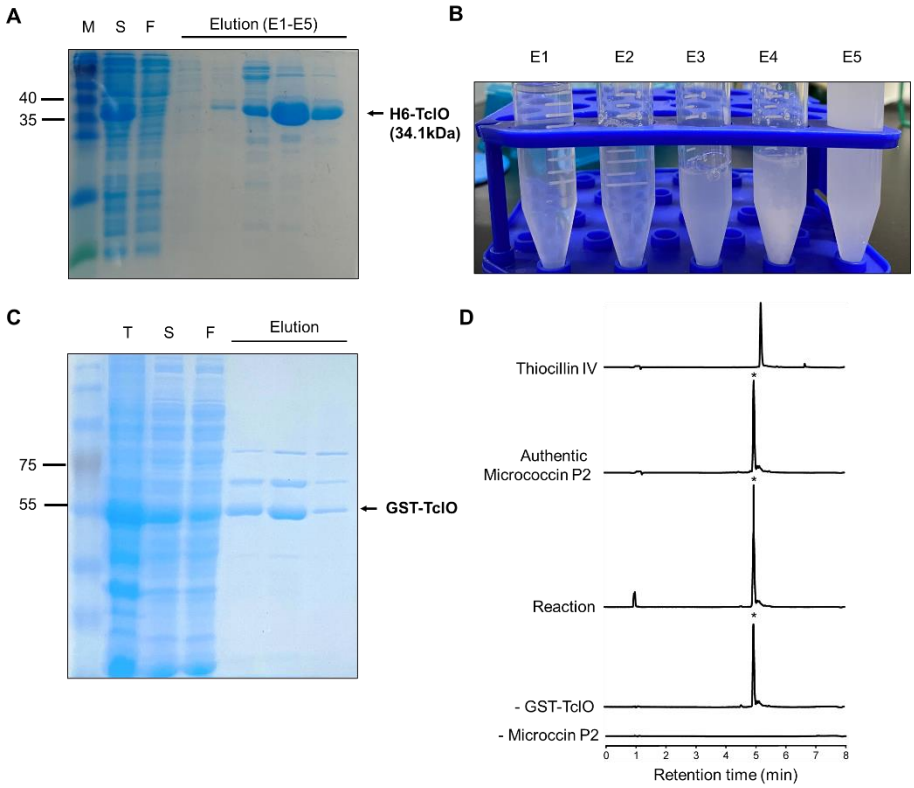
A
M S F
Elution (E1-E5)
40
35
H6-TclO
(34.1kDa)
B
E1 E2 E3 E4 E5
C
T S F
Elution
75
55
GST-TclO
D
Thiocillin IV
Authentic
Micrococcin P2
Reaction
- GST-TclO
- Microccin P2
0 1 2 3 4 5 6 7 8
Retention time (min)

Figure 20. *In vivo* feeding result of micrococcin P2 in expression of TclO.

(A) Schematic map of plasmids used in this experiment. (B) UPLC-MS analysis of *in vivo* feeding samples. A thiocillin IV peak was not detected in the presence of micrococcin P2 and TclO. (C) Proposed TclO enzymatic reaction for biosynthetic procedures. Prior to macrocyclization, TclO-mediated an O-methyl transfer reaction.

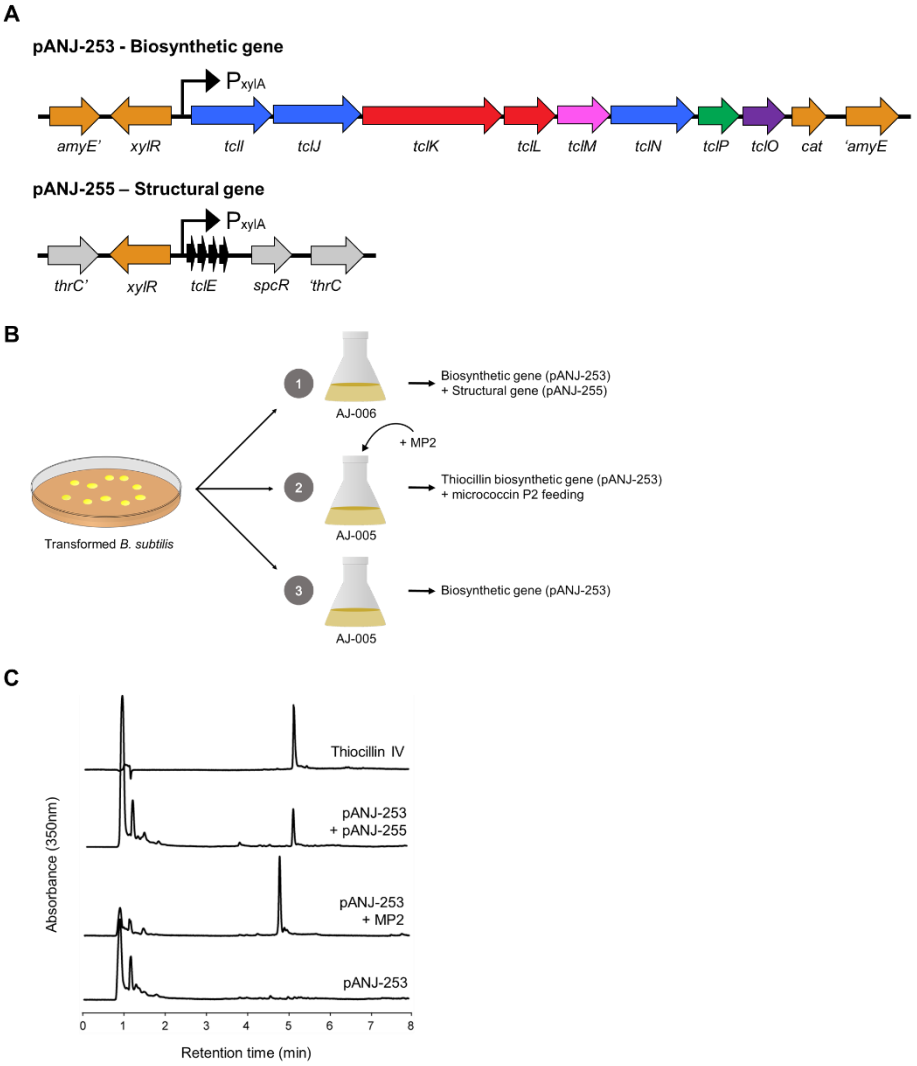
A
pANJ-253 - Biosynthetic gene
PxylA
amyE'
xylR
tclI
tclJ
tclK
tclL
tclM
tclN
tclP
tclO
cat
'amyE
pANJ-255 – Structural gene
PxylA
thrC'
xylR
tclE
spcR
'thrC
B
Transformed B. subtilis
1
AJ-006
Biosynthetic gene (pANJ-253)
+ Structural gene (pANJ-255)
+ MP2
2
AJ-005
Thiocillin biosynthetic gene (pANJ-253)
+ micrococcin P2 feeding
3
AJ-005
Biosynthetic gene (pANJ-253)
C
Absorbance (350nm)
Thiocillin IV
pANJ-253
+ pANJ-255
pANJ-253
+ MP2
pANJ-253
0
1
2
3
4
5
6
7
8
Retention time (min)

MALDI-TOF analysis of linear peptide intermediates

The first attempts to purify recombinant His_6-TclO for *in vitro* assays were unsuccessful, perhaps due to ectopically expressed tagged TclO instability. *In vivo* feeding studies have been conducted to determine whether MP2 was methylated in the presence of active TclO, but the required enzymatic reaction did not occur.

Lastly, to determine when the substrate was methylated by TclO, His_6-TclE precursor peptides were intended to facilitate the purification of biosynthetic intermediates in *B. subtilis* extracts. A procedure follows a similar published method (Bewley et al., 2016). The designed peptide sequence and target molecules are summarized (Figure 21 and Table 13). First, to validate whether the newly introduced His_6-tag affected the thiocillin IV biosynthesis process, untagged *tclE* and His_6-*tclE* genes were induced with *tcl* biosynthetic enzymes (i.e., Strain 1, 2, and 3 in Table 14). Notably, while native TclE produced the desired natural products (Strain 1 in Table 14), the His_6-TclE-1 and -2 did not (Strain 2 and 3 in Table 14). Thus, there is strong evidence that the N-terminal His_6-tag may interfere with or hinder essential enzymatic sequences, such as TclM, which is intolerant to changes in the leader sequence (Fleming et al., 2019).

Therefore, the *tclM* gene was removed from the *tcl* clusters to determine whether the linear sequence was a viable substrate for O-methylation prior to macrocyclization (i.e., Strain 4 and 5 in Table 14). Unfortunately, the corresponding mass (6538.44 and 6521.41) was not observed in MALDI-TOF

analysis (Figure S15-S18). According to this negative result, even the simplest His_6-tag appears blocked during the synthesis of thiopeptides.

Figure 21. Molecular structure of thiocillin IV and linear intermediates.

Target 1
(Thiocillin IV)

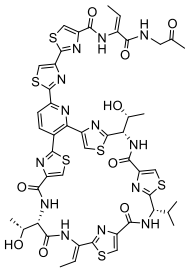

Molecular Weight: 1142.3460

Target 2
(Uncyclized thiocillin IV)

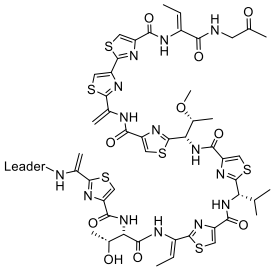

Molecular weight : 6538.44

Target 3
Uncyclized micrococcin P2

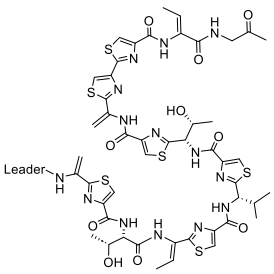

Molecular weight : 6524.41

Table 13. Designed precursor peptide (TclE) sequence.

No.	Amino acid sequence	Remark
1	MSEIKKALNTLEIEDFDAIEMVDVDAMPENEALEIMGASCTTCVCTCSCCTT	Native TclE
2	MGSSHHHHHHSSGLVPRGSHMASMTGGQQMGRGSMSEIKKALNTLEIEDFDAIEMVDVDAMPENEALEIMGASCTTCVCTCSCCTT	His_6-TclE-1
3	MGSHHHHHHGGGMSEIKKALNTLEIEDFDAIEMVDVDAMPENEALEIMGASCTTCVCTCSCCTT	His_6-TclE-2

Underlined: leader peptide, yellow: his tag, blue: thrombin cleavage site, brown: T7 tag

Table 14. Summary of *B. subtilis* strain construction for *tcl* linear intermediate detection.

Strain	*amyE* locus	*thrC* locus	Structure (in Figure 12)	Result
1	*tcl-IJKLMNOP*	tclE	Target 1	thiocillin IV
2	*tcl-IJKLMNOP*	His_6-tclE-1	Target 1	Not detected
3	*tcl-IJKLMNOP*	His_6-tclE-2	Target 1	Not detected
4	*tcl-IJKLNOP*	His_6-tclE-1	Target 2	Not detected
5	*tcl-IJKLNOP*	His_6-tclE-2	Target 3	Not detected

Discussion

This chapter reports research findings on identifying the characteristics of thiocillin IV, a previously characterized putative antibiotic. Thiocillin IV was expected to be methylated by MP2 at 8-Thr since the mass difference to a methyl group and some structural congeners had O-methylated threonines. Biosynthesis of thiocillin IV enabled to characterize the structure of thiocillin by NMR, HR-Mass, and UV. Structural analysis revealed that TclO-mediated methyl group transfer only at 8-Thr and all other structures were verified as the same as MP2

Strategic biosynthesis and optimization of thiocillin IV production

In *B. cereus* ATCC 14579, eight thiocillin compounds can be synthesized from *tcl* gene clusters. In Chapter 1, MP2 was synthesized by reconstructing the *tcl* gene cluster and excluding putative post-translational modification enzymes. Thiocillin IV, a structural congener produced from *tcl* gene cluster, was not obtained in simple cultures because too little was synthesized. To synthesize thiocillin IV, *B. subtilis* was used for selective synthesis of thiocillin IV. Reconstructed *tcl* gene cluster, therefore, provided the opportunity to engage in selective biosynthesis and to elucidate the function of the thiocillin IV and TclO.

The prototype of thiocillin IV production strain (AJ-004) had limited production yield, so additional metabolic engineering, including gene insertion, deletion, RBS modification, and cultural optimization, was needed. Structural peptide insertion significantly contributed to increasing thiocillin IV production

(Figure 16). Moreover, even when the same number of genes were added, their effect differed greatly depending on insertion location (i.e., *tcl* operon vs. other sites). Previous studies have also suggested that if the linear polypeptide is not post-translationally modified immediately by the biosynthetic enzyme, then it will be degraded by other proteases in the cell (Griffith and Grossman, 2008).

In contrast to the effect of structural genes, the insertion of other biosynthetic genes like *tclP* and *tclM* did not effectively increase thiocillin IV production (data not shown). In addition, another study was conducted to optimize the genes and culture conditions to increase production by controlling culture time and xylose concentration. These results confirmed that maximizing production by optimizing genes and culture conditions is possible. In particular, optimization can be achieved by controlling the amount of oxygen and testing the carbon and nitrogen source types available in the medium (Tabbene et al., 2009). Future studies may provide the basis for strains that could be applied industrially.

Site-selective methylation may produce structural variety

Thiopeptides are thought to have evolved as a means of defense against other microorganisms, including bacteria and fungi, that compete with the producing organism for nutrients and other resources (Bleich et al., 2015). Thiopeptides' highly unusual sulfur-containing structures make them highly effective against a wide range of target microorganisms. A demand for thiopeptides has led to a structural diversification of these compounds over time and the structural

variety of thiocillins may also be part of thiopeptide evolution (Baym et al., 2016).

In thiocillin compounds, structural changes occur via hydroxylation of Val-6, O-methylation of Thr-8, and/or dehydrogenation of Thr-14. Of these change sites, Val-6 and Thr-8 sites are located in the macrocyclic ring, which are contributing factors to the potency of this class of antibiotics against bacterial pathogens. Their conformational states are controlled by the rigidity of the macrocyclic core, especially by heterocycles and dehydrobutyrine (Tran et al., 2017). The variation among functional groups in the macrocycle ring results in multiple conformational states. Structural rigidity is related to the antimicrobial activities of the thiocillins (Tran et al., 2017). Since the potency and mode of action of thiocillin IV are comparable to MP2, incorporating a methyl group in the macrocyclic ring does not significantly impact the macrocyclic core's rigidity. In brief, the O-methylation of MP2 does not affect its antibacterial inhibitory effect but that this modification has other effects.

The structural modification of the macrocyclic ring seems to be related to points other than structural rigidity. The hydroxylation of valine residues might be responsible for the inhibitory activity of the peptide. For example, thiocillin I, the 6-Val hydroxylated form of MP1, is known to have superior antibacterial activity relative to MP1 (Akasapu et al., 2019). TclO-mediated O-methylated products did not show improved potency or altered mode of action in spontaneous mutants (i.e., MP2 vs. thiocillin IV). Thiocillin IV O-methylation was also ~~not~~ unrelated to simple antibacterial effects. Since the

function of methylation could not be demonstrated in this chapter, the purpose of modification must be inferred from other examples.

Other representative 26-member thiopeptides that contain small rings, such as thiostrepton and nosiheptide, have been produced from *Streptomyces laurentii* ATCC 31255 and *Streptomyces actuosus* ATCC 25421 (Mocek et al., 1989; Hang and Nonek, 2005). The small ring was constructed by crosslinking of quinalic acid or an indolic moiety with connections to macrocyclic residues (Melby et al., 2011). Structural similarity caused thiostrepton and nosiheptide to bind to the same molecular targets as MP2, but they showed different mechanisms of action (Baumann et al., 2010). Notably, target mutations induced by MP2 were not affected by the activity of thiostrepton or nosiheptide. Therefore, evolutionary complexity progresses with the structural diversity of thiopeptides and O-methylation is involved in that process.

The timing of O-methylation by TclO

Additionally, apart from its function in describing the role of TclO, one of the objectives was to identify the substrate that could initiate an enzyme reaction in the biosynthetic process. However, the expression of the TclO protein in *E. coli* resulted in its instability and inability to maintain functional competence (Figure 19). Through a feeding study conducted in *B. subtilis*, it was indirectly determined that MP2 is not the substrate for TclO, suggesting that the methylation reaction must take place prior to the macrocyclization step (Figure 20). Thiocillin IV is not synthesized directly from MP2; instead, it undergoes

O-methylation followed by macrocyclization using an unknown exact substrate (Figure 22).

Due to the potential interference of the attached polyhistidine tag with biosynthetic steps (Table 14), the detection of methylated linear intermediates was not possible in the *tclM* gene deletion strains. While the polyhistidine tag was considered to have minimal impact, the presence of consecutive histidine residues could affect protein stability or interfere with protein interactions (Booth et al., 2018). Affinity tags play a crucial role in facilitating MALDI-TOF analysis, and alternative options such as flag-tag, strep-tag, or sequence-specific antibodies could be utilized instead of the polyhistidine tag (Terpe, 2003). By using appropriate affinity tags, sequential gene deletion of biosynthetic genes could directly demonstrate TclO activity. Genes could be selectively deleted to identify specific intermediates. For instance, *tclK* and *tclL*, responsible for the metabolization of Ser/Thr to the dha/dhb group, could be targeted to investigate the importance of substrate rigidity. If no reaction occurs, *tclP*, responsible for terminal decarboxylation, could be deleted, followed by modifications in thiazole formation genes to observe the methylation of intermediates.

In the event that all attempted tags interfere with the biosynthetic processes, chemically synthesized authentic materials could be used as standards to compare characteristic patterns in mass spectrometry data, aiding in the identification of protein sequences (Altenburg et al., 2022). By enriching specific intermediates, organic solvent extraction, known for its hydrophobic

properties, could be employed to assist in determining the structure of the TclO substrate and the timing of enzyme activation.

Even though the enzyme reaction was not confirmed accurately here, it was possible to predict unknown factors could act as prerequisites for a reaction to occur. First, the TclO sequence was analyzed by using RREFiner v 1.0, a bioinformatic tool for identifying RRE domains (Kloosterman et al., 2020b). The RREFinder tool was run in precision and exploratory modes (using a set bit score cutoff 25). However, no RRE sequences were detected in TclO gene using either mode (Figure S19). It is well known that the leader peptide is crucial for thiopeptide biosynthesis, but this may not be related to the TclO reaction for enzyme reactions mediated by TclO (Vinogradov and Suga, 2020). There is also a possibility that the enzyme was recognizing and methylating the surrounding structure. In the case of TbtI, a thiazole-methylating enzyme of thiomuracin, enzymatic specificity occurs by recognizing adjacent thiazole structures (Mahanta et al., 2017). In this case, the thiocillin macrocyclic ring contains two unmodified threonine residues, Thr-3 and Thr-8, but only Thr-8 is selectively methylated; Thr-3 remains unmodified in all thiocillin structures. TclO is likely to recognize the two threonine residues differently since different chemical structures surround them. Furthermore, the dehydrobutyrine structure next to 3-Thr is expected to be less accessible due to its reduced structural flexibility (Tran et al., 2017).

Considering this assumption, it becomes challenging to draw a definitive conclusion regarding whether TclO recognizes the peripheral structure of threonine residues or specific leader peptide sequences. Future

research should prioritize identifying the precise timing of enzyme reactions. Through the characterization of TclO, a deeper understanding of thiopeptide biosynthesis can be achieved, leading to significant advancements in the field.

Figure 22. Proposed mechanism of TclO mediated O-methylation.

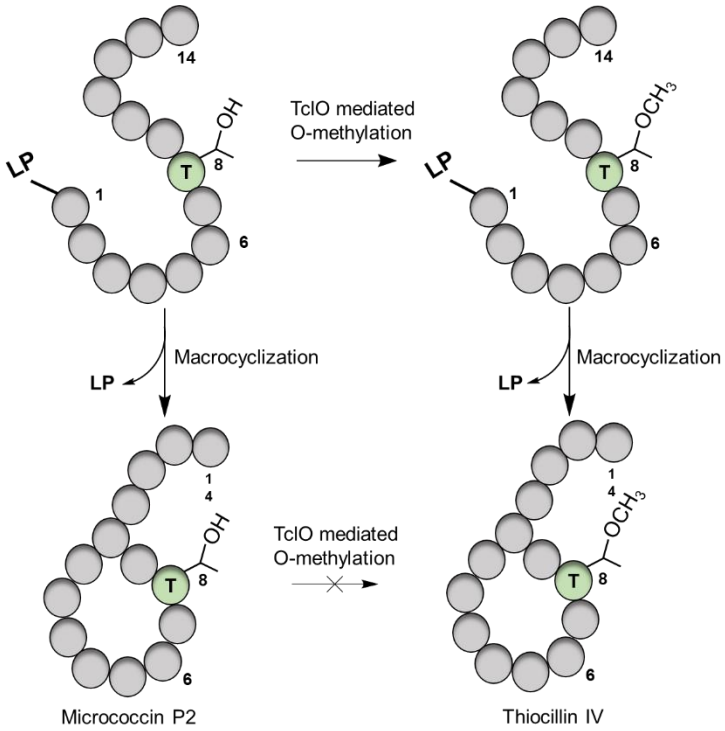
14
OH
TclO mediated
O-methylation
14
OCH3
LP
T
8
1
6
LP
T
8
1
6
Macrocyclization
LP
Macrocyclization
LP
1
4
OH
TclO mediated
O-methylation
T
8
6
1
4
OCH3
T
8
6
Micrococcin P2
Thiocillin IV

Conclusion

The emergence of antibiotic-resistant bacteria poses a significant threat to public health, necessitating the development of new agents with novel modes of action. Thiopeptide antibiotics offer a promising platform for such endeavors.

This dissertation describes the biosynthesis of micrococcin P2 and thiocillin IV from the *Bacillus subtilis* by incorporating *Bacillus cereus* ATCC 14579 genes responsible for the production of the thiocillins. Investigations of the two natural product's structural characterization, mode of action studies, and industrial application as first-in-class antibiotics have been conducted. The antimicrobial activity of these natural products is extensively evaluated through *in vitro* and *in vivo* studies, demonstrating their efficacy comparable to existing first-line treatments. Furthermore, the mild hydrolysis of MP2 to generate micrococcin P acid opens up exciting opportunities for further research, including the exploration of structure-activity relationships and the simplification of manufacturing processes. The developed semi-synthetic technology holds the promise of simplifying the rigorous Chemistry, Manufacturing & Control issues in the development of new antibiotics.

Ultimately, the work described in this dissertation. may aid in reinforcing the ongoing efforts to combat antimicrobial resistance, addressing the urgent need for new antibiotics with diverse modes of action.

References

Abda EM, Adugna Z, and Assefa A (2020) Elevated level of imipenem-resistant Gram-negative bacteria isolated from patients attending health centers in North Gondar, Ethiopia. *Infect Drug Resist* 13, 4509-4517.

Abraham EP, Heatley NG, Brookes P, Fuller AT, and Walker J (1956) Probable identity of an antibiotic produced by a spore-bearing *Bacillus* of the *B. pumilus* group with micrococcin. *Nature* 178, 44-45.

Acker MG, Bowers AA, and Walsh CT (2009) Generation of thiocillin variants by prepeptide gene replacement and *in vivo* processing by *Bacillus cereus. J Am Chem Soc* 131, 17563-17565.

Agrawal RK, Linde J, Sengupta J, Nierhaus KH, and Frank J (2001) Localization of L11 protein on the ribosome and elucidation of its involvement in EF-G-dependent translocation. *J Mol Biol* 311, 777-787.

Akasapu S, Hinds AB, Powell WC, and Walczak MA (2019) Total synthesis of micrococcin P1 and thiocillin I enabled by Mo (VI) catalyst. *Chem Sci* 10, 1971-1975.

Altenburg T, Giese SH, Wang S, Muth T, and Renard BY (2022) Ad hoc learning of peptide fragmentation from mass spectra enables an interpretable detection of phosphorylated and cross-linked peptides. *Nat Mach Intell* 4, 378-388.

Arndt HD, Schoof S, and Lu JY (2009) Thiopeptide antibiotic biosynthesis. *Angew Chem Int Ed Engl* 48, 6770-6773.

Arnison PG, Bibb MJ, Bierbaum G, Bowers AA, Bugni TS, Bulaj G et al. (2013) Ribosomally synthesized and post−translationally modified peptide natural products: overview and recommendations for a universal nomenclature. *Nat Prod Rep* 30, 108-160.

Aslam B, Wang W, Arshad MI, Khurshid M, Muzammil S, Rasool MH et al. (2018) Antibiotic resistance: a rundown of a global crisis. *Infect Drug Resist* 11, 1645-1658.

Bagley MC, Dale JW, Merritt EA, and Xiong X (2005) Thiopeptide antibiotics. *Chem Rev* 105, 685-714.

Bailly C (2022) The bacterial thiopeptide thiostrepton. An update of its mode of action, pharmacological properties and applications. *Eur J Pharmacol* 914, 174661.

Baumann S, Schoof S, Bolten M, Haering C, Takagi M, Shin−ya K et al. (2010) Molecular determinants of microbial resistance to thiopeptide antibiotics. *J Am Chem Soc* 132, 6973-6981.

Baym M, Stone LK, and Kishony R (2016) Multidrug evolutionary strategies to reverse antibiotic resistance. *Science* 351, aad3292.

Bennallack PR, Bewley KD, Burlingame MA, Robison RA, Miller SM, and Griffitts JS (2016) Reconstitution and minimization of a micrococcin biosynthetic pathway in *Bacillus subtilis. J Bacteriol* 198, 2431-2438.

Bennallack PR, Burt SR, Heder MJ, Robison RA, and Griffitts JS (2014) Characterization of a novel plasmid-borne thiopeptide gene cluster in *Staphylococcus epidermidis* strain 115. *J Bacteriol* 196, 4344-4350.

Bérdy J (2012) Thoughts and facts about antibiotics: where we are now and where we are heading. *J Antibiot* 65, 385-395.

Bewley KD, Bennallack PR, Burlingame MA, Robison RA, Griffitts JS, and Miller SM (2016) Capture of micrococcin biosynthetic intermediates reveals C-terminal processing as an obligatory step for *in vivo* maturation. *Proc Natl Acad Sci U S A* 113, 12450-12455.

Bhavsar AP, Zhao X, and Brown ED (2001) Development and characterization of a xylose-dependent system for expression of cloned genes in *Bacillus subtilis*: conditional complementation of a teichoic acid mutant. *Appl Environ Microbiol* 67, 403-410.

Bleich R, Watrous JD, Dorrestein PC, Bowers AA, and Shank EA (2015) Thiopeptide antibiotics stimulate biofilm formation in *Bacillus subtilis. Proc Natl Acad Sci U S A* 112, 3086-3091.

Booth WT, Schlachter CR, Pote S, Ussin N, Mank NJ, Klapper V et al. (2018) Impact of an N-terminal polyhistidine tag on protein thermal stability. *ACS Omega* 3, 760-768.

Bowers AA, Acker MG, Koglin A, and Walsh CT (2010a) Manipulation of thiocillin variants by prepeptide gene replacement: structure, conformation, and activity of heterocycle substitution mutants. *J Am Chem Soc* 132, 7519-7527.

Bowers AA, Walsh CT, and Acker MG (2010b). Genetic interception and structural characterization of thiopeptide cyclization precursors from *Bacillus cereus*. *J Am Chem Soc* 132, 12182-12184.

Boyce JM (2007) Environmental contamination makes an important contribution to hospital infection. *J Hosp Infect* 65, 50-54.

Brown LCW, Acker MG, Clardy J, Walsh CT, and Fischbach MA (2009) Thirteen posttranslational modifications convert a 14-residue peptide into the antibiotic thiocillin. *Proc Natl Acad Sci U S A* 106, 2549-2553.

Burkhart BJ, Hudson GA, Dunbar KL, and Mitchell DA (2015). A prevalent peptide-binding domain guides ribosomal natural product biosynthesis. *Nat Chem Biol* 11, 564-570.

Burkhart BJ, Kakkar N, Hudson GA, Van Der Donk WA, and Mitchell DA (2017a) Chimeric leader peptides for the generation of non-natural hybrid RiPP products. *ACS Cent Sci* 3, 629-638.

Burkhart BJ, Schwalen CJ, Mann G, Naismith JH, and Mitchell DA (2017b) YcaO-dependent posttranslational amide activation: biosynthesis, structure, and function. *Chem Rev* 117, 5389-5456.

Bycroft BW and Gowland MS (1978) The structure of the highly modified peptide antibiotics micrococcin P1 and P2. *J Chem Soc Chem Commun* 6, 256-258.

Caesar LK, Montaser R, Keller NP, and Kelleher NL (2021) Metabolomics and genomics in natural products research: complementary tools for targeting new chemical entities. *Nat Prod Rep* 38, 2041-2065.

Chain E, Florey HW, Gardner AD, Heatley NG, Jennings MA, Orr-Ewing J et al. (1940) Penicillin as a chemotherapeutic agent. *Lancet* 236, 226-228.

Chan DC and Burrows LL (2021) Thiopeptides: antibiotics with unique chemical structures and diverse biological activities. *J Antibiot* 74, 161-175.

Cheung WL, Chen MY, Maksimov MO, and Link AJ (2016) Lasso peptide biosynthetic protein LarB1 binds both leader and core peptide regions of the precursor protein LarA. *ACS Cent Sci* 2, 702-709.

Ciufolini MA, and Lefranc D (2010) Micrococcin P1: structure, biology and synthesis. *Nat Prod Rep* 27, 330-342.

Clinical and Laboratory Standards Institute (1999) Methods for determining bactericidal activity of antimicrobial agent, (1st ed.). CLSI, USA.

Clinical and Laboratory Standards Institute (2018) Methods for dilution antimicrobial susceptibility test for bacteria that grow aerobically, (11th ed.). CLSI, USA.

Cogan DP, Hudson GA, Zhang Z, Pogorelov TV, Van Der Donk WA, Mitchell DA et al. (2017) Structural insights into enzymatic [4+2] aza-cycloaddition in thiopeptide antibiotic biosynthesis. *Proc Natl Acad Sci U S A* 114, 12928-12933.

Cox CL, Doroghazi JR, and Mitchell DA (2015) The genomic landscape of ribosomal peptides containing thiazole and oxazole heterocycles. *BMC Genom* 16, 1-16.

Cui W, Han L, Suo F, Liu Z, Zhou L, and Zhou Z (2018) Exploitation of *Bacillus subtilis* as a robust workhorse for production of heterologous proteins and beyond. *World J Microbiol Biotechnol* 34, 1-19.

Czepiel J, Biesiada G, Brzozowski T, Ptak-Belowska A, Perucki W, Birczynska M et al. (2014) The role of local and systemic cytokines in patients infected with *Clostridium difficile. J Physiol Pharmacol* 65, 695-703.

Dadgostar P (2019) Antimicrobial resistance: implications and costs. *Infect Drug Resist* 12, 3903-3910.

Dai J, Gong J, and Guo R (2022) Real-world comparison of fidaxomicin versus vancomycin or metronidazole in the treatment of *Clostridium difficile* infection: a systematic review and meta-analysis. *Eur J Clin Pharmacol* 78, 1727-1737.

Daniels LM and Kufel WD (2018) Clinical review of *Clostridium difficile* infection: An update on treatment and prevention. *Expert Opin Pharmacother* 19, 1759-1769.

Degiacomi G, Personne Y, Mondesert G, Ge X, Mandava CS, Hartkoorn RC, et al. (2016) Micrococcin P1 − A bactericidal thiopeptide active against *Mycobacterium tuberculosis*. *Tuberculosis* 100, 95-101.

Dhingra S, Rahman NAA, Peile E, Rahman M, Sartelli M, Hassali MA et al. (2020) Microbial resistance movements: an overview of global public health threats posed by antimicrobial resistance, and how best to counter. *Front Public Health* 8, 531.

DiFeo TJ (2003) Drug product development: A technical review of chemistry, manufacturing, and controls information for the support of pharmaceutical compound licensing activities. *Drug Dev Ind Pharm* 9, 939-958.

Dunbar KL, Scharf DH, Litomska A, and Hertweck C (2017). Enzymatic carbon–sulfur bond formation in natural product biosynthesis. *Chem Rev* 117, 5521-5577.

Eastgate MD, Schmidt MA, and Fandrick KR (2017). On the design of complex drug candidate syntheses in the pharmaceutical industry. *Nat Rev Chem* 1, 0019.

Ehling−Schulz M, Lereclus D, and Koehler TM (2019) The *Bacillus cereus* group: *Bacillus* species with pathogenic potential. *Microbiol Spectr* 7, 7.3.6.

Engelhardt K, Degnes KF, Kemmler M, Bredholt H, Fjærvik E, Klinkenberg G et al. (2010) Production of a new thiopeptide antibiotic, TP-1161, by a marine *Nocardiopsis* species. *Appl Environ Microbiol* 76, 4969-4976.

Fan Y, Chen H, Mu N, Wang W, Zhu K, Ruan Z et al. (2021) Nosiheptide analogues as potential antibacterial agents via dehydroalanine region modifications: semi-synthesis, antimicrobial activity and molecular docking study. *Bioorg Med Chem Lett* 31,115970.

Ferri M, Ranucci E, Romagnoli P, and Giaccone V (2017) Antimicrobial resistance: A global emerging threat to public health systems. *Crit Rev Food Sci Nut* 57, 2857-2876.

Fleming SR, Bartges TE, Vinogradov AA, Kirkpatrick CL, Goto Y, Suga H, Hicks LM, et al. (2019) Flexizyme enabled benchtop biosynthesis of thiopeptides. *J Am Chem Soc* 141, 758-762.

Flinspach K, Kapitzke C, Tocchetti A, Sosio M, and Apel AK (2014) Heterologous expression of the thiopeptide antibiotic GE2270 from *Planobispora rosea* ATCC 53733 in *Streptomyces coelicolor* requires deletion of ribosomal genes from the expression construct. *PLoS One* 9, e90499.

Foulston L (2019) Genome mining and prospects for antibiotic discovery. *Curr Opin Microbiol* 51, 1-8.

Fymat AL (2017) Antibiotics and antibiotic resistance. *Biomed J Sci Tech Res* 1, 1-16.

Gabrovska N, Spasova A, Galacheva A, Kostadinov D, Yanev, N, Milanov V et al. (2022) Tuberculosis in adolescents in Bulgaria for a three-year period: 2018–2020. *Children* 6, 785.

Garg N, Salazar-Ocampo LM, and Van Der Donk WA (2013). *In vitro* activity of the nisin dehydratase NisB. *Proc Natl Acad Sci U S A* 110, 7258-7263.

Grabowski H, Vernon J, and DiMasi JA (2002) Returns on research and development for 1990s new drug introductions. *Pharmacoeconomics* 20, 11-29.

Griffith KL and Grossman AD (2008) Inducible protein degradation in *Bacillus subtilis* using heterologous peptide tags and adaptor proteins to target substrates to the protease ClpXP. *Mol Microbiol* 70, 1012-1025.

Guan Z, Xue D, Abdallah II, Dijkshoorn L, Setroikromo R, Lv G, and Quax WJ (2015) Metabolic engineering of *Bacillus subtilis* for terpenoid production. *Appl Microbiol Biotechnol* 99, 9395-9406.

Haft DH, Basu MK, and Mitchell DA (2010). Expansion of ribosomally produced natural products: a nitrile hydratase-and Nif11-related precursor family. *BMC biol* 8, 1-15.

Hall W (2018) Superbugs: An arms race against bacteria. *Harvard University Press,* USA.

Hang PC and Honek JF (2005) Electronic structure calculations on the thiazole-containing antibiotic thiostrepton: molecular mechanics, semi-empirical and ab initio analyses. *Bioorg Med Chem Lett* 15, 1471-1474.

Hare R (1982) New light on the history of penicillin. *Med Hist* 26, 1-24.

Harms JM, Wilson DN, Schluenzen F, Connell SR, Stachelhaus T, Zaborowska Z et al. (2008) Translational regulation via L11: molecular switches on the ribosome turned on and off by thiostrepton and micrococcin. *Mol Cell* 30, 26-38.

Harvey AL, Edrada-Ebel R, and Quinn RJ (2015) The re-emergence of natural products for drug discovery in the genomics era. *Nat Rev Drug Discov* 14, 111-129.

Harwood CR, Pohl S, Smith W, and Wipat A (2013) *Bacillus subtilis*: model Gram−positive synthetic biology chassis, *Methods Microbiol* 40, 87-117. Academic Press, USA.

Helle S, Cameron D, Lam J, White B, and Duff S (2003) Effect of inhibitory compounds found in biomass hydrolysates on growth and xylose fermentation by a genetically engineered strain of *S. cerevisiae. Enzyme Microb Technol* 33, 786-792.

Hetrick KJ and van der Donk WA (2017) Ribosomally synthesized and post-translationally modified peptide natural product discovery in the genomic era. *Curr Opin Chem Biol* 38, 36-44.

Hudson GA and Mitchell DA (2018) RiPP antibiotics: biosynthesis and engineering potential. *Curr Opin Microbiol* 45, 61-69.

Hutchings MI, Truman AW, and Wilkinson B (2019) Antibiotics: past, present and future. *Curr Opin Microbiol* 51, 72-80.

Hwang HJ, Son YJ, Kim D, Lee J, Shin YJ, Kwon Y et al. (2022) Diversity-oriented routes to thiopeptide antibiotics: total synthesis and biological evaluation of micrococcin P2. *Org Biomol Chem* 20, 1893-1899.

Ishida N, Kumagai K, Niida T, Tsuruoka T, and Yumoto H (1967) Nojirimycin, a new antibiotic. II. Isolation, characterization and biological activity. *J Antibiot* 20, 66-71.

Jarrad AM, Karoli T, Blaskovich MAT, Lyras D and Cooper MA (2015) *Clostridium difficile* drug pipeline: Challenges in discovery and development of new agents. *J Med Chem* 58, 5164-5185

Jin L, Wu X, Xue Y, Jin Y, Wang S, Chen Y (2017) Mutagenesis of NosM leader peptide reveals important elements in nosiheptide biosynthesis. *Appl Environ Microbiol* 83, e02880-16.

Just−Baringo X, Albericio F, and Álvarez M (2014) Thiopeptide antibiotics: retrospective and recent advances. *Mar Drugs* 12, 317-351.

Karaiskos I and Giamarellou H (2014) Multidrug-resistant and extensively drug-resistant Gram-negative pathogens: current and emerging therapeutic approaches. *Expert Opin Pharmacother* 15, 1351-1370.

Kaur J, Kumar A, and Kaur J (2018) Strategies for optimization of heterologous protein expression in *E. coli*: Roadblocks and reinforcements. *Int J Biol Macromol* 106, 803-822.

Kim TH, Hanh BTB, Kim G, Lee DG, Park JW, Lee SE. et al. (2019) Thiostrepton: a novel therapeutic drug candidate for *Mycobacterium abscessus* infection. *Molecules* 24, 4511.

Khadye VS, Sawant S, Shaikh K, Srivastava R, Chandrayan S and Odaneth AA (2021). Optimal secretion of thermostable Beta-glucosidase in *Bacillus subtilis* by signal peptide optimization. *Protein Expr Purif* 182, 105843.

Kloosterman AM, Cimermancic P, Elsayed SS, Du C, Hadjithomas M, Donia MS et al. (2020a) Expansion of RiPP biosynthetic space through integration of pan-genomics and machine learning uncovers a novel class of lanthipeptides. *PLoS Biol* 18, e3001026.

Kloosterman AM, Shelton KE, van Wezel GP, Medema MH and Mitchell DA (2020b) RRE-Finder: a genome-mining tool for class-independent RiPP discovery. *mSystems* 5, e00267-20.

Koon HW, Wang J, Mussatto CC, Ortiz C, Lee EC, Tran DHN et al. (2018) Fidaxomicin and OP-1118 inhibit *Clostridium difficile* toxin A and B mediated inflammatory responses via inhibition of NF-κB activity. *Antimicrob Agents Chemother* 62, e01513-01517.

LaMarche MJ, Leeds JA, Amaral A, Brewer JT, Bushell SM, Deng G et al. (2012) Discovery of LFF571: an investigational agent for *Clostridium difficile* infection. *J Med Chem* 55, 2376-2387.

LaMarche MJ, Leeds JA, Amaral K, Brewer JT, Bushell SM, Dewhurst JM et al. (2011) Antibacterial optimization of 4-aminothiazolyl analogues of the natural product GE2270A: identification of the cycloalkylcarboxylic acids. *J Med Chem* 54, 8099-8109.

Ledneczki I, Tapolcsányi P, Gábor E, Éles J, Greiner I, Schmidt É et al. (2017) Discovery of novel steroidal histamine H3 receptor antagonists/inverse agonists. *Bioorg Med Chem Lett* 27, 4525-4530.

Leeds JA, Sachdeva M, Mullin S, Dzink-Fox J, and LaMarche MJ (2012) Mechanism of action of and mechanism of reduced susceptibility to the novel anti-*Clostridium difficile* compound LFF571. *Antimicrob Agents Chemother* 56, 4463-4465.

Leeds JA (2016) Antibacterials developed to target a single organism: mechanisms and frequencies of reduced susceptibility to the novel anti-*Clostridium difficile* compounds fidaxomicin and LFF571. *Cold Spring Harb Perspect Med* 6, a025445.

Lefranc D and Ciufolini MA (2009) Total synthesis and stereochemical assignment of micrococcin P1. *Angew Chem Int Ed* 48, 4198-4201.

Lewis K (2013) Platforms for antibiotic discovery. *Nat Rev Drug Discov* 12, 371-387.

Liao R, Duan L, Lei C, Pan H, Ding Y, Zhang Q et al. (2009). Thiopeptide biosynthesis featuring ribosomally synthesized precursor peptides and conserved posttranslational modifications. *Chem Biol* 16, 141-147.

Maarten L, Snoeck N, De Maeseneire SL, and Soetaert WK (2018) Hidden antibiotics: Where to uncover? *Biotechnol Adv* 36, 2201-2218.

Mahanta N, Zhang Z, Hudson, GA, Van Der Donk WA, and Mitchell DA (2017) Reconstitution and substrate specificity of the radical S-adenosyl-methionine thiazole C-methyltransferase in thiomuracin biosynthesis. *J Am Chem Soc* 139, 4310-4313.

Matsumoto H, Shiotani A, and Graham DY (2019) Current and future treatment of *Helicobacter pylori* infections. *Adv Exp Med Biol* 1149, 211-225.

Melby JO, Nard NJ, and Mitchell DA (2011) Thiazole/oxazole-modified microcins: complex natural products from ribosomal templates. *Curr Opin Chem Biol* 15, 369-378.

Miao CC, Han LL, Lu YB, and Feng H (2020) Construction of a high-expression system in *Bacillus* through transcriptomic profiling and promoter engineering. *Microorganisms* 8, 1030.

Mocek U, Chen LC, Keller PJ, Houck DR, Beale JM, and Floss HG (1989) ^{1}H and ^{13}C NMR assignments of the thiopeptide antibiotic nosiheptide. *J Antibio*t 42, 1643-1648.

Mordhorst S, Ruijne F, Vagstad AL, Kuipers OP, and Piel J (2023) Emulating nonribosomal peptides with ribosomal biosynthetic strategies. *RSC Chem Biol* 4, 7-36.

Morris RP, Leeds JA, Naegeli HU, Oberer L, Memmert K, Weber E et al. (2009) Ribosomally synthesized thiopeptide antibiotics targeting elongation factor Tu. *J Am Chem Soc* 131, 5946-5955.

Mullane K. Lee C, Bressler A, Buitrago M, Weiss K, Dabovic K et al. (2015) Multicenter, randomized clinical trials to compare the safety and efficacy of LFF571 and vancomycin for *Clostridium difficile* infections. *Antimicrob Agents Chemother* 59, 1435-1440.

Myers CL, Hang PC, Ng G, Yuen J, and Honek JF. (2010) Semi-synthetic analogues of thiostrepton delimit the critical nature of tail region modifications in the control of protein biosynthesis and antibacterial activity. *Bioorg Med Chem Lett* 18, 4231-4237.

Nagai K, Kamigiri K, Arao N, Suzumura KI, Kawano Y, Yamaoka M et al. (2003) YM-266183 and YM-266184, novel thiopeptide antibiotics produced by *Bacillus cereus* isolated from a marine sponge i. taxonomy, fermentation, isolation, physico-chemical properties and biological properties. *J Antibiot* 56, 123-128.

Naidu BN, Sorenson ME, Zhang Y, Kim OK, Matiskella JD, Wichtowski JA et al. (2004) Nocathiacin I analogues: synthesis, *in vitro* and *in vivo* biological activity of novel semi-synthetic thiazolyl peptide antibiotics. *Bioorg Med Chem Lett* 14, 5573-5577.

Oka D, Yamaya N, Kuno T, Asakawa Y, Shiragiku T, Chen L et al. (2021) *In vitro* and *in vivo* antibacterial activities of a novel quinolone compound, OPS-2071, against *Clostridioides difficile*. *Antimicrob Agents Chemother* 65, e01170-20.

Oman TJ and Van Der Donk WA (2010) Follow the leader: the use of leader peptides to guide natural product biosynthesis. *Nat Chem Biol* 6, 9-18.

Ortega MA and Van Der Donk WA (2016) New insights into the biosynthetic logic of ribosomally synthesized and post-translationally modified peptide natural products. *Cell Chem Biol* 23, 31-44.

Ovchinnikov KV, Kranjec C, Telke A, Kjos M, Thorstensen T, Scherer S et al. (2021) A strong synergy between the thiopeptide bacteriocin micrococcin P1 and rifampicin against MRSA in a murine skin infection model. *Front Immunol* 12, 676534.

Porse BT, Cundliffe E, and Garrett RA (1999) The antibiotic micrococcin acts on protein L11 at the ribosomal GTPase centre. *J Mol Biol* 287, 33-45.

Renwick MJ, Brogan DM, and Mossialos E (2016) A systematic review and critical assessment of incentive strategies for discovery and development of novel antibiotics. *J Antibiot* 69, 73-88.

Rodríguez V (2022) Insights into post−translational modification enzymes from RiPPs: A toolkit for applications in peptide synthesis. *Biotechnol Adv* 107908.

Saleh MM, Frisbee AL, Leslie JL, Buonomo EL, Cowardin CA, Ma JZ et al. (2019) Colitis-induced Th17 cells increase the risk for severe subsequent *Clostridium difficile* infection. *Cell Host Microbe* 25, 756-765.

Schwalen CJ, Hudson GA, Kille B, and Mitchell DA (2018). Bioinformatic expansion and discovery of thiopeptide antibiotics. *J Am Chem Soc* 140, 9494-9501.

Shen X, Mustafa M, Chen Y, Cao Y, and Gao J (2019) Natural thiopeptides as a privileged scaffold for drug discovery and therapeutic development. *Med Chem Res* 28, 1063-1098.

Shoji JI, Kato T, Yoshimura Y, and Tori K (1981) Structural studies on thiocillins I, II and III (studies on antibiotics from the genus *Bacillus*. Xxix). *J Antibiot* 34, 1126-1136.

Son YJ, Kim YR, Oh SH, Jung S, Ciufolini MA, Hwang HJ et al. (2022). Micrococcin P2 Targets *Clostridioides difficile*. *J Nat Prod* 85, 1928-1935.

Son YJ, Hwang HJ, and Kwon Y (2023) Heterologous synthesis and characterization of thiocillin IV. *ACS Chem Biol* 18, 265-272.

Stelzmueller I, Goegele H, Biebl M, Wiesmayr S, Berger N, Tabarelli W et al. (2007) *Clostridium difficile* colitis in solid organ transplantation-a single center experience. *Dig Dis Sci* 52, 3231-3236.

Su T (1948) Micrococcin. An antibacterial substance formed by a strain of micrococcus. *Br J Exp Pathol* 29, 473-481.

Su Y, Liu C, Fang H, and Zhang D (2020) *Bacillus subtilis*: a universal cell factory for industry, agriculture, biomaterials and medicine. *Microb Cell Fact* 19, 1-12.

Sugden R, Kelly R, and Davies S (2016) Combatting antimicrobial resistance globally. *Nat Microbiol* 1, 1-2.

Sukmarini L (2022) Marine bacterial ribosomal peptides: Recent genomics and synthetic biology-based discoveries and biosynthetic studies. *Mar Drugs* 20, 544.

Tabbene O, Slimene IB, Djebali K, Mangoni ML, Urdaci MC, and Limam F (2009) Optimization of medium composition for the production of antimicrobial activity by *Bacillus subtilis* B38. *Biotechnol Prog* 25, 1267-1274.

Tacconelli E, Carrara E, Savoldi A, Harbarth S, Mendelson M, Monnet DL et al. (2018) Discovery, research, and development of new antibiotics: the WHO priority list of antibiotic-resistant bacteria and tuberculosis. *Lancet Infect Dis* 18, 318-327.

Tang C, Wang L, Zang L, Wang Q, Qi D, and Dai Z (2023) On-demand biomanufacturing through synthetic biology approach. *Mater Today Bio* 18, 100518.

Taubes G (2008) The bacteria fight back. *Science* 321, 356-361.

Terpe K (2003) Overview of tag protein fusions: from molecular and biochemical fundamentals to commercial systems. *Appl Microbiol Biotechnol* 60, 523-533.

Theuretzbacher U, Outterson K, Engel A, and Karlén A (2020) The global preclinical antibacterial pipeline. *Nat Rev Microbiol* 18, 275-285.

Tran HL, Lexa KW, Julien O, Young TS, Walsh CT, Jacobson MP et al. (2017) Structure-activity relationship and molecular mechanics reveal the importance of ring entropy in the biosynthesis and activity of a natural product. *J Am Chem Soc* 139, 2541-2544.

Truax NJ and Romo D (2020) Bridging the gap between natural product synthesis and drug discovery. *Nat Prod Rep* 37, 1436-1453.

Valiente E, Cairns M, and Wren B (2014) The *Clostridium difficile* PCR ribotype 027 lineage: a pathogen on the move. *Clin Microbiol Infect* 20, 396-404.

Ventola CL (2015) The antibiotic resistance crisis: Part 1: Causes and threats. *Pharm Ther* 40, 277-283.

Vinogradov AA and Suga H (2020) Introduction to thiopeptides: Biological activity, biosynthesis, and strategies for functional reprogramming. *Cell Chem Biol* 27, 1032-1051.

Waksman SA (1953) Streptomycin: Background, isolation, properties, and utilization. *Science* 118, 259-266.

Walker J, Olesker A, Valente L, Rabanal R, and Lukacs G (1977) Total structure of the polythiazole-containing antibiotic micrococcin P. A ^{13}C nuclear magnetic resonance study. *J Chem Soc Chem Commun* 20, 706-708.

Walsh CT (2003) Where will new antibiotics come from? *Nat Rev Microbiol* 1, 65-70.

Walsh CT and Wright G (2005) Introduction: antibiotic resistance. *Chem Rev* 105, 391-394.

Wang RW, Qiu XL, Bols M, Ortega-Caballero F, and Qing FL (2006) Synthesis and biological evaluation of glycosidase inhibitors: gem−difluoromethylenated nojirimycin analogues. *J Med Chem* 49 2989-2997.

Wever WJ, Bogart JW, Baccile JA, Chan AN, Schroeder FC, and Bowers AA (2015) Chemoenzymatic synthesis of thiazolyl peptide natural products featuring an enzyme-catalyzed formal [4+2] cycloaddition. *J Am Chem Soc* 137, 3494-3497.

Wright GD (2017) Opportunities for natural products in 21st century antibiotic discovery. *Nat Prod Rep* 34, 694-701.

Wright PM, Seiple IB, and Myers AG (2014) The evolving role of chemical synthesis in antibacterial drug discovery. *Angew Chem Int Ed Engl* 53, 8840-8869.

Yang X and Van Der Donk WA (2013) Ribosomally synthesized and post-translationally modified peptide natural products: new insights into the role of leader and core peptides during biosynthesis. *Chem Eur J* 19, 7662-7677.

Young TS and Walsh CT (2011) Identification of the thiazolyl peptide GE37468 gene cluster from *Streptomyces* ATCC 55365 and heterologous expression in *Streptomyces lividans*. *Proc Natl Acad Sci U S A* 108, 13053-13058.

Xiang M, Kang Q, and Zhang D (2020) Advances on systems metabolic engineering of *Bacillus subtilis* as a chassis cell. *Synth Syst Biotechnol* 5, 245-251.

Zaman K (2010) Tuberculosis: a global health problem. *J Health Popul Nutr* 28, 111-113.

Zheng Q, Wang Q, Wang S, Wu J, Gao Q, and Liu W (2015) Thiopeptide antibiotics exhibit a dual mode of action against intracellular pathogens by affecting both host and microbe. *Chem Biol* 22, 1002-1007.

Zhou F, Hamza T, Fleur AS, Zhang Y, Yu H, Chen K et al. (2018) Mice with inflammatory bowel disease are susceptible to *Clostridium difficile* infection with severe disease outcomes. *Inflamm Bowel Dis* 24, 573-582.

Zhu D, Sorg JA, and Sun X (2018) *Clostridioides difficile* biology: sporulation, germination, and corresponding therapies for *C. difficile* infection. *Front Cell Infect Microbiol* 8, 29.

Supplementary Materials

Figure S1. ^{1}H-NMR of micrococcin P acid (400 MHz, DMSO-d_6).

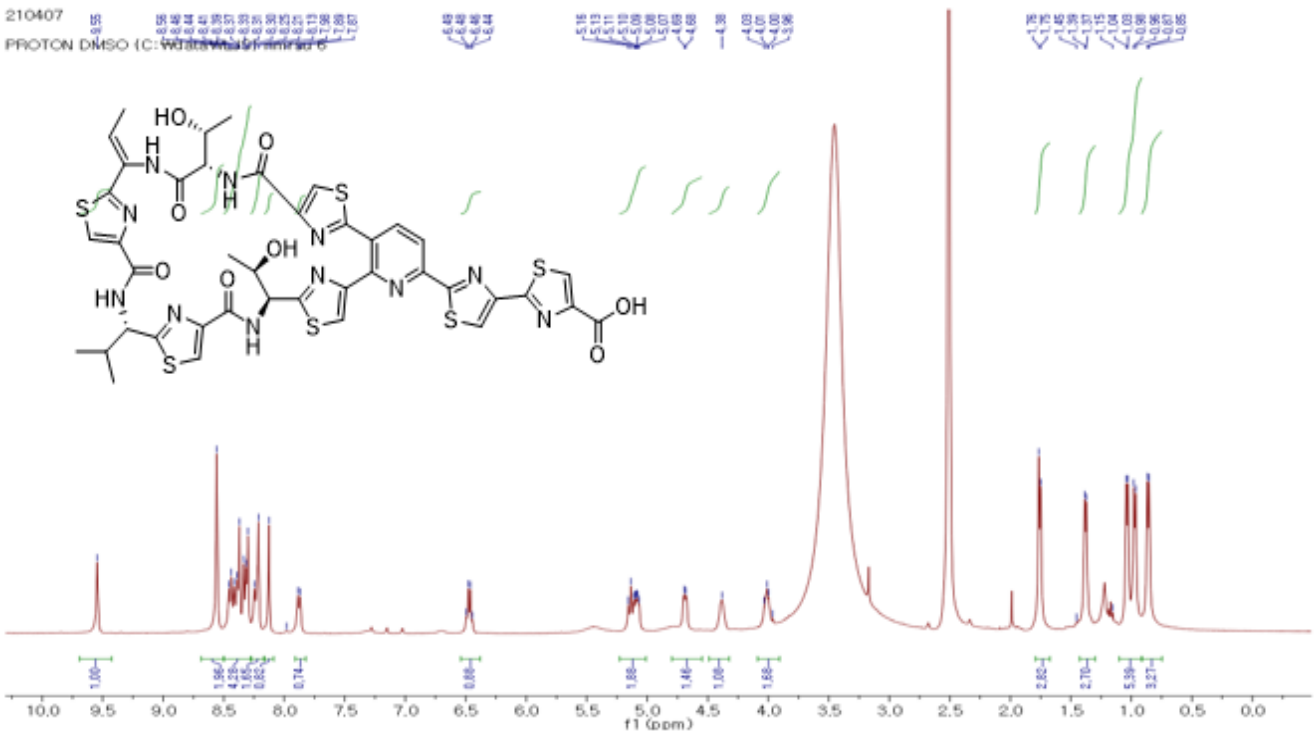

Figure S2. ^{13}C-NMR of micrococcin P acid (400 MHz, DMSO-d_6).

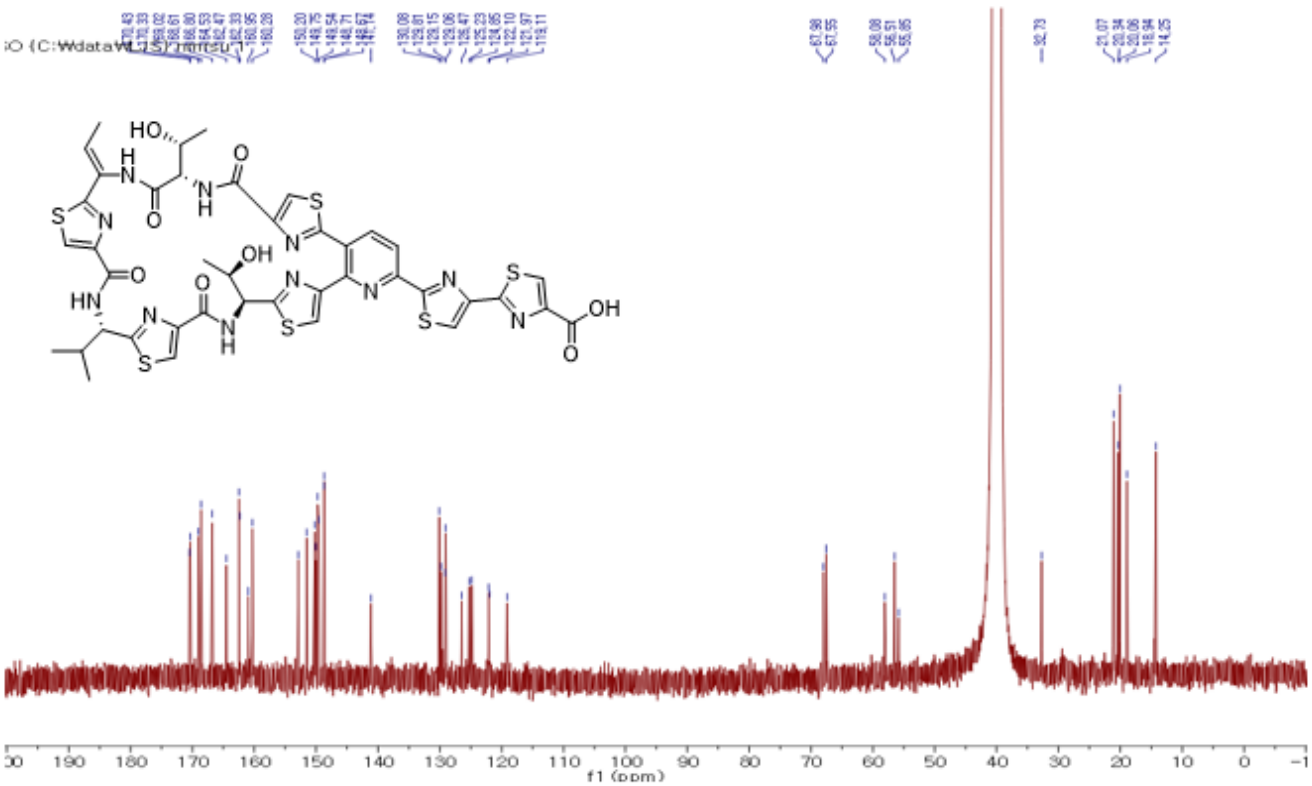

Figure S3. Mass spectra of purified thiocillin IV (A) and micrococcin P2 (B). Additional methyl groups in Thiocillin IV correspond to the mass differences.

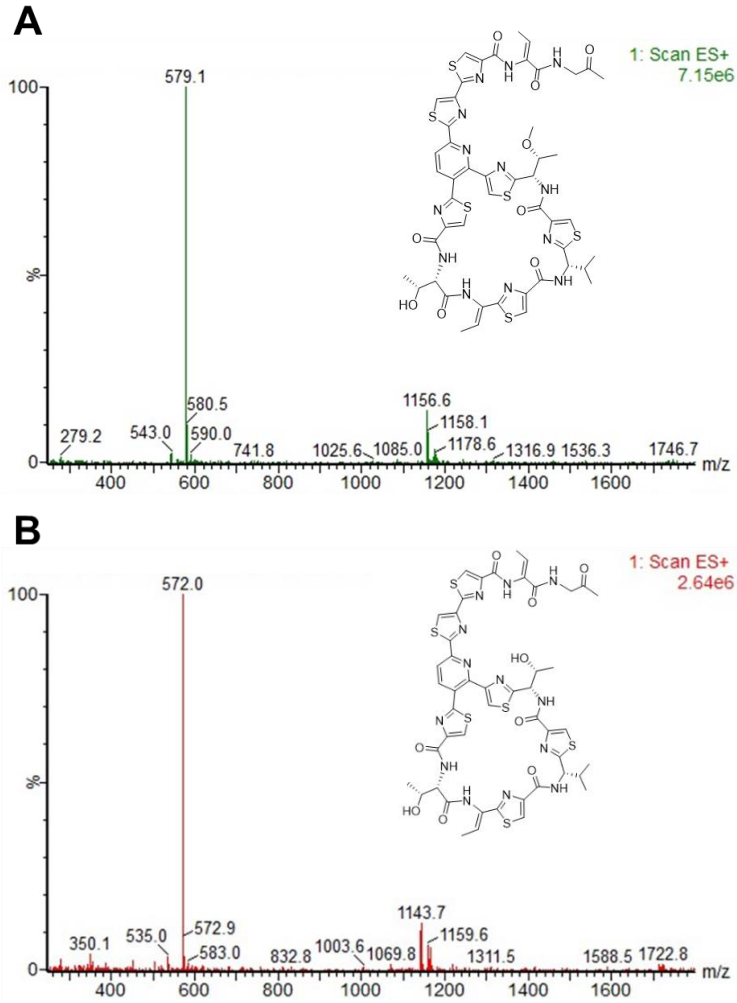

Figure S4. UV absorption spectra of purified thiocillin IV (A) and micrococcin p2 (B). These two thiopeptides showed an identical UV absorption spectrum.

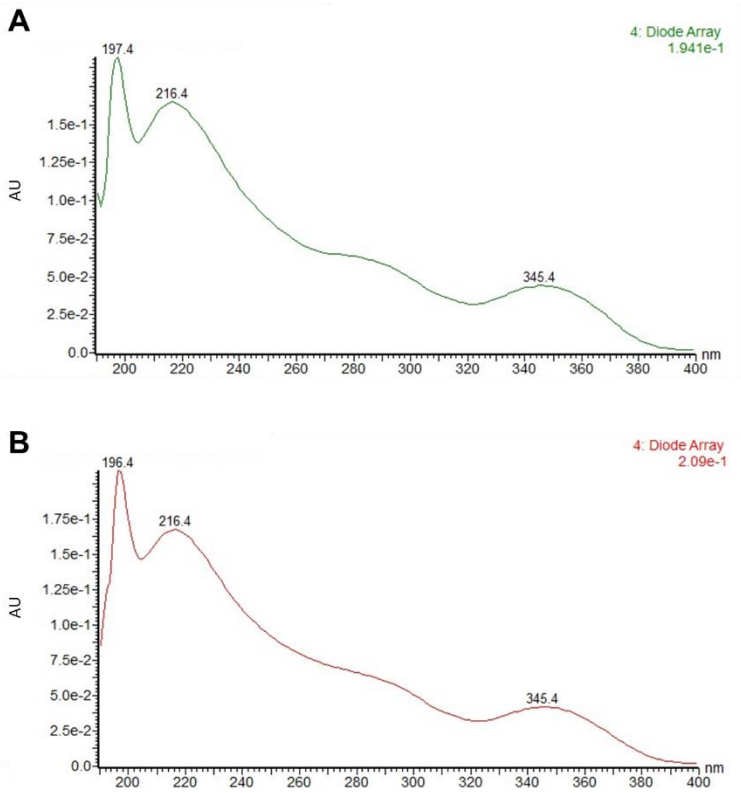

Figure S5. High-resolution electrospray ionization mass spectrometry (HR ESI-MS) analysis of thiocillin IV.

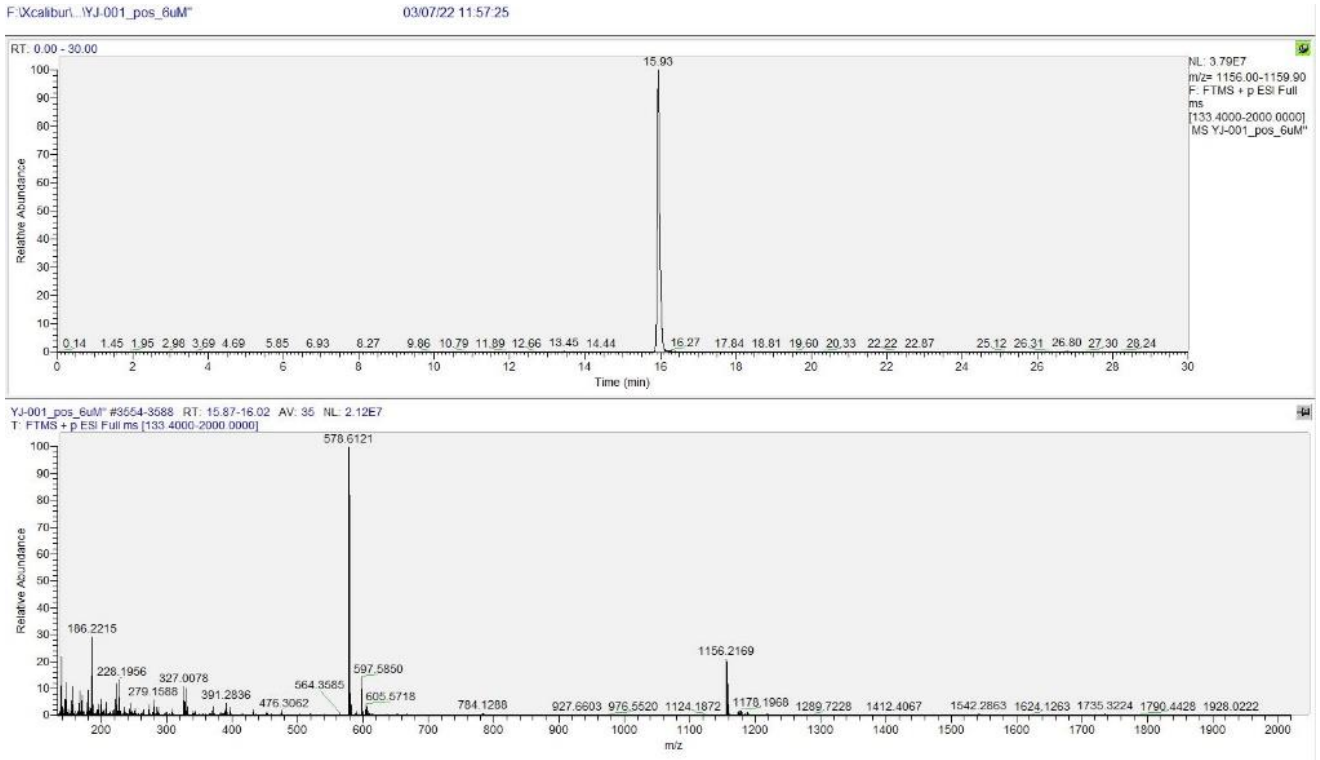

Figure S6. ^{1}H-NMR spectra of thiocillin IV (600 MHz, $CDCl_3$).

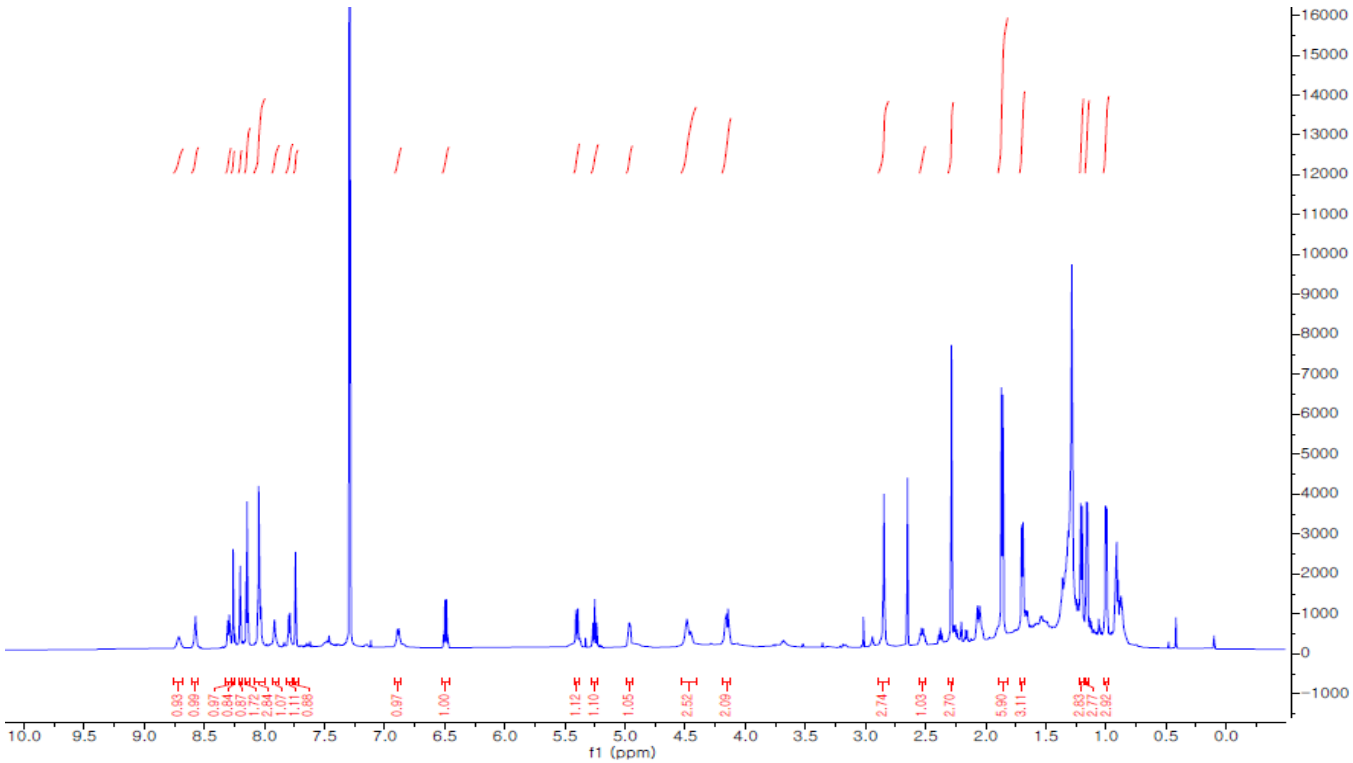

Figure S7. ^{13}C-NMR spectra of thiocillin IV (151 MHz, $CDCl_3$).

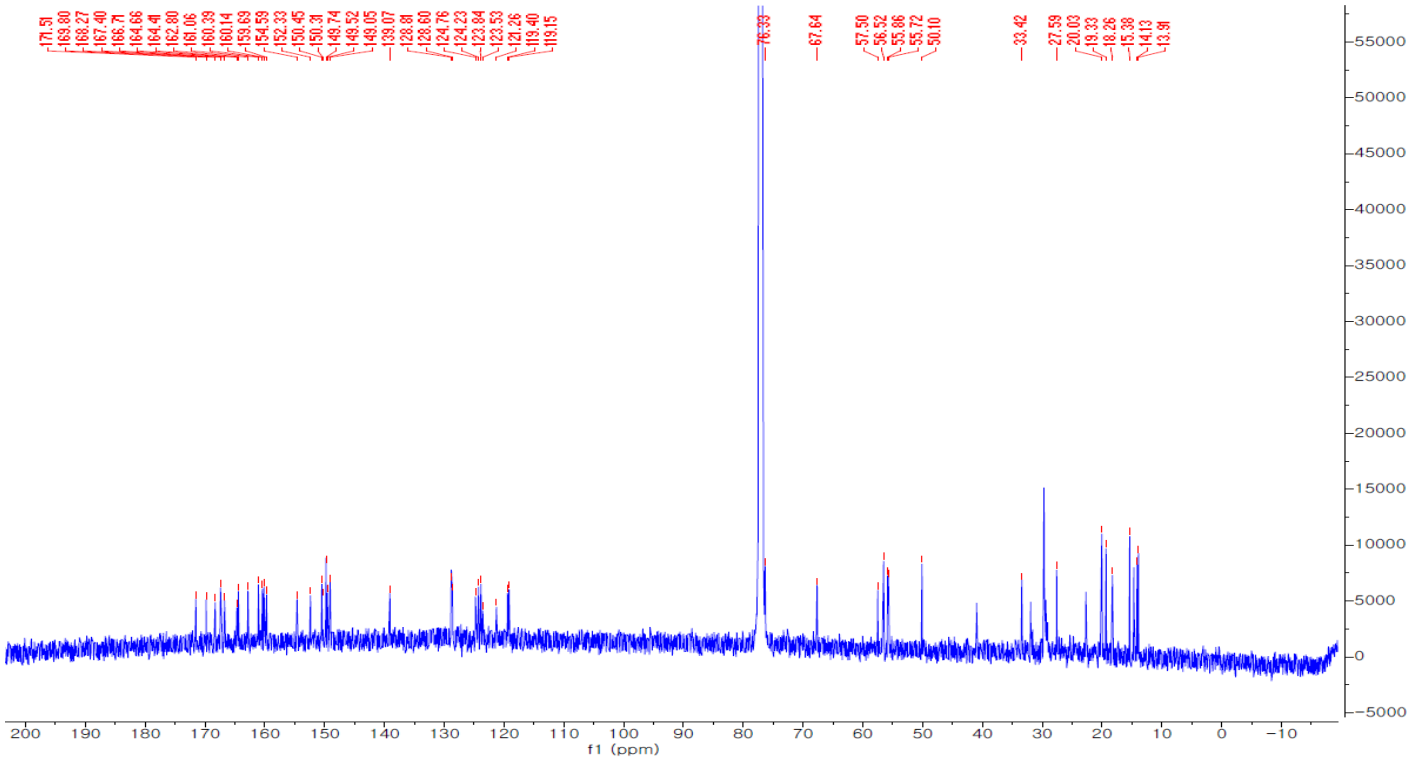

Figure S8. HMBC spectra of thiocillin IV (600 MHz, $CDCl_3$).

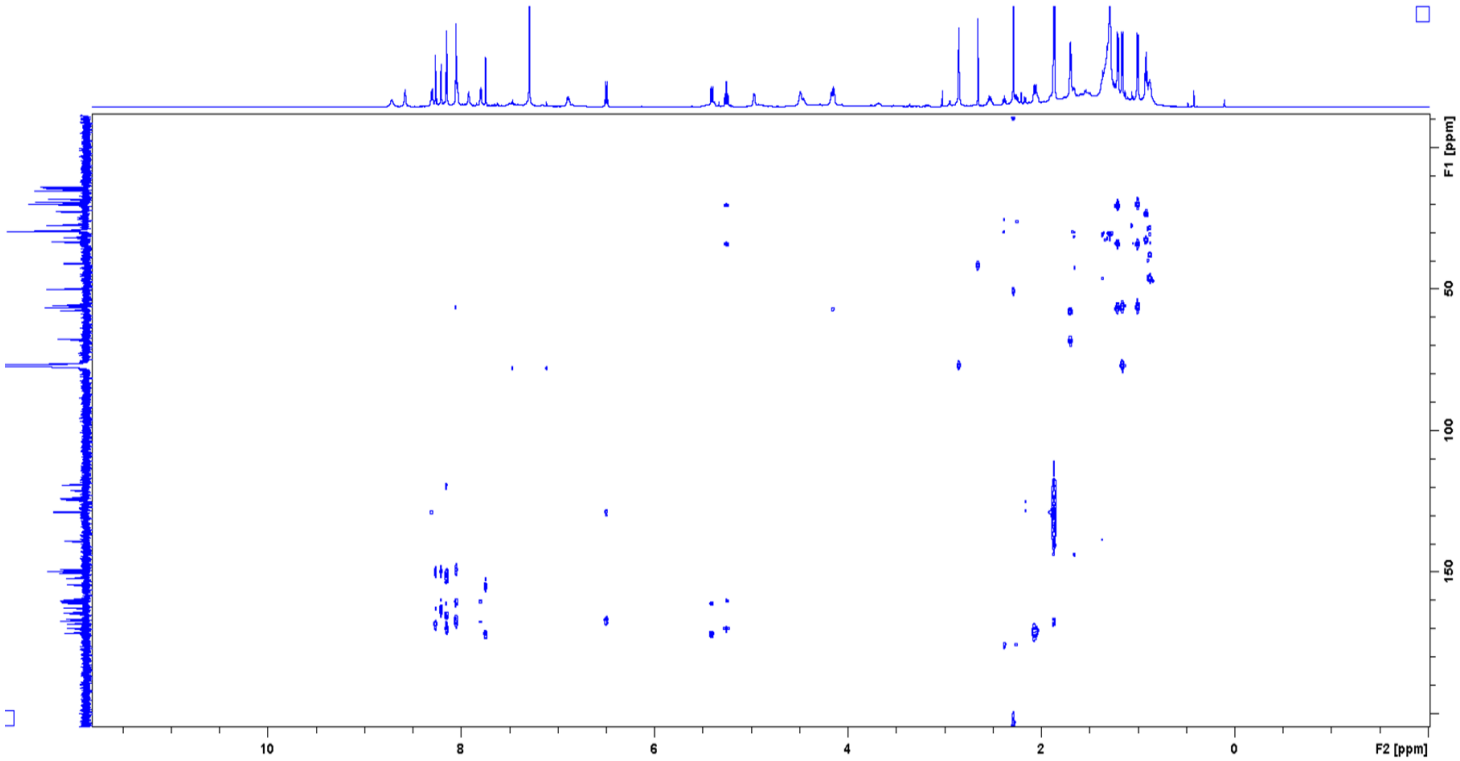

Figure S9. Enlarged HMBC spectra of thiocillin IV (^{1}H: 0-3.0 ppm, ^{13}C: 0-90 ppm). Curved arrows in thiocillin IV structure indicate key HMBC correlations. Linear arrows in HMBC spectra indicate assigned signals.

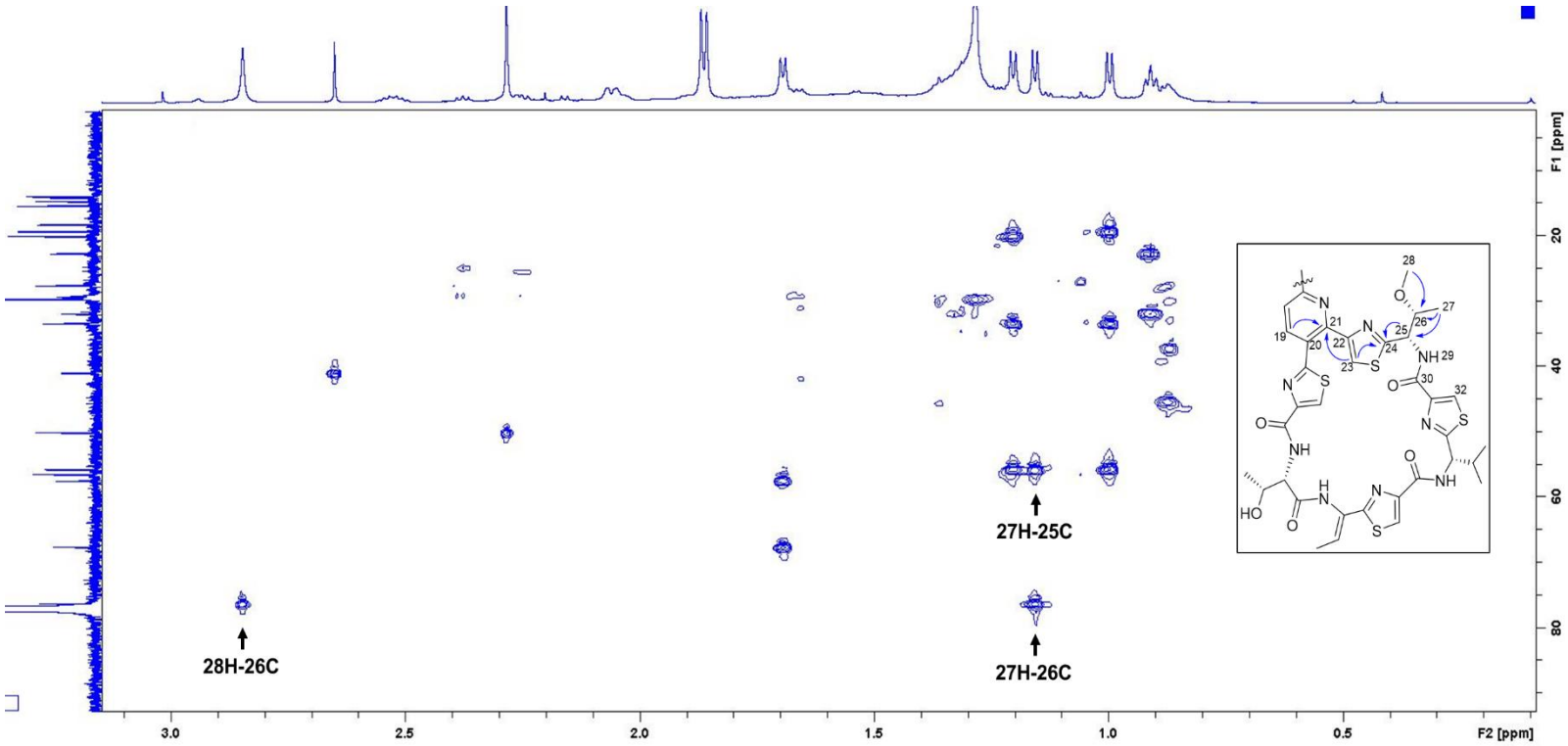

Figure S10. Enlarged HMBC spectra of thiocillin IV (^{1}H: 5-8.5 ppm, ^{13}C: 80-190 ppm). Curved arrows in thiocillin IV structure indicate key HMBC correlations. Linear arrows in HMBC spectra indicate assigned signals.

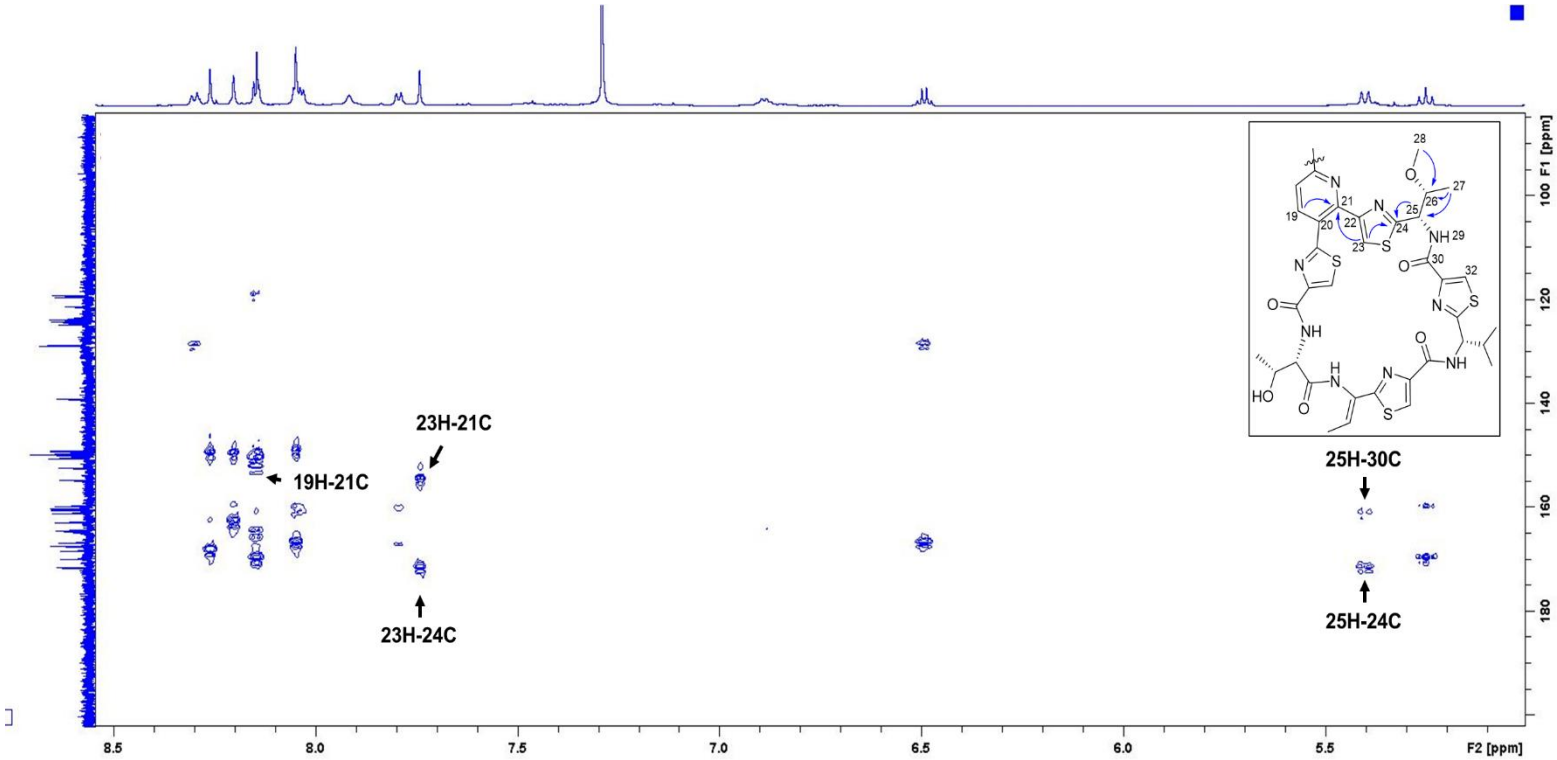

Figure S11. HSQC spectra of thiocillin IV (600 MHz, $CDCl_3$).

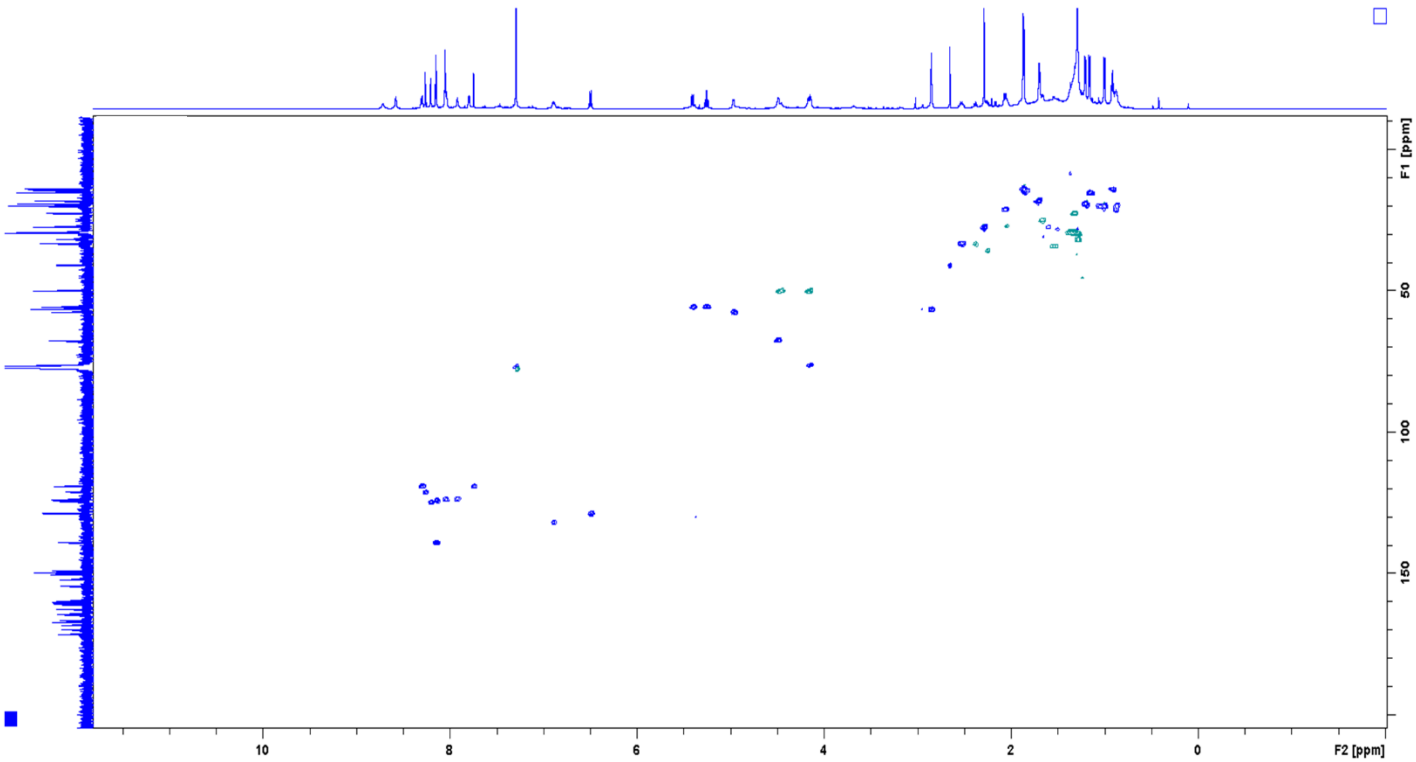

Figure S12. Assigned key HSQC signals in thiocillin IV. Key signals were noted with numbers in HSQC spectra.

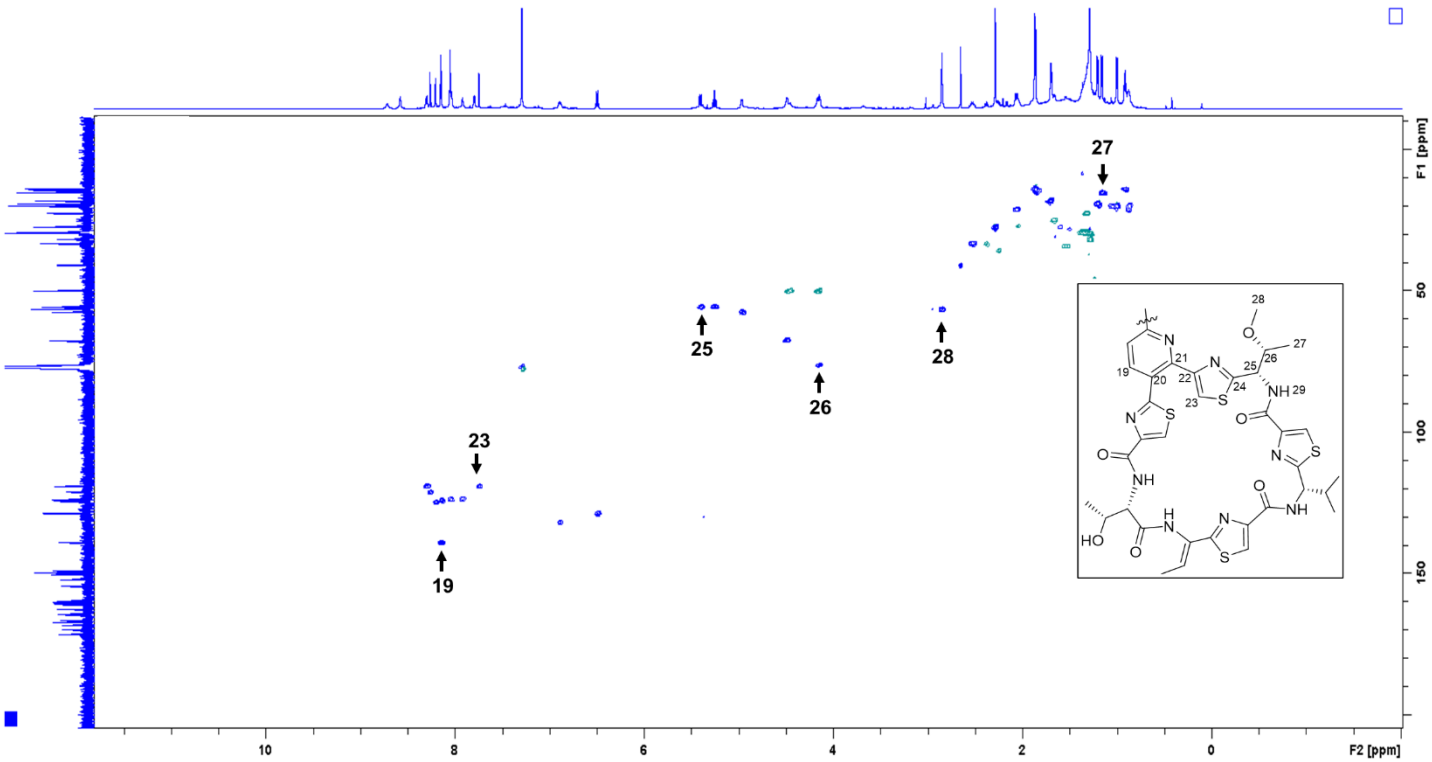

Figure S13. COSY spectra of Thiocillin IV (400 MHz, $CDCl_3$).

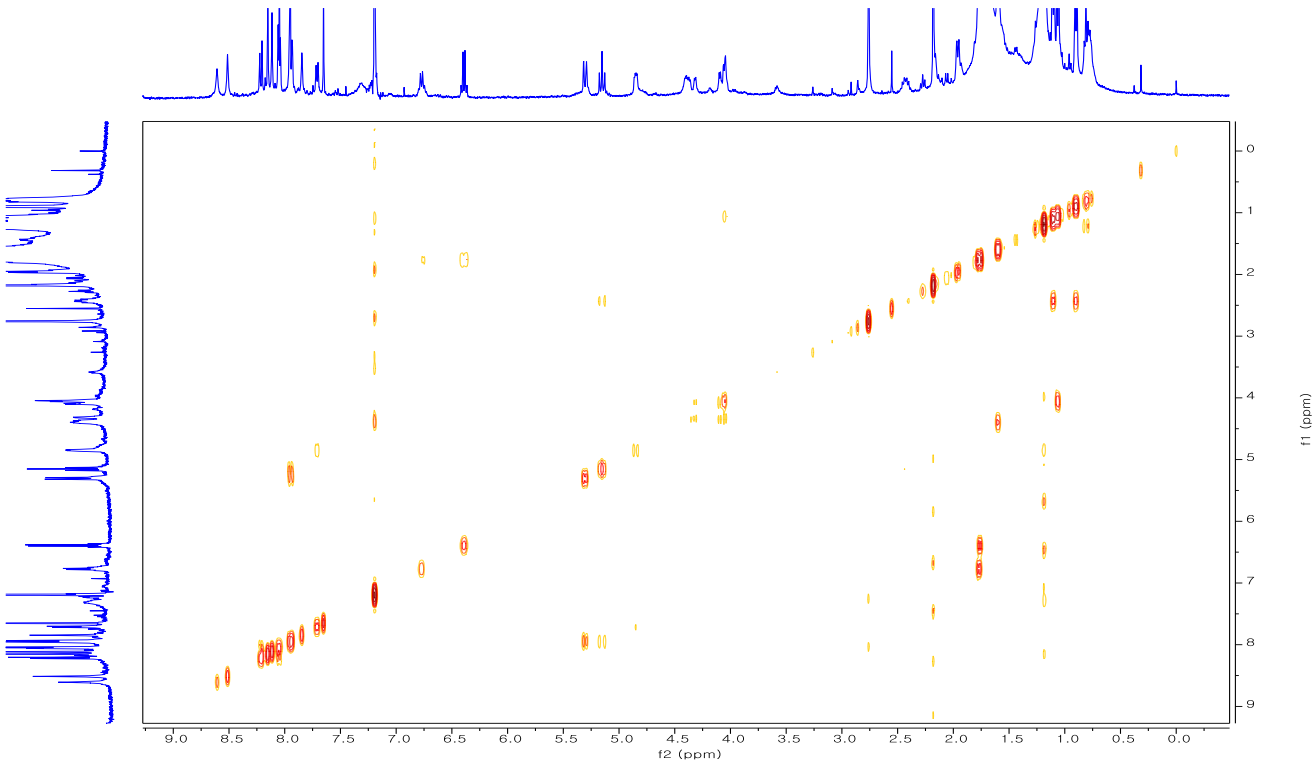

Figure S14. TOCSY spectra of thiocillin IV (400 MHz, $CDCl_3$).

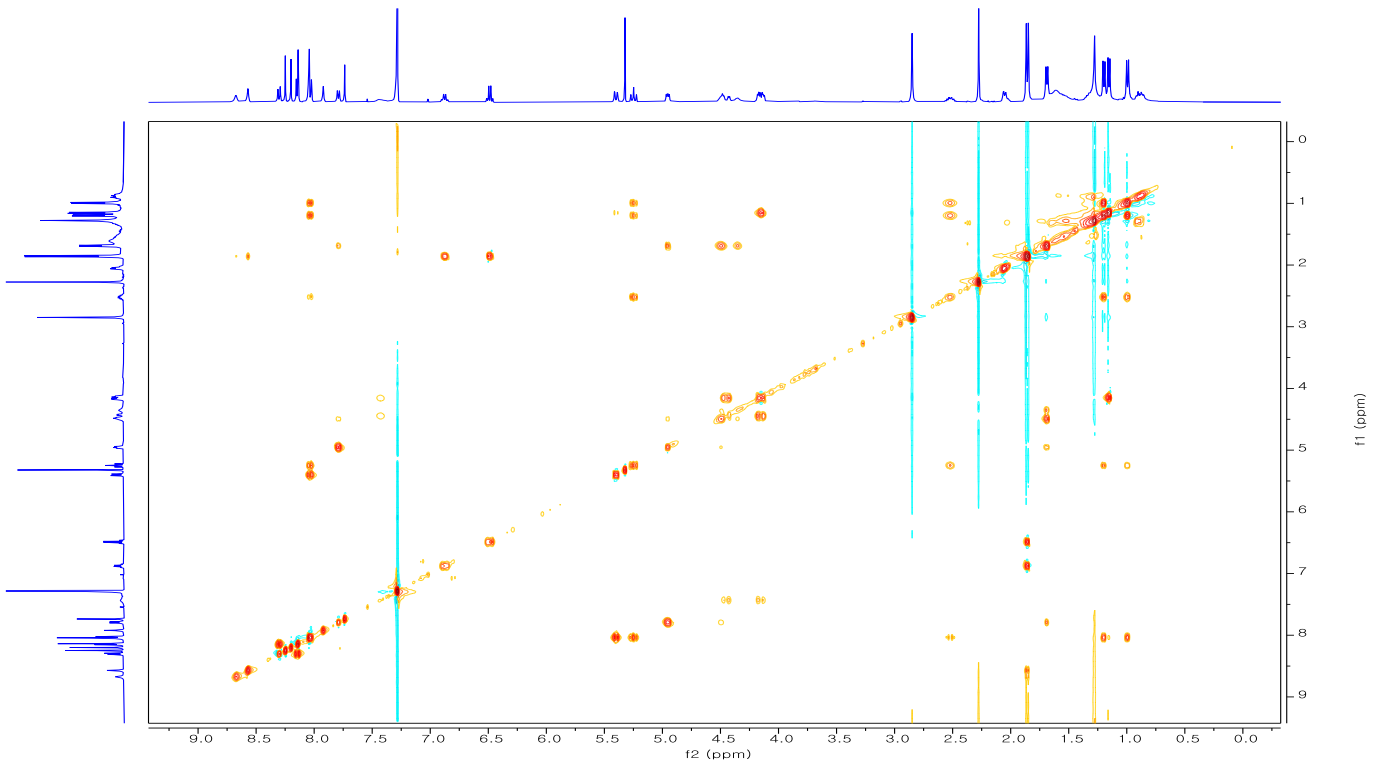

Figure S15. MALDI-TOF-MS spectra of sample 1 (Detect target 2) in reflector mode. Target Mass = 6538.44.

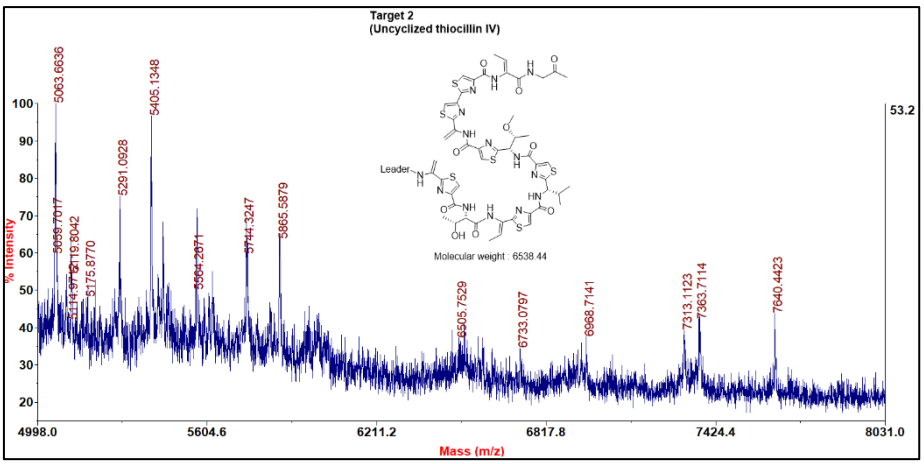

Figure S16. MALDI-TOF-MS spectra of sample 1 (Detect target 2) in linear mode. Target Mass: 6538.44

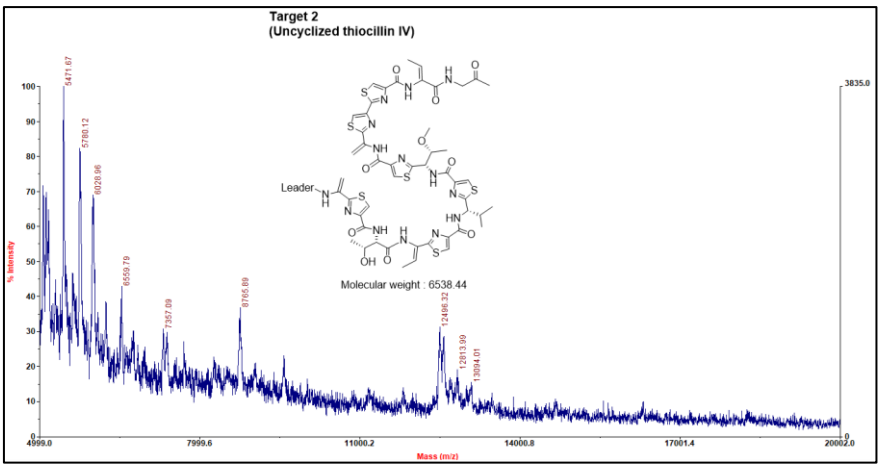

Figure S17. MALDI-TOF-MS spectra of target 3 in reflector mode. Target Mass = 6524.41.

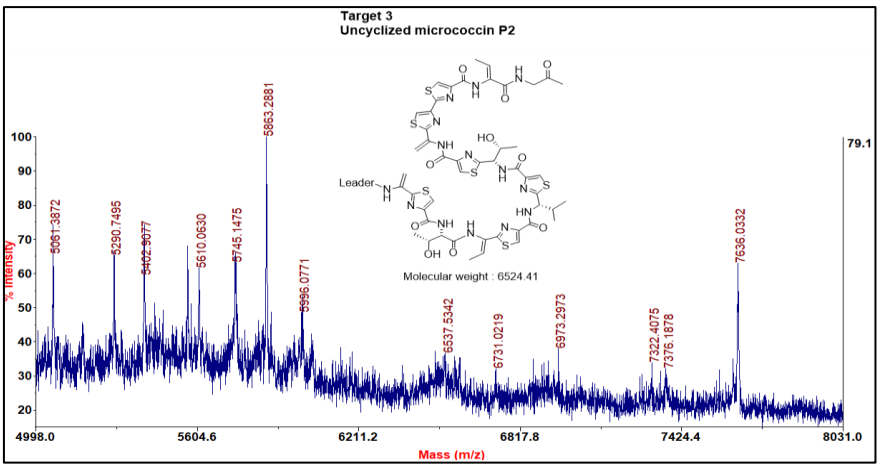

Figure S18. MALDI-TOF-MS spectra of target 3 in linear mode. Target Mass = 6524.41.

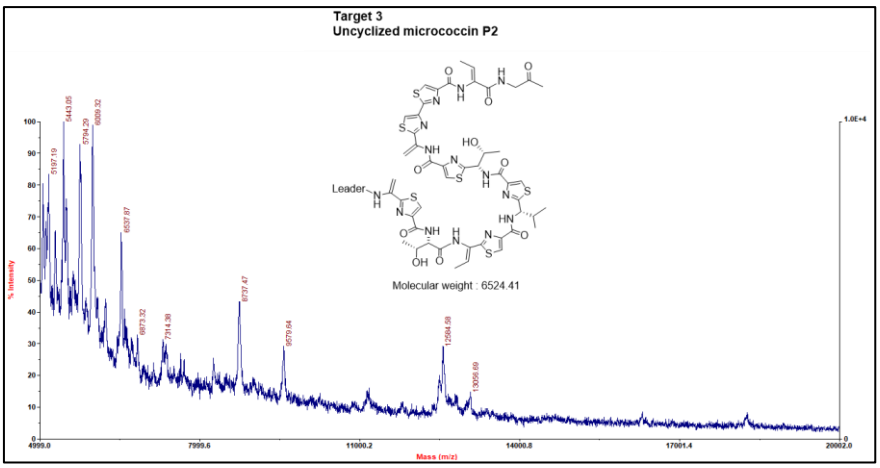

Figure S19. RREfinder analysis result using *tclO* sequence as query.

```
(RREFinder) son@DESKTOP-JROSMQ4:~/RREFinder$ python RRE.py -m exploratory -i input.fast
a -t fasta test3
Reading in file input.fasta
Continuing with 1 queries
Rewriting fasta
hmmsearch --cpu 1 -o output/test3/results/RREfinder_hmm_results.txt --domtblout output/
test3/results/RREfinder_hmm_results.tbl -T 25 data/hmm/RRE_v7_phmms_3_iter.hmm output/t
est3/fastas/fasta_all.fasta
Resubmitting 0 found RREs
Finished. Total time: 1.14 seconds (on 1 cores)
RREfinder exploratory mode preliminary hits found: 0 out of 1
RREfinder exploratory mode resubmitted hits found: 0 out of 1
```

Table S1. ^{1}H NMR structural correlation of thiocillin IV.

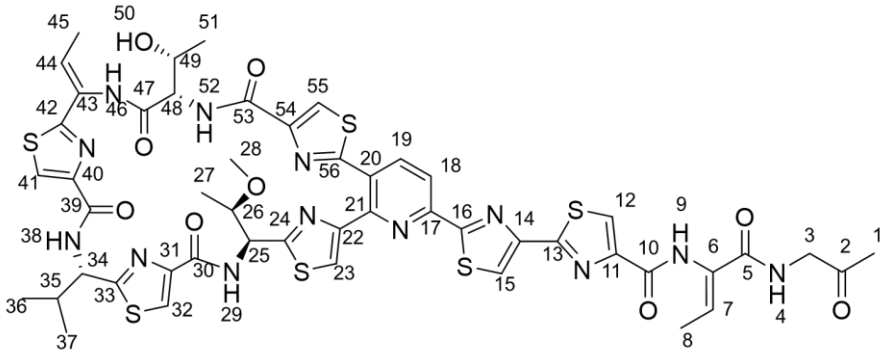

Position	thiocillin IV (ppm, 600 MHz, $CDCl_3$)
46-H^b	8.71 (s, 1H)
9-H^b	8.57(s, 1H)
18-H	8.30 (d, *J* = 8.0 Hz, 1H)
55-H	8.26 (s, 1H)
15-H	8.20 (s, 1H)
19-H 41-H	8.17 – 8.14 (m, 2H)
29-H^b 32-H 38-H^b	8.08 – 7.99 (m, 3H)
12-H	7.92 (s, 1H)
52-H^b	7.79 (d, *J* = 7.1 Hz, 1H)
23-H	7.74 (s, 1H)
7-H	6.89 (d, *J* = 7.0 Hz, 1H)
44-H	6.49 (q, *J* = 6.9 Hz, 1H)
25-H	5.40 (d, *J* = 10.2 Hz, 1H)
34-H	5.25 (t, *J* = 9.7 Hz, 1H)
48-H	4.96 (dd, *J* = 6.8, 3.5 Hz, 1H)
49-H 50-H^b	4.51-4.44 (m, 3H)
26-H 3-2H	4.19-4.11 (m, 2H)
28-3H	2.85 (s, 3H)
35-H	2.53 (ddd, *J* = 16.3, 13.4, 6.7 Hz, 1H)

1-3H	2.28 (s, 3H)
8-3H 45-3H	1.86 (d, *J* = 7.0 Hz, 6H)
51-3H	1.69 (d, *J* = 6.3 Hz, 3H)
37-3H[c]	1.20 (d, *J* = 6.6 Hz, 3H)
27-3H	1.16 (d, *J* = 6.3 Hz, 3H)
37-3H[c]	1.00 (d, *J* = 6.6 Hz, 3H)

a. Data collected for NMR spectra comparison to thiocillin IV
b. NH, OH peaks of thiocillin IV
c. Diastereotopic methyl groups

^{1}H NMR (600 MHz, $CDCl_3$) δ 8.71 (s, 1H), 8.57(s, 1H), 8.30 (d, *J* = 8.0 Hz, 1H), 8.26 (s, 1H), 8.20 (s, 1H), 8.17 – 8.14 (m, 2H), 8.08 – 7.99 (m, 3H), 7.92 (s, 1H), 7.79 (d, *J* = 7.1 Hz, 1H), 7.74 (s, 1H), 6.89 (d, *J* = 7.0 Hz, 1H), 6.49 (q, *J* = 6.9 Hz, 1H), 5.40 (d, *J* = 10.2 Hz, 1H), 5.25 (t, *J* = 9.7 Hz, 1H), 4.96 (dd, *J* = 6.8, 3.5 Hz, 1H), 4.51 – 4.44 (m, 3H), 4.19-4.11(m, 2H), 2.85(s, 3H), 2.53 (ddd, *J* = 16.3, 13.4, 6.7 Hz, 1H), 2.28 (s, 3H), 1.86 (d, *J* = 7.0 Hz, 6H), 1.69 (d, *J* = 6.3 Hz, 3H), 1.20 (d, *J* = 6.6 Hz, 3H), 1.16 (d, *J* = 6.3 Hz, 3H), 1.00 (d, *J* = 6.6 Hz, 3H)

^{13}C NMR (151 MHz, $CDCl_3$) δ 171.5, 169.8, 168.3, 167.4, 166.7, 164.7, 164.4, 162.8, 161.1, 160.4, 160.1, 159.7, 154.6, 152.3, 150.4, 150.3, 149.7, 149.5, 149.1, 139.0, 128.8, 128.6, 124.8, 124.2, 123.8, 123.5, 121.3, 121.2, 119.4, 119.1, 76.3, 67.6, 57.5, 56.5, 55.9, 55.7, 50.1, 33.4, 27.6, 20.0, 19.3, 18.3, 15.4, 14.1, 13.9.

Abstracts in Korean

병원균의 항생제 저항성 문제는 점점 심각해지고 있기 때문에 지속적인 항생 물질의 연구가 필요하다. 티오펩타이드 천연물은 새로운 작용 기전, 낮은 독성, 높은 항생 효능을 지니고 있기 때문에 항생제로 개발하기 좋은 천연물이다. 본 학위논문은 티오펩타이드 천연물 micrococcin P2 와 thiocillin IV 의 생합성, 효능, 구조 동정 연구를 통해 천연물의 특성을 밝히고자 하였다. Chapter 1 에서는 *B. cereus* ATCC 14579 의 thiocillin 유전자 클러스터를 재구성하여 *B. subtilis* 으로부터 생합성한 micrococcin P2 의 물질의 구조 및 항생효과를 검증하였다. Micrococcin P2 는 그람 양성균, 결핵균, 클로스트리디오이데스 디피실 임상분리균주에서 높은 저해 효능을 확인하였다. 특히 낮은 세포독성, 항염증 효능, 체내로 흡수되지 않는 약동학적 특성과 마우스 감염 모델을 통해 micrococcin P2 의 클로스트리디움 감염증 치료제로의 개발 가능성을 확인하였다. 염기 조건에서 micrococcin P2 로부터 생성되는 중간체 micrococcin P acid 는 micrococcin P2 골격을 이용한 항생 물질의 반합성 공정 핵심 물질이 될 가능성을 확인하였다. Chapter 2 에서는 *B. cereus* ATCC 14579 에서 미량 생산되어 정확한 구조 및 활성에 대한 정보가 없었던 thiocillin IV 을 생합성하여 구조 동정 및 생리 활성에 대해 연구하였다. thiocillin IV 은 micrococcin P2 생합성 유전자와 *tclO* 유전자를 *B. subtilis* 에서 함께 발현하여 얻을 수 있었다. Thiocillin IV 생산량은

최적화를 통해 2.4 mg/L 수준을 확보하였다. 구조 분석을 통해 thiocillin IV 구조는 8 번 트레오닌의 잔기에 선택적으로 O-methylation 되어 있음을 확인하였다. 항균 활성은 그람 양성균에 특이적이고 다른 항생제와 교차 내성이 없음을 확인하였다. 항생제 저항성은 ribosomal protein L11 의 프롤린 잔기 돌연변이를 통해 나타났다. 또한 thiocillin IV 생합성은 micrococcin P2 에서 O-methylation 이 일어나는 것이 아니라 선형 중간체에서 methylation 이 일어난 후에 고리화 반응이 일어나 thiocillin IV 가 만들어 지는 것을 확인하였다. 결과적으로 본 연구는 티오펩타이드에 대한 이해를 한층 확장하였으며, 최근 들어 급속도로 확산되고 있는 항생제 내성문제 극복에 있어 새로운 방안을 제시해줄 수 있을 것이다.

중심어: 항생제, 티오펩타이드, 티오실린 생합성 유전자, 생합성, 미생물 생산